Published in final edited form as:
*Prog Chem Org Nat Prod*. 2011 ; 94: 1–58. doi:10.1007/978-3-7091-0748-5_1.

# Chemistry and Biology of Rocaglamides (= Flavaglines) and Related Derivatives from *Aglaia* Species (Meliaceae)

**Sherif S. Ebada**,
Institute of Pharmaceutical Biology and Biotechnology, Heinrich-Heine University of Duesseldorf, Universitaetsstrasse 1, D-40225, Duesseldorf, Germany. Department of Pharmacognosy and Phytochemistry, Faculty of Pharmacy, Ain-Shams University, Organization of African Unity 1, 11566 Cairo, Egypt

**Neil Lajkiewicz**,
Department of Chemistry and Center for Chemical Methodology and Library Development (CMLD-BU), Boston University, Commonwealth Avenue 590, Boston, MA 02215, USA

**John A. Porco Jr.**,
Department of Chemistry and Center for Chemical Methodology and Library Development (CMLD-BU), Boston University, Commonwealth Avenue 590, Boston, MA 02215, USA

**Min Li-Weber**, and
Tumor Immunology Program (D030), German Cancer Research Center (DKFZ), Im Neuenheimer Feld 280, D-69120, Heidelberg, Germany

**Peter Proksch**
Institute of Pharmaceutical Biology and Biotechnology, Heinrich-Heine University of Duesseldorf, Universitaetsstrasse 1, D-40225, Duesseldorf, Germany

Sherif S. Ebada: sherif.elsayed@uni-duesseldorf.de; Neil Lajkiewicz: neiljl@bu.edu; John A. Porco: porco@bu.edu; Min Li-Weber: m.li-weber@dkfz-heidelberg.de; Peter Proksch: proksch@uni-duesseldorf.de

## 1. Introduction

Throughout the ages, humans have relied on Nature for fulfilling their basic needs for foodstuffs, shelter, clothing, means of transportation, fertilizers, flavors and fragrances, and, last but not least, medicines. Natural products have played, for thousands of years, an important role throughout the world in treating and preventing human diseases. Natural product medicines have come from various source materials including terrestrial plants, terrestrial microorganisms, marine organisms, and terrestrial vertebrates and invertebrates (1). The importance of natural products in modern medicine can be assessed using three criteria: (a) the rate of introducing new chemical entities of wide structural diversity, which may serve as templates for semisynthetic and total synthetic modification, (b) the number of diseases treated or prevented by these substances, and (c) their frequency of use in the



Correspondence to: Peter Proksch, proksch@uni-duesseldorf.de.

John A. Porco, Min Li-Weber, and Peter Proksch contributed equally to the writing of this chapter. Dedicated to Dr. Bambang Wahyu Nugroho, a pioneer of rocaglamide research (9, 14, 16, 17, 27, 54–56, 58, 59, 75, 84, 85) who passed away far too early.

treatment of disease (2, 3). An analysis of the origin of drugs developed between 1981 and 2007 indicated that almost half of the drugs approved since 1994 were based on natural products (2, 3). Over 20 new drugs launched into the pharmaceutical market between 2000 and 2005 represent natural products (2, 3), whereas more than 13 natural-product-related drugs were approved from 2004 to 2007; four of them represent the first members of new classes of drugs: the peptide ziconotide, and the small molecules ixabepilone, retapamulin, and trabectedin (ET-743) (Fig. 1) (3, 4). Interestingly, over a hundred natural-product-derived compounds are currently undergoing clinical trials and at least a hundred similar substances are under preclinical development, with most of these derived from leads from plant and microbial sources (3). In spite of challenges facing drug discovery from plants, including the legal and logistical difficulties involved in the procurement of plant materials, and the lengthy and costly process of bioassay-guided fractionation and compound isolation, plants still provide new drug leads that prove to be of potential preclinical and/or clinical use against serious ailments such as cancer, malaria, *Alzheimer*'s disease, and AIDS (5).

The family Meliaceae (= Mahogany family, order Sapindales) is an angiosperm plant family of mostly trees and shrubs together with a few herbaceous plants. This family includes about 50 genera and 550 species, with a panotropical geographical distribution. Two genera, namely, *Swietenia* (Mahogany) and *Khaya* (African mahogany), are important sources of high-quality woods for building shelters and furniture due to their physical properties and also due to their resistance to insect invasion (6).

The genus *Aglaia* Lour. (Fig. 2) is the largest genus of the family Meliaceae, comprising about 120 woody species ranging from small to large trees up to 40 m high, mainly distributed in the tropical rainforests of southeast Asia from Sri Lanka and India, through Burma, south China and Taiwan, Vietnam, Malaysia, Indonesia, the Philippines, New Guinea, the Solomon Islands, Vanuatu (New Hebrides), New Caledonia, Australia (Queensland, Northern Territory and Western Australia), Fiji, as far east as the island of Samoa in Polynesia and north to the Marianne Islands (Saipan, Roti and Guam), and the Caroline Islands (Palau and Ponape) in Micronesia (7). A molecular phylogeny has demonstrated that the genus is divided into three sections, section *Amoora*, section *Neoaglaia*, and section *Aglaia* (8). They are distinguishable morphologically, mainly on fruit characteristics and the numbers of flower parts (8). Like the two genera *Swietenia* (Mahogany) and *Khaya*, the timber of many *Aglaia* species is used locally for house-building, fence-posts, canoes, paddles, axe-handles, spear-shafts, and firewood. The fragrant flowers are used for scenting tea and are kept in cupboards to perfume and to protect clothing from moths. They produce sweet, fleshy fruits that are cultivated in villages in Thailand and peninsular Malaysia and are eaten in the forest by indigenous forest peoples.

The fruits of *Aglaia* (Fig. 2) are also a source of food for birds and mammals in the forests of the Indo-Malayan and Australasian regions where they occur. In West Malaysia, the fruits of species in the section *Aglaia* are indehiscent and primates break open the orange, yellow or brown, fibrous, inedible pericarp and extract the one or two seeds from within. The translucent, sweet aril adheres firmly to the seed, and the seed is often swallowed whole. Analysis of the nutrient content of the aril reveals that it contains sugars and other sweet-tasting constituents and it is thought that these are attractive to the gibbons that disperse the

seeds (7). The fruits of sections *Amoora* and *Neoaglaia* are dehiscent and contain up to three seeds. The outer pericarp is pink or reddish-brown and contrasts with the white inner pericarp and the red aril surrounding the seed. The aril is easily detached from the testa and is removed by the action of a bird's gizzard, without destroying the rest of the seed. The aril, surrounding a relatively large seed, is rich in lipids and provides the birds that disperse the large seed with a high-calorie reward (7).

Several species of the genus *Aglaia*, such as *A. odorata*, are used traditionally in folk medicine for heart stimulant and febrifuge purposes, and for the treatment of coughs, diarrhea, inflammation, and injuries (9). Extracts have also been used as bactericides, insecticides, and in perfumery (10).

During the last few decades, species in the genus *Aglaia* Lour. have received an increasing scientific focus due to their bioactivity potential. Phytochemical interest in the natural constituents of *Aglaia* Lour. can be traced back to the discovery in 1982 of the first cyclopenta[*b*]benzofuran derivative, rocaglamide (**1**), from *A. elliptifolia* (11). To date, more than a hundred naturally occurring rocaglamide-type (= flavagline) compounds have been isolated from over 30 *Aglaia* species (9, 12). Rocaglamides exhibit potent insecticidal (13–18) and antiproliferative (12, 19–21) activities. In addition, antiviral (22), antifungal (23), and anti-inflammatory (24, 25) activities were also reported for these compounds, which are so far only known from *Aglaia* species. Other classes of natural products occurring in *Aglaia* include lignans (13, 26–29), flavonoids, and bisamides (18, 22, 26, 30–36). Some of these metabolites exhibit cytotoxic and antiviral properties as well (22, 30). Furthermore, many terpenoids have been reported from the genus *Aglaia* Lour. (10, 36–51).

The present contribution surveys the group of the rocaglamide derivatives (also known as "flavaglines" or "rocaglate derivatives") and related compounds obtained from the genus *Aglaia*, with an emphasis on their structural diversity, and highlights their potential pharmacological significance, which is the main reason for attracting a greater attention by natural product chemists and cell biologists to this class of natural products and provides a comprehensive overview on their total synthesis.

## 2. Structural Classification of Rocaglamides and Related Compounds

### 2.1. Rocaglamide Derivatives

Rocaglamide (**1**), a 1*H*-2,3,3a,8b-tetrahydrocyclopenta[*b*]benzofuran, was first structurally elucidated in 1982 by *King et al*. through single-crystal X-ray analysis (Fig. 3) (11). Its absolute stereochemistry was determined unambiguously to be (1*R*,2*R*,3*S*,3a*R*,8b*S*) using enantioselective synthesis in 1990 by *Trost et al*. (52). Comparative MS and 1D and 2D NMR spectroscopic data of rocaglamide (**1**) and its analogues, desmethylrocaglamide (**7**), methyl rocaglate (**18**), and rocaglaol (**28**) were first presented in 1993 by *Ishibashi et al*. (53). Rocaglamide congeners differ basically with regard to their substituents at C-1, C-2, C-8b, and C-3′ at ring B. Major variations in the substitution pattern occur at C-2 while the hydroxy substituents at C-1 or C-8b can either be acetylated, methylated, or ethylated (*e.g.* congeners **4**, **5**, and **6**). The position C-3′ is either hydroxylated or methoxylated (*e.g.* congeners **2** and **3**). However, oxidation (16) and esterification (17) of the hydroxy group at

C-1 have been also reported. The structures of rocaglamides known so far are summarized in Fig. 4.

The mass spectra of rocaglamide and its derivatives often show characteristic pairs of fragments at *m/z* 300 and 313 dependent on the substitution pattern. Plausible structures for the ions *m/z* 300 and 313 arising from fragmentation of rocaglamide-type compounds under EI conditions have been described (54), as summarized in Fig. 5. Changes in the fragmentation pattern in the range *m/z* 300–343 indicate the type of substitution at ring B and C-8b of the furan ring. For example, the presence of a hydroxy substituent at C-3′ shifts the characteristic pair of fragments at *m/z* 300 and 313 (as in rocaglamide) to *m/z* 316 and 329 while a methoxy substituent at the same position gives rise to fragments at *m/z* 330 and 343 in the EI mass spectrum of the respective derivative (55). Modification of the hydroxy substituent at C-8b (*e.g.* methylation) can also be determined initially by comparison of its diagnostic fragments to those of the more common structural analogues featuring a hydroxy group at that position (56). Rocaglamide analogues exhibit $^{1}$H and $^{13}$C NMR signals for aromatic protons and aromatic methoxy groups typical for those of substituted phenols. Investigation of the $^{1}$H NMR spectra of several rocaglamide derivatives showed empirically that hydroxylation at C-3′ causes a deshielding effect on the aromatic protons at ring B in the following order: H-2′ > H-6′ > H-5′. Consequently, methylation of the hydroxy group at C-3′ causes a deshielding of the aromatic protons accordingly: H-6′ > H-5′ > H-2′. Moreover, substitution at C-3′ changes the symmetrical $^{1}$H NMR resonance pattern for the AA′BB′ system for the *para*-substituted ring B to an ABC pattern of methines comparable to a threefold substituted phenyl ring system. Assignment of the relative configuration at C-2 has also been deduced by inspection of their $^{1}$H NMR spectra. The vicinal coupling constant values of the methine protons at the C-1, C-2, and C-3 positions ($J_{1,2}$ *ca.* 5–7 Hz and $J_{2,3}$ *ca.* 13–14 Hz) indicated the 1$\alpha$,2$\alpha$,3$\beta$ configuration as well as the *cis*-BC ring junction (53). N*O*ESY experiments have been used to confirm the stereochemical relationship of the substituents from different carbon ring junctions. The N*O*ESY spectrum showed a N*O*E correlation peak between H-2′ and both H-1$\alpha$ and H-2$\alpha$ but not between H-2′ and H-3$\beta$ (53).

The CD spectra of the rocaglamides show prominent negative *Cotton* effects between 217 and 220 nm as the most characteristic feature (54). Their CD spectra are dominated by the nature of the cyclopenta[*b*]tetrahydrobenzofuran moiety forming the backbone of the rocaglamide derivatives with stereocenters at C-1, C-2, C-3, C-3a, and C-8b and thus by the 3D array of the main molecular chromophores, the three aromatic rings. However, the asymmetric carbon C-2 apparently can influence the CD spectra of rocaglamide congeners, as exemplified by the $\alpha$-sugar-substituted derivative **30** (54), which shows virtually the same CD spectrum as rocaglamide (**1**), but it lacks the stereocenter at C-2.

Considering rocaglamide (**1**) as the parent compound, major modifications in the substitution patterns occur at C-2, which in **1** is attached to a dimethylamino substituent characterized by two $NCH_3$ resonance signals at *ca*. 2.90–3.40 ppm in the $^{1}$H NMR spectrum. Derivatives **2**, **5**, and **6**, with a hydroxy function at C-3′ of ring B, were isolated from the twigs (55) and flowers (56) of the Vietnamese species *Aglaia duperreana* while its methoxylated form known as aglaroxin E (**3**) was purified from the bark of the Sri Lankan

species *A. roxburghiana* (57). Compounds with an acetoxy function at C-1 (**4** and **5**) (55, 58) and ethoxylated substituent at C-8b (**6**) (56) were obtained from the same *A. duperreana* specimen.

*N*-Desmethylrocaglamide congeners **7**–**11** feature a –$CONHCH_3$ group at C-2. *N*-Desmethylrocaglamide (**7**) was isolated from twigs and leaves of *A. odorata* (14, 53), whereas congeners with an acetylated hydroxy function at C-1 have been isolated from the flowers of *A. odorata* (59) and the roots of *A. duperreana* (58) collected in Vietnam. An ethylated form of substitution at C-8b occurs in compound **11**, which was obtained from the flowers of the same collection (56). Derivatives with an amino acyl substituent at C-2, as in congeners **12** and **13**, were isolated from *Aglaia harmsiana* (54). From the same species, the cyclized form of the amino acyl chain yielding the tetrahydrofuran ring, which is present in congener **14**, was isolated in its two stereoisomeric configurations. The *N*-didesmethylrocaglamide derivatives **15**–**17** are widely distributed among various *Aglaia* species from different geographical origins, *e.g. A. odorata* from Indonesia (59), *A. argentea* from Malaysia (60), and *A. duperreana* from Vietnam (56).

The methyl rocaglate congeners **18**–**26** were identified by their methyl ester functionality at C-2, which is indicated by a $^{13}C$ NMR resonance at *ca.* 170 ppm as well as by a three-proton singlet at *ca.* 3.70 ppm in its $^{1}H$ NMR spectrum. Methyl rocaglate (**18**) was isolated initially from *Aglaia odorata* (53), then later from *A. forbesii* (60) and *A. elaeagnoidea* (61). Methyl rocaglate was also named aglafoline (62). Compounds with acetylated substituents at C-1 (**21** and **22**) were isolated from *A. duperreana* (56), and also from *A. odorata* (59) while the formylated congeners **23** and **24** were obtained from the bark of *A. spectabilis* collected from Vietnam (17). An unusual C-1 oxime derivative **25** of a rocaglate was isolated from the leaves of *A. odorata* (14), which was exemplified by a large downfield shift of 153.0 ppm as compared to the C-1 resonance for methyl rocaglate at 80.6 ppm in addition to the loss of the H-1 resonance at 4.90 ppm. The H-2 resonance in congener **25** was observed as a doublet that coupled only with H-3, instead of a double doublet as observed in methyl rocaglate (**18**).

Rocagloic acid (**27**) is the demethylated form of methyl rocaglate or the acid congener of this series of cyclopenta[*b*]tetrahydrobenzofuran compounds. It was obtained from the leaves of the Taiwanese species *Aglaia elliptifolia* (63) and also from the leaves of *A. dasyclada* (64) collected in Yunnan Province (China). The $^{1}H$ NMR and $^{13}C$ NMR spectra of **27** are comparable to those of methyl rocaglate (**18**), with the exception of the loss of methyl ester resonance signals.

The rocaglaol derivatives **28**–**32** are unsubstituted at C-2. Rocaglaol (**28**) itself was first isolated from the leaves of *A. odorata* (53) and later proved to be identical to ferrugin, which was reported from *A. ferruginaea* (65) but had been initially assigned a different structure (66). The $^{13}C$ NMR spectra of compounds **28**–**32** exhibit no signal indicative of a carbonyl group (usually in the range of 171–175 ppm), whereas they do feature an aliphatic methylene signal at *ca.* 38 ppm for C-2, as detected from the DEPT-135 spectrum (54). In their $^{1}H$ NMR spectra, the resonances for the methylene protons at *ca.* 2.15 and 2.80 ppm appear as a pair of geminally coupled multiplets splitting as a *ddd* due to coupling with the

vicinal methine protons, H-1 and H-3. Modification of the substitution pattern for compounds **28**–**32** occurs either at C-3′ or C-8b. Methoxylation (**29**) and glycosidation (**30**) at C-3′ have been reported for compounds isolated from the flowers of *A. odorata* (59) and leaves of *A. harmsiana* (54). Inspection of the $^{1}$H NMR spectrum of the glycoside congener **30** revealed an *α*-linked modified rhamnose unit with a methoxy group at the C-3″ position as confirmed by N*O*E experiments (54). This sugar-substituted rocaglaol derivative **30** was the first rocaglamide glycoside isolated from Nature. From the leaf extract of the Malaysian species *A. laxiflora*, a similar rocaglaol rhamnoside, **31**, was isolated, which was reported to contain an additional acetyl group at the C-2″ position of the modified rhamnose unit as confirmed by HMBC (67). Methylation (**32**) and ethylation (**33**) of the hydroxy group at C-8b occur in compounds isolated from the roots of *A. duperreana* (58) and the bark of *A. forbesii* (60).

The three cyclopenta[*b*]tetrahydrobenzofuran derivatives **34**–**36** were isolated by *Kinghorn et al.* from two specimens of *Aglaia* species collected in Indonesia (42, 68, 69). 1-*O*-Acetylrocaglaol (**34**) was isolated from the twigs of *A. rubiginosa* (42). The absolute stereochemistry of **34** was deduced by a comparison of the CD spectrum with that of rocaglamide (**1**). Two methyl rocaglate congeners with an unusual dioxyanyloxy unit at C-6, silvestrol (**35**) and episilvestrol (**36**), were obtained from the fruits and twigs of *A. foveolata* (68). The CD spectrum of silvestrol (**35**) was very similar to that of methyl rocaglate (**18**) implying that the tricyclic cores of both molecules have the same stereochemistry. However, the relative configuration of the dioxyanyloxy unit was difficult to confirm from the available NMR data. Accordingly, the absolute configuration of **35** was established by a single-crystal X-ray analysis of its 5‴,6‴-di-*p*-bromobenzoate derivative, and was found to be (1*R*,2*R*,3 *S*,3a*R*,8b*S*,1‴*S*,2‴*R*,4‴*R*,5‴*R*) (68). From a comparison of its 2D NMR data with those of silvestrol (**35**), compound **36** was assigned as the C-5‴ epimer of **35** (68). Initially, the plant material was wrongly identified as *Aglaia silvestris* (M. Roemer) Merrill, hence the name silvestrol was given to **35**. However, the species was later re-identified as *A. foveolata* Pannell (69).

From the fruits of *Aglaia spectabilis* (syn. *Amoora cucullata*) (Meliaceae) collected from Thailand in 2004, two rocaglamide derivatives, namely, 1-*O*-formylrocagloic acid (**37**) and 3′-hydroxyrocagloic acid (**38**) were isolated (70). The absolute stereochemistry of **37** was defined as having the (1*R*,2*R*,3 *S*,3a*R*,8b*S*)-configuration by comparing its CD spectrum, which revealed a prominent negative *Cotton* effect at 274 nm, with that of rocaglamide (**1**) (70).

The group of 6,7-methyenedioxy rocaglamide analogues (**39**–**41**) was isolated from the stem bark of the Sri Lankan species *Aglaia roxburghiana* (57) and were accorded the trivial names aglaroxins A, B, and F. Compared to the fundamental structure of the rocaglamides, the $^{1}$H NMR resonances for $OCH_3$-6 and H-7 were absent and instead replaced by a methylenedioxy singlet at *ca.* 5.90 ppm. The doublet for H-5 at *ca.* 6.30 ppm in the $^{1}$H NMR spectrum of rocaglamide (**1**) was replaced by a singlet (13). The resonance for $OCH_3$-8 was also shifted downfield from $\delta$3.85 to $\delta$4.10 ppm due to the deshielding effect of the adjacent methylenedioxy function. The presence of a methylenedioxy function was also

evident from a triplet resonance at *ca.* 103 ppm as revealed in its DEPT spectra (16). The absolute configuration of aglaroxin A (**39**) was first determined by calculation of its CD spectrum using molecular dynamics (MD) simulations (16). Variations for the analogues occur at ring B in which aglaroxin B (**40**) was methoxylated at C-3′ while aglaroxin F (**41**) was both methoxylated and hydroxylated at C-3′ and C-4′ (57). Two further aglaroxin A analogues, the 1-*O*-acetate (**42**) and the 3′-methoxy-1-*O*-acetate (**43**), were isolated from an Indonesian collection of the bark of *A. edulis* (71).

The pannellins **44**–**46** were isolated from *Aglaia elaeagnoidea* collected from Thailand (13). For this group of analogues, the amide function at C-2 in aglaroxins A, B, and F was replaced by a methyl ester. Pannellin-1-*O*-acetate (**45**) is the acetylated product of **44** while 3′-methoxypannellin (**46**) is characterized by an additional $–OCH_3$ function in ring B.

*Proksch et al*. described the isolation of a similar group of congeners from the twigs of a Vietnamese collection of *A. oligophylla*, including isothapsakon A (**47**), a C-1-oxo derivative of aglaroxin A (**39**), bearing a bisamide side chain at C-2 that is derived from piriferine (16). The ketone substituent at C-1 was identified by the carbon resonance at $\delta$206 ppm consequently resulting in a downfield shift of H-2, which appeared as a doublet coupling only with H-3.

Derivatives **48**–**52**, featuring a 3′,4′-methylenedioxy substitution in the B ring, have been first reported from *Aglaia elliptica* (20) collected in Thailand and the Vietnamese species *A. spectabilis* (17) while the congeners **39**–**47** possess the same 3′,4′-methylenedioxy functionality but in ring A.

The last group of rocaglamide congeners (**53**–**62**) is characterized by a pyrimidinone subunit fused at C-1 and C-2. The resulting pentacyclic skeleton can be considered conceptually as a rocaglamide with a 2-aminopyrrolidine amide substituent at C-2 linked to C-1 via the primary amino group. This pyrimidinone-type rocaglamide **53** was first isolated from the roots of *A. odorata* collected in Thailand and was elucidated structurally by X-ray crystallography (72). Later, **53** was also isolated from the leaves and twigs of the Vietnamese species *A. duperreana* (55) while its flowers yielded the 3′-hydroxy derivative **54** (56). Aglaroxin D (aglaiastatin) (**55**), the dihydro derivative of **53**, has been isolated from the leaves of *A. duperreana* (55) and *A. odorata* (73) and from the stem bark of the Sri Lankan species *A. roxburghiana* (57). The latter collection yielded four further pyrimidinone analogues with an additional 6,7-methylenedioxy substituent in ring A, known as aglaroxins C (**59**) and G–I (**60**–**62**) (57).

Three further pyrimidinone-type congeners, marikarin (**56**) and 3′-hydroxy-marikarin (**57**), were isolated from the root bark of *Aglaia gracilis* collected in Fiji (18), while aglaiformosanin (**58**) was obtained from the stem bark of *A. formosana* collected in Taiwan (74). In 2003, aglaroxin F (**41**) was isolated from *A. oligophylla* twigs collected in Vietnam together with its 8b,10-anhydro analogue, cyclorocaglamide (**63**) (75). Cyclorocaglamide (**63**) was identified as the first bridged cyclopenta[*b*]benzofuran between C-8b and C-2′ of ring B, whereas to the best of our knowledge aglaroxin F (**41**) represents the only

rocaglamide derivative with three oxygen functions in the B ring, bearing an additional hydroxy group at C-2′.

### 2.2. Aglain Derivatives

Aglains (see Fig. 6) are characterized by a cyclopenta[*bc*]benzopyran(2,5-methano-1-benzoxepin) skeleton, thought to be derived biogenetically from the addition of a flavonoid precursor and a bisamide such as odorine (**103**), odorinol (**104**), or piriferine (**105**) (Fig. 6) (14, 60). Formally, rocaglamides can also be considered as derivatives from aglains by cleaving the C-C bond between C-10 and C-5a, and linking C-10 and C-5a instead. The nature of the ring system of aglains was proven unambiguously by X-ray crystallography of the first congener of this group, aglain A (**64**), thus also revealing the relative configuration (60). The aglain skeleton was confirmed through key HMBC correlations including H-10 to C-5, C-5a, H-4 to C-11, C-5, C-5a, and H-3 to C-2″/6″, C-2, C-5 (60).

The aglains, aglaforbesins as well as the forbaglins contain bisamide side chains that are derived from a cinnamic acid bisamide. These low molecular weight precursors, namely, odorine (**103**) (76, 77), odorinol (**104**) (19, 76), and piriferine (**105**) (78), are composed of cinnamic acid, the bifunctional amine 2-aminopyrrolidine, and 2-methylbutanoic acid (in odorine), 2-hydroxy-2-methylbutanoic acid (in odorinol) or 2-methylpropanoic acid (in piriferine). In 33 of the total of 37 aglain derivatives isolated so far, the bisamide side chain is directly analogous to a naturally occurring cinnamic acid bisamide, odorine (**103**), odorinol (**104**), or piriferine (**105**). The four remaining compounds, **77** and **92**–**94**, can be formally obtained by dehydration of the hydroxy group at C-19 resulting in a double bond between C-19 and C-20. Aglains differ in regard to their configuration at C-19, which can be either (*R*) or (*S*), but more often remains uncertain. This finding parallels the situation of the cinnamic acid bisamides, which also occur as diastereomers at the analogous position. Similarly, the configuration at C-13 can either be (*R*) or (*S*), which again is consistent with the occurrence of both (+)- or (−)-forms of odorine (**103**), odorinol (**104**), and piriferine (**105**) in Nature. It is noteworthy that this aminal position is prone to epimerization in low molecular weight precursors (77), and, frequently, aglains are isolated as diastereomeric mixtures (15).

In their cyclic core, aglains display structural variability at the following positions: the bridging carbon atom, C-10, nearly always carries one proton as well as one oxygen-containing substituent, the latter being either a hydroxy, an acetoxy, or a sugar moiety. The substituents can be either *endo* or *exo* with regard to ring A. Only two derivatives, **88** and **89**, are known to feature a carbonyl group at C-10. In the oxepine ring, H-3 and H-4 are mostly *trans*-oriented, but both possible diastereomeric forms, *i.e.* H-3$\alpha$, H-4$\beta$ as well as H-3$\beta$, H-4$\alpha$, occur more or less evenly distributed in Nature. For compounds with the opposite configuration at C-10, NOE correlation peaks are observed between the $\beta$-protons, H-3 or H-4, and OH-10 (in aprotic solvent) or $OCOCH_3$-10. Furthermore, these NOEs have also been used to assign the relative configurations of the H-3 and H-4 stereocenters. Additionally, the vicinal coupling constant between H-3 and H-4 can be utilized to confirm their configurations. For the H-3$\beta$, H-4$\alpha$ configuration, the $^1$H NMR vicinal coupling constant varies between 5 and 6 Hz, while for the H-3$\alpha$, H-4$\beta$ configuration, the coupling

constant amounts to 9–11 Hz (14, 60, 67). One exception is 4-epiaglain A (**65**), which features the *β*-configuration for both H-3 and H-4, and displays a coupling constant of 7.4 Hz (79).

As in the case of rocaglamides, ring A of aglains is usually substituted by two *m*-positioned methoxy groups at C-6 and C-8, but is also known to carry a 7,8-methylenedioxy substituent, mostly in addition to the methoxy group at C-6 except for congeners **81** and **82**, which feature no methoxy group at C-6. Ring B always carries a 4′-methoxy substituent, in some cases accompanied by a hydroxy or a methoxy group at C-3′, while ring C is always unsubstituted. These substitution patterns are again parallel to those of rocaglamide, whereas a methylenedioxy substituent in ring B has not been encountered in aglains so far.

In spite of the numerous structural analogies between rocaglamides and aglains, and the postulated similar biogenetic pathways leading to both classes of compounds, it is interesting to note that bisamide-derived side chains occur mainly in aglains (and in aglaforbesins as well as in forbaglins, see below), but are rarely encountered in rocaglamides such as in isothapsakon A (**47**). It may be speculated that bulky substituents, such as those present in odorine (**103**), odorinol (**104**), or piriferine (**105**), cannot easily be incorporated into rocaglamides, and thus are usually replaced by simpler amide or nitrogen-free side chains.

The assignment of the relative configuration of aglain A (**64**), the parent compound of this series of cyclopenta[*bc*]benzopyran derivatives, was determined from NOESY NMR correlations (60). In 2000, the first X-ray structure of this type of compounds was obtained for aglaxiflorin A (**74**), thus confirming the relative stereochemistry (67). Previously, the relative configuration of aglains had been assigned from 2D NOE data, while the absolute configuration was deduced on the grounds of biogenetic comparison with rocaglamide (**1**). According to *Greger* and colleagues, formal conversion of cyclopenta[*bc*]benzopyran into cyclopenta[*b*] benzofuran would leave the absolute configuration at C-2 (C-3a in rocaglamides) unchanged, as was deduced by inspecting *Dreiding* models (15). Thus, the structures of aglain derivatives are commonly drawn with the methylene bridge (C-10) oriented upwards, while the aromatic ring B and OH-5 are oriented downwards (9).

Aglains A (**64**), B (**67**), and C (**69**) were isolated from the leaves of *Aglaia argentea* collected in Malaysia (60), while 4-epiaglain A (**65**) and 10-*O*-acetylaglain B (**68**) were obtained from an Indonesian collection of *A. elliptica* leaves (79). The relative configurations of **65** and **68** were solved using NOESY NMR data. Deacetylaglain A (**66**), isolated from the leaves of *A. gracilis* collected in Fiji (18), is very similar to aglain A (**64**), except for the hydroxy group at C-10. Recently, ponapensin, the only congener featuring a methoxy group at C-13 instead of the amide side chain in aglain B (**67**), was isolated from the Micronesian species *Aglaia ponapensis* (80).

In thapsakones A (**88**) and B (**89**), obtained from the root bark of *Aglaia edulis* (southwest Thailand), which lack a proton at C-10, the stereochemistry of H-3 and H-4 was deduced in an elegant manner by observing a shift stronger than a lanthanide-induced shift (LIS) to the respective *β*-proton (4 in **88**, 3 in **89**) (15). The configuration of the aminal proton H-13 was

assigned as being (13*S*) by observing N*O*Es between H-4 and H-13 as well as between the terminal methyl group(s) H-21 (and H-20 in the case of piriferine-derived side chains) and H-2″/6″, while no such N*O*E correlations were detected for (13*R*)-derivatives as confirmed by close inspection of *Dreiding* models (15, 60).

Edulirin A (**90**), 10-*O*-acetyledulirin A (**91**), and 19,20-dehydroedulirin A (**92**), together with aglaroxin A analogues **42** and **43**, were reported from an Indonesian collection of the bark of *Aglaia edulis* (71).

The two glycosidic derivatives **94** and **95** have been isolated from the leaves of *Aglaia dasyclada* collected in Yunnan Province, People's Republic of China (64). These two compounds have a hydroxytiglic amidic putrescine moiety instead of the cinnamic acid bisamides previously found as the amine substituents in other aglain derivatives.

The last group of aglain congeners with compounds **96**–**100** exhibits a benzoyl-1,4-butanebisamide moiety at C-4 along with the open oxepine ring congener, secofoveoglin (**101**). Pyrimidaglain A (**96**) and B (**97**) were the first congeners of this group isolated from the leaves of *Aglaia andamanica* collected in Thailand (36). Recently, three further congeners, desacetylpyrimidaglains A, C, and D (**98**–**100**), have been reported from the leaves of *A. forbesii* collected also in Thailand (46). The latter has been given the trivial name, isofoveoglin, and was isolated together with the open oxepine ring congener, secofoveoglin (**102**), from the leaves and stem bark of *A. foveolata* (Indonesia) (81). The only difference between the pyrimidaglains **96** and **97** and the desacetylpyrimidaglains **98**–**100** is the lack of acetylation of the OH-10 function in the latter compounds. The relative configurations of the deacetyated pyrimidaglains has been proven through the observation of the characteristic N*O*ESY cross peaks H-3 to H-4, N*H*-12, H-2′/6′, and H-2″/6″, H-4 to H-3, OH-10, N*H*-12, and H-2″/6″, and H-10 to H-2″/6″, and the most important cross peak between OH-10 and H-4, which directly proved the relative configuration at C-3, C-4, and C-10 (46). Cyclofloveoglin (**101**), isolated from the leaves and stem bark of *A. foveolata* (Indonesia) (81), represents a hitherto unprecedented five membered-cyclic amide moiety among the rocaglamide-type compounds isolated from the genus *Aglaia* so far (9, 12). The structure of **101** was proposed through the DEPT NMR spectrum, which revealed a quaternary carbon resonance at $\delta$90.6 ppm that replaced the signal of a hydroxymethine carbon at position C-10 in **100**. Furthermore, a HMBC spectrum confirmed the structure of cyclofloveoglin through correlations between the quaternary carbon, C-10, with H-4 and H-13, indicating that N-12 is bonded to C-10 (81).

### 2.3. Aglaforbesin Derivatives

The aglaforbesins are closely related to the aglains, but with a cinnamic acid bisamide-derived side chain at C-3 and the unsubstituted phenyl ring C at C-4 mutually interchanging (as in congener **95**). This structural feature was evidenced by HMBC correlations from H-3 to C-11 as well as H-4 to C-2″/6″ (60). To date, only ten aglaforbesin derivatives (see Fig. 7) have been described from Nature, which differ with regard to the substitution pattern of ring A as well as in the stereochemistry at C-3, C-4, and C-13. Unlike the aglains, no structural variants from the 4′-methoxy substituted ring B are known, however, in ring A, a

methylendioxy functionality between C-7 and C-8 has been reported in the three congeners **109**–**111** (16, 71). Side chains are derived from odorine (**103**) (in **106** and **107**) (60), odorinol (**104**) (in **108**) (67), and piriferine (**105**) (in **109**) (16). However, foveoglins A (**112**) and B (**113**) feature a benzoyl-1,4-butanebisamide moiety at C-3 (71, 81) unlike the pyrimidaglains **96**–**100**, which exhibit the same moiety at C-4 (36, 46).

Assignment of the stereochemistry of aglaforbesins is based on the same principles as for aglains. Consequently, the configuration of the aminal proton H-13 was deduced as being (*R*) in aglaforbesins A (**106**) and B (**107**) due to N*O*Es observed between H-3 and H-13 as well as between H-21 and H-2″/6″ (60). Interestingly, the H-3$\alpha$/H-4$\beta$ configuration leads to a pronounced upfield shift of $OCH_3$-6 ($\delta$ approx. 3.1 ppm), since in this case the methoxy group is placed inside the shielding zone of the unsubstituted benzene ring at C-4$\alpha$ (60, 67), while a normal chemical shift ($\delta$ approx. 4.1 ppm) is observed in the case of reversed stereochemistry at C-3 and C-4 (16). By analogy to the aglains, configurations at their respective positions are also reflected by the magnitude of the vicinal coupling constant: $^3J_{(H\text{-}3,\ H\text{-}4)}$ amounts to 10–11 Hz when H-3 is $\alpha$ and H-4 is $\beta$ (60, 67), while the coupling constant is 6–7 Hz when in the opposite configuration (16).

### 2.4. Forbagline Derivatives

Forbaglines are benzo[*b*]oxepines naturally occurring in the genus *Aglaia*, in which the pyran ring of the aglains is replaced by an oxepine ring. The benzo[*b*]oxepine skeleton of the forbagline derivatives can be formally obtained from the aglains by oxidative cleavage at the methylene bridge between C-5 and C-10 (60). As for the aforementioned groups of rocaglamide-type compounds, the aromatic rings A, B, and C share common characteristics with their benzofuran and benzopyran counterparts. The aromatic ring A can carry either an 8-methoxy or a 7,8-methyl-enedioxy substituent in addition to a 6-methoxy group, while ring B may show a *p*-methoxy (as in **114**–**124**) or a *p*-hydroxy (as in **125**) substituent, and ring C is unsubstituted. The benzo[*b*]oxepine core is conserved in all but derivative **125**, which has a carboxylic acid functional group instead of the methyl ester group at C-10 (64). The only major variation in the skeleton occurs in the type of the bisamide side chain substituent at C-4.

The structure of the first derivative, forbaglin A (**114**), was established by X-ray crystallographic analysis, thus revealing the relative stereochemistry (60). The configurations at H-3 and H-4 of the forbagline derivatives reflect those of the aglains and aglaforbesins with only *trans* isomers having been isolated so far. By analogy to the benzopyran series, the magnitude of the vicinal coupling constant $^3J_{(H\text{-}3,\ H\text{-}4)}$ can be used to determine the relative stereochemistry at C-3 and C-4.

To date, 12 forbagline derivatives (see Fig. 8) have been isolated, including the 7 derivatives **114**–**120** with an odorine or a piriferine side chain. The other 5 analogues **121**–**125** revealed bisamide side chains derived from substituents other than odorine or piriferine (64, 82). Both derivatives **124** and **125** have a hydroxytiglic amidic putrescine moiety similar to that of **94** and **95**, and all of them were isolated from the same *Aglaia* species (64). Compound **124** is the only forbagline glucoside derivative isolated so far, with the glucose attached to C-21

(the bisamide side chain), whereas compound **125** has a very similar structure to **124** except for the absence of the sugar moiety at C-21, and the presence of a carboxylic acid and a hydroxy functional group at positions C-10 and C-4′ (64).

Edulisones A (**121**), B (**122**), and 19,20-dehydroedulisone A (**123**) were isolated from the bark of *Aglaia edulis* collected in Indonesia (71, 82). The relative stereochemistry of edulisone A (**121**) was determined by single-crystal X-ray diffraction analysis, revealing the (*R*) configuration at C-13 (82). Furthermore, the two epimers **121** and **122** showed different $^{1}$H NMR chemical shifts for protons close to the C-13 epimeric site, which may be used to assign the relative stereochemistry at C-13. For the (13*R*)-epimer **121**, H-14a and H-14b displayed two signals in the $^{1}$H NMR spectrum, while for the (13*S*)-epimer, these two protons were overlapped in a relatively upfield region (82). For H-16a and H-16b of the (13*R*)-epimer, the two protons overlapped in the $^{1}$H NMR spectrum, while for the (13*S*)-epimer, these two protons were clearly separated, one at a higher field and one at a lower field relative to those of its (13*R*)-counterparts (82). The same phenomenon was also observed in forbaglins A ((13*R*), **114**) and B ((13*S*), **115**) (60).

## 3. Biosynthesis of Rocaglamides and Related Metabolites

The cyclopenta[*b*]benzofurans (rocaglamides), and the two structurally related groups, the cyclopenta[*bc*]benzopyrans (including the aglains and aglaforbesins), and the benzo[*b*]oxepines (known also as the “forbaglines”), are considered characteristic secondary metabolites of the genus *Aglaia*, because they have been only isolated from this taxon (9). Therefore, the collective name “flavagline” has been proposed for these compounds because their mutual biogenetic origin has been postulated to arise from common structurally related precursors that include cinnamic acid amides and the flavonoid nucleus (9, 13–15). A postulated biosynthetic origin was firstly proposed by *Nugroho et al*. in 1999 as depicted in Fig. 9 (14). According to this hypothesis, the initial *C*-*C*-connecting step (step A) between C-2 of the flavonoid **I** and C-3 of the cinnamic acid amide **II** is a *Michael*-type 1,4-addition of the enolate subunit of **I** to the *α*,*β*-unsaturated amide **II**. The C-2 atom of the resulting amide enolate of **III** can now attack C-4 of the previous flavonoid, which has now become a strongly activated carbonyl group, to yield a five-membered ring, giving rise to **IV** (step B). According to this concept, **IV** constitutes the biosynthetic key intermediate and precursor both to aglain and rocaglamide derivatives. Moreover, **IV** can already be considered as a dehydroaglain derivative, and a simple reduction step (*e.g.* with $[H]^{-}$ possibly through NADPH or a related H-nucleophile), will yield the corresponding aglain derivative **V′** (step C′).

This reduction to give **V** stabilizes the strained molecule **IV**, which, as the key intermediate, may otherwise undergo a rearrangement by an intramolecular migration of the electron-rich substituted (phloroglucinol-type) aromatic ring from the previous C-4 to C-3 of the flavonoid. Mechanistically, this can be considered as an electrophilic aromatic *ipso*-substitution via the cyclopropyl derivative **V** as the *σ*-complex (steps C and D), thus ultimately transforming the hydroxyketone **IV** into the isomeric hydroxyketone **VI**, which is already a dehydrorocaglamide derivative. Again, this is possibly a reversible process, which

becomes definite by a stabilizing final reduction step (step E), to give rise to rocaglamide derivatives **VII**.

Although aglaforbesin derivatives are not depicted in Fig. 9, they also fit into the biogenetic scheme proposed, but differ in comparison to the aglains by the opposite orientation of the cinnamic acid amide **II** with respect to flavonoid **I**. In addition, forbaglines can be proposed as being biosynthesized through oxidative cleavage between C-5 and C-10 of hydroxyketone **IV** (numbering as in aglains and aglafor-besins). Apparently, the addition of **II** to **I** is neither regio- nor stereoselective, since all four possible stereoisomers do exist in Nature, *i.e.* both (H-3$\alpha$,H-4$\beta$) and (H-3$\beta$, H-4$\alpha$) derivatives have been reported.

From these aforementioned considerations, a search for the probably unstable, possibly interconverting, intermediates **IV** and **VI** of the postulated biosynthesis pathway of dehydroaglain and rocaglamide derivatives, would provide further support for the hypothetical biogenetic scheme and be rewarding, if successful.

For the bisamide-containing flavaglines, a proposed biosynthesis pathway is depicted in Fig. 10, in which a similar initial *C*-*C*-addition occurs between C-2 of the flavonoid and C-3 of piriferine (**105**), odorine (**103**), or odorinol (**104**). This step leads to the formation of the aglain derivative, thapsakon A (**88**), which can be transformed into isothapsakon A (**47**) through an α-ketol rearrangement similar to steps (C–E) in Fig. 9.

## 4. Pharmacological Significance of Rocaglamides and Related Compounds

### 4.1. Insecticidal Activity

The first report on the remarkable insecticidal activity of extracts from *Aglaia* species in the literature originates from 1985, when Chiu *et al*. (83) described the antifeedant properties of a crude extract derived from *A. odorata* towards larvae of the cabbage worm, *Pieris rapae*. The active principles of *A. odorata* responsible for the strong antifeedant properties of the respective crude extracts against *P. rapae* and against other insects, however, were only identified in 1993 when *Ishibashi et al*. (53) reported on the bioassay-guided isolation of rocaglamide (**1**) and three of its congeners using larvae of the polyphagous noctuid, *Peridroma saucia*, as experimental insects. Interestingly, rocaglamide (**1**) had already previously been isolated in 1982 from *A. elliptifolia* and described as having inhibitory properties against a human epidemoid carcinoma of the nasopharynx (KB) cell line *in vitro* ($IC_{50}$ = 8.7 μ*M*) (11), thereby providing an early hint to the parallelism between insecticidal and antiproliferative properties of rocaglamide and its derivatives that became even more obvious in subsequent studies (84, 85).

Sparked by these findings, a more directed search for new rocaglamide derivatives from Nature aiming also at a better understanding of their pronounced insecticidal properties commenced, which up to now has led to the isolation of more than 60 naturally occurring rocaglamide congeners as well as numerous other biogenetically related compounds isolated from over 30 different *Aglaia* species collected mainly in Indonesia, the People’s Republic of China, Thailand, and Vietnam.

The majority of the 63 naturally occurring rocaglamide derivatives known so far were analyzed for their insecticidal activity employing various Lepidopteran larvae including *Peridroma saucia* (53), *Ostrinia nubilalis* (86), *Helicoverpa armigera* (87), or *Spodoptera littoralis* as experimental insects. Most of these studies, however, have been performed with larvae of the polyphagous pest insect *Spodoptera littoralis* (14, 16, 17, 54–56, 58, 59) thereby permitting the formulation of preliminary structure-activity relationships based on a larger set of data obtained with the same insect species. In the studies with *S. littoralis*, different rocaglamide derivatives were usually added at a range of concentrations to artificial diet, which was subsequently offered to newly hatched larvae in a no choice chronic feeding bioassay. From the larval survival rates, $LC_{50}$ values can be calculated for the various rocaglamide congeners and compared to other insecticides of natural origin, such as azadirachtin from *Azadirachta indica* (family Meliaceae) (Fig. 11). With only a few exceptions, all naturally occurring rocaglamide congeners evaluated exhibited potent insecticidal activity toward the larvae of *S. littoralis*. The most active compounds, including the parent compound rocaglamide (**1**) itself or its didesmethyl analogue **15**, exhibited $LC_{50}$ values ranging between 1 and 2 ppm, so their insecticidal activity was thus comparable to that of azadirachtin (14, 54, 55, 59).

Acylation of the OH group at C-1 (*e.g.* with formic or acetic acid) led to a reduction of insecticidal activity, as exemplified by comparison of the $LC_{50}$ values of compound **2** (1.5 ± 0.7 ppm) and its acetyl derivative **5** (8.0 ± 1.4 ppm) or of congener **12** (1.1 ± 0.6 ppm) and its acetyl derivative **13** (14.7 ± 2.8 ppm) (14, 54, 55). On the other hand, the nature of the amide substituent present at C-2 showed little or no influence on the insecticidal activity of the resulting rocaglamide congeners, even when the dimethylamino group present in the parent compound rocaglamide (**1**) ($LC_{50}$ of 0.9 ± 0.4 ppm) was exchanged for a rather bulky group, as, for example, in compound **14** ($LC_{50}$ of 1.6 ± 0.6 ppm). The same findings were true when the amide group was exchanged to an ester substituent, which likewise had no significant effect on the resultant insecticidal activity of the respective compounds. However, a diminution in insecticidal activity by a factor of 5 or 6 was usually observed for rocaglamide derivatives featuring an unsubstituted C-2 when compared to analogues with an amide or carboxylic acid ester substituent at this particular position (14, 54, 55, 59).

In rings A or B, the occurrence of an additional oxygen substituent, when compared to the substitution pattern of the parent compound, rocaglamide (**1**), revealed only marginal influences on the insecticidal activity of the respective products (54). However, a dramatic effect with regard to structure-activity relationships of rocaglamide derivatives was observed for analogues with a substituted OH group at C-8b. For example, compounds featuring a methoxy group at C-8b that were isolated from the roots of *A. duperreana* proved to be completely inactive as insecticides even when tested at concentrations of more than 100 ppm. Thus, these results point out the presence of a free OH group at C-8b as being the most important structural prerequisite for insecticidal activity of rocaglamide analogues determined so far (56, 58).

It is difficult to decide whether the mortality of the *S. littoralis* larvae observed in chronic feeding bioassays described above is mainly caused by starvation due to feeding deterrence or by a direct toxicity of the rocaglamide derivatives evaluated or from a combination of

both effects. When neonate larvae of *S. littoralis* were given the choice between an artificial diet treated with rocaglamide (**1**) and a control diet, they avoided the former and showed a clear preference for the latter (the $IC_{50}$ values in these experiments varied between 0.2 and 0.25 ppm), indicating that **1** and its congeners have strong antifeedant properties (54, 55). The toxicity of rocaglamide (**1**) was proven by injecting known amounts of this cyclopenta[*b*] benzofuran derivative into the hemolymph of last instar larvae of *S. littoralis*. In these experiments, the $LC_{50}$ of rocaglamide varied between 5.6 and 7.5 ppm (54, 55). Further proof for the effects of **1** on a cellular level was obtained using *in vitro* cultures of *Spodoptera frugiperda* cells. Addition of rocaglamide (**1**) to the *in vitro* cultures resulted in an arrest of cellular division as indicated by the severely reduced incorporation of [$^3$H]-thymidine. The $IC_{50}$ of **1** amounted to 1.9 μg/cm$^3$ (= 3.8 μ*M*) (84, 85).

A more recent study was conducted to assess the insecticidal activity of rocaglamide (**1**) isolated from *Aglaia elaeagnoidea* against the gram pod borer, *Helicoverpa armigera* (Hübner) (87). In this study, rocaglamide was added to an artificial diet and this led to growth retardation of neonate larvae in a dose-dependent manner with an $IC_{50}$ value of 0.76 ppm, which could be compared to that of azadirachtin ($IC_{50}$ = 0.23 ppm). However, azadirachtin (Fig. 11) was determined as being more potent than rocaglamide in inducing growth inhibition via oral administration to the first stadium larvae utilized. By topical application, rocaglamide (**1**) was found to have $LD_{50}$ and $LD_{95}$ values of 0.40 and 1.02 μg per larvae against third instar larvae 96 h post-treatment, whereas the analogous values for azadirachtin were 8.16 and 25.8 μg per larva for the same period (87).

In spite of the severe morphological larval deformities observed in azadirachtin-treated larvae during the process of ecdysis, the cytotoxic nature of rocaglamide (**1**) was established by evaluating dietary utilization, for which the results did not implicate any antifeedant effect, but rather a toxicity-mediated effect due to the reduced efficiency of the conversion of ingested food. Conclusively, feeding deterrence was deduced not to be the primary mode of insecticidal activity of rocaglamide, with this compound having instead a centrally mediated effect, which could be due to induced cytotoxicity at non-specific cellular levels (87).

However, the molecular target of rocaglamide (**1**) and its congeners in insects is still unknown, and the insecticidal activity of these compounds can be linked to distinct structural features, such as the OH group at C-8b, which is an indispensable prerequisite for bioactivity. Interestingly, rocaglamide derivatives often co-occur in *Aglaia* species with biogenetically closely related compounds of the aglain, aglaforbesin, or forbagline type (14, 16, 60). In these latter compounds, the oxygen heterocycle of the dihydrobenzofuran nucleus in rocaglamides is replaced by a bridged pyran or by an oxepine ring. These structural differences, however, lead to a complete loss of insecticidal activity for aglain, aglaforbesin, or forbagline derivatives (14, 16). The putative biogenetic precursors of rocaglamides as well as aglains, aglaforbesins, and forbaglines – methylated flavonoids and 2-aminopyrrolidines, such as odorine (**103**) – are likewise devoid of any significant insecticidal activity (54, 55), implying that the integrity of the cyclopenta[*b*]-tetrahydrobenzofuran moiety of the rocaglamide skeleton is essential for the insecticidal activity of this unique group of natural products.

### 4.2. Anti-inflammatory Activity

In several countries of Southeast Asia (*e.g.* Vietnam), the leaves and flowers of *A. duperreana* and *A. odorata* are used in traditional medicine for the treatment of asthma and inflammatory skin diseases. Inflammatory diseases arise from inappropriate activation of the immune system, leading to abnormal expression of genes encoding pro-inflammatory cytokines and tissue-destructive enzymes (88). Overproduction of cytokines such as TNF-α and IFN-γ has been shown to be tightly associated with autoimmune and inflammatory diseases, whereas, uncontrolled expression of the cytokine IL-4 causes allergic disorders including asthma (88, 89). It has been shown that rocaglamide (**1**), 1-*O*-acetylrocaglamide (**4**), and 1-oxo-11,12-methylendioxyrocaglaol (**50**) can inhibit TNF-α, IFN-γ, and IL-4 production in human peripheral blood T cells at very low doses (25–50 n*M*) (25). This effect may partially explain the anti-inflammatory and anti-asthmatic activities of *Aglaia* species. Importantly, at the concentrations required for inhibition of cytokine expression, these compounds do not show obvious toxicities on primary blood T cells (21, 25).

Many inflammatory cytokine genes including IL-4 are regulated at the transcriptional level by pro-inflammatory transcription factors, such as NF-κB and AP-1 and by nuclear factor of activated T cells (NF-AT) (89–91). Several rocaglamide derivatives were reported to have an inhibitory effect on the activity of NF-κB. It was shown that at n*M* concentrations, rocaglamide (**1**), desmethyl-rocaglamide (**7**), *N*,*N*-didesmethyl-*N*-4-hydroxybutyl-rocaglamide (**12**), and didesmethyl-rocaglamide (**15**) inhibited NF-κB-mediated transcription induced by TNF-α or phorbol 12-myristate 13-acetate (PMA) in Jurkat leukemic T cells by more than 90%, as determined by a stably transfected NF-κB-regulated luciferase reporter gene (24). This effect, however, was not seen in non-lymphoid cells transiently transfected with the NF-κB-regulated luciferase reporter gene (24). The authors concluded that rocaglamide derivatives may be potent inhibitors of NF-κB in T lymphocytes but not in other types of cells. The NF-κB pathway can be activated by various stimuli. In resting T cells, NF-κB is sequestered in an inactive state by the cytoplasmic inhibitor of NF-κB (IκB). Stimulation of T cells, *e.g.* through the T cell receptor, the TNF receptor, or using PMA, leads to rapid activation of the IκB kinases (IKKs) and results in phosphorylation, ubiquitylation, and subsequent degradation of IκB proteins, which allows the nuclear translocation of NF-κB (92). Rocaglamide (**1**) probably interferes with the NF-κB activation pathway upstream of the IKK complex but downstream of the TNF receptor-associated proteins (24).

Recently, several rocaglamide derivatives were reported to inhibit NF-AT activity in a more sensitive and selective way than NF-κB (25). It was shown that rocaglamide (**1**), 1-*O*-acetylrocaglamide (**4**), and 1-oxo-11,12-methylendioxy-rocaglaol (**50**) inhibit NF-AT-dependent transcription at doses that did not impair NF-κB- and AP1-mediated transcription in Jurkat T cells stimulated with PMA and ionomycin (25). Rocaglamide (**1**), which was previously reported to inhibit PMA-induced NF-κB activation in Jurkat T cells at concentrations of 25–100 n*M* (24), did not show inhibition of PMA-induced IκB degradation and also did not block PMA-induced nuclear translocation of p65 (a subunit of NF-κB) (21, 25). Instead, at concentrations <100 n*M*, rocaglamide (**1**), as well as 1-*O*-acetylrocaglamide (**4**) and 1-oxo-11,12-methylendioxy-rocaglaol (**50**), even substantially

increased NF-κB-mediated transcription (25). In addition, using an enzyme-based NF-κB activity readout it was shown that rocaglamide (**1**) inhibited NF-κB activity only at a high dose ($IC_{50}$ = 2 μ*M*) (80). Since rocaglamide also inhibits protein synthesis (see below), it is, therefore, unclear whether the observed inhibition of NF-κB activity at high concentrations of this compound is due to inhibition of NF-κB activation signalling pathway or is rather the consequence of translation inhibition. Apparently, the latter studies do not support rocaglamide as a potent NF-κB inhibitor. Nevertheless, a newly identified compound of the group of aglain derivatives named ponapensin, which is the only congener featuring a methoxy group at C-13 instead of an amide side chain in aglain B (**67**), was shown to inhibit NF-κB activity with an $IC_{50}$ of 60 n*M* determined by the NF-κB ELISA method (80). So far, there are no further studies on whether and how ponapensin inhibits NF-κB activity in cells.

Members of the NF-AT family of proteins are calcium- and calcineurin-regulated transcription factors. In resting T cells, NF-AT proteins are phosphorylated and reside in the cytoplasm. T cell activation leads to activation of the calcium-dependent phosphatase calcineurin, resulting in rapid dephosphorylation of NF-AT which leads to its nuclear translocation and the induction of NF-AT-mediated gene transcription. NF-AT activities are negatively controlled by several kinases including glycogen-synthase kinase 3 (GSK3) and casein kinase 1 (CK1), which maintain NF-AT in a phosphorylated state in the cytosol (maintenance kinases), and inducible MAPKs p38 (the mitogen-activated protein kinases) and JNK (the stress-activated c-Jun N-terminal protein kinase), which induce the re-phosphorylation of nuclear NF-AT to expose a nuclear-export signal and translocate NF-AT back to the cytosol (export kinases) (91). Investigation of the molecular mechanism by which rocaglamide (**1**), 1-*O*-acetylrocaglamide (**4**), and 1-oxo-11,12-methylendioxyrocaglaol (**50**) inhibit NF-AT activation in Jurkat T cells revealed that these compounds can enhance T-cell-activation-induced p38 and JNK activity (25). Increase of p38 and JNK activity resulted in acceleration of nuclear export of NF-AT. Prevention of NF-AT nuclear translocation in activated Jurkat T cells was visualized by confocal laser scan microscopy after rocaglamide (**1**) treatment (25). These data suggest that rocaglamide derivatives may function as immunosuppressive agents by targeting NF-AT activity in T cells. However, later studies revealed that, in contrast to malignant T cells, rocaglamides do not activate p38 and JNK in normal T cells and have apparently little effect on the NF-AT-dependent transcription in normal T cells (21). How the expression of TNF-α, IFN-γ, and IL-4 in normal T cells are suppressed by rocaglamide remains unknown.

### 4.3. Anticancer Activity

**4.3.1. Antitumor Activities *In Vivo* in Mouse Tumor Models—**In 1982, rocaglamide (**1**) was shown for the first time to increase lifespan of tumor-bearing mice in a leukemic model using P388 murine lymphocytic leukemia cells (11). In this study, administration of rocaglamide (**1**) at a dose of 1 mg/kg/day was shown to prolong survival with a T/C value (median survival time of treated *vs.* control group) of 156% (11). This observation has attracted the attention of scientists and more and more newly isolated rocaglamide derivatives have been evaluated for their antitumor potential in different cancer cell lines. A battery of rocaglamide derivatives has been found to have potent inhibitory effects on

proliferation in different tumor cell lines *in vitro* (summarized in Ref. (12)). The $IC_{50}$ values of the antiproliferative activities of most of the rocaglamide derivatives range from 1 to 200 n*M* depending on the cell line investigated (12). Several rocaglamide derivatives were further tested *in vivo* in mice tumor models (21, 68, 93, 94). For instance, intraperitoneal treatment with 4′-demethoxy-3′,4′-methylenedioxy-methyl rocaglate (**48**) at 10 mg/kg body weight three times per week was shown to lead to delayed growth of the xenografted human breast cancer cell line BC1 in athymic mice (93). Treatment with silvestrol (**35**) at 2.5 mg/kg/injection, when given intraperitoneally for five consecutive days in the ip P388 murine leukemia model, afforded a lifespan increase corresponding to a T/C of 150% (68). Silvestrol (**35**) was also shown to inhibit growth of the xenografted human breast cancer cells MDA-MB-231 at doses of 0.5 mg/kg/day for 8 days (94). Significant delay in growth and tumor size (*P* value = 0.021) of the mouse lymphoma RMA was observed after 16 days intraperitoneal treatment with desmethyl-rocaglamide (**7**) at 5 mg/kg three times per week (21). These animal studies have confirmed the anticancer activities of rocaglamide derivatives. All animal studies showed that these compounds had no toxicity to liver evaluated by glutamate pyruvate transaminase (GPT) activity and showed also no body weight loss.

**4.3.2. Cytostatic Activity and Inhibition of Translation—**Since rocaglamide (**1**) and its derivatives have been found to have anticancer activities in experimental animal models, efforts have been taken to explore the molecular mechanisms of their actions. In several early publications, rocaglamide derivatives were reported to function mainly in a cytostatic rather than a directly cytotoxic manner (11, 84, 85, 93). It was shown that treatment of the human lung carcinoma cells Lu1 with 4′-demethoxy-3′,4′-methylenedioxy-methyl rocaglate (**48**) resulted in inhibition of tumor cell proliferation with cell accumulation in the G1/G0 phase of the cell cycle with only marginal cell death (93). Thereafter, didesmethyl-rocaglamide (**15**), aglaroxin D (aglaiastatin) (**55**), and silvestrol (**35**) were shown to inhibit cell proliferation of different human malignant cell lines with the cell cycle blocked at the G2/M phase with negligible death (85, 95, 96). Furthermore, 4′-demethoxy-3′,4′-methylenedioxy-methyl rocaglate (**48**) was found to strongly inhibit protein biosynthesis in tumor cells as determined by $^{3}$H-leucine incorporation (93). Based on these observations, it was thought that inhibition of translation is the key mode of action by which cyclopenta[*b*]benzofurans exert their antitumor activities.

Although rocaglamide (**1**) was found to inhibit translation more than 10 years ago, its mode of function was only recently explored. Translational control involves a highly regulated process (schematically depicted in Fig. 12). Translation is initiated by binding of the initiation factor eIF4E to the mRNA 5′ cap structure. After binding to the 5′ cap structure, eIF4E interacts with eIF4G, which serves as a scaffold protein for the assembly of eIF4E and eIF4A to form the eIF4F complex. The eIF4F complex is then directed to the 5′ terminus of the mRNA and unwinds the mRNA 5′ secondary structure to facilitate ribosome binding and promotes ribosome recruitment and translation (97). Using a small molecule screening approach, 1-*O*-formylaglafoline (**23**) and silvestrol (**35**) were found to inhibit translation by interfering with eIF4A activity (98). It is thought that eIF4A exists as a free form or as part of the eIF4F complex and recycles through the eIF4F complex during

translation initiation. 1-*O*-Formylaglafoline (**23**) and silvestrol (**35**) were shown to stimulate the RNA-binding activity of eIF4A and this action prevents incorporation of free eIF4A into the eIF4F complex (98).

In eukaryotes, most mRNAs are translated in a cap-dependent manner. The rate-limiting step of translation is largely controlled by binding of the initiation factor eIF4E to the mRNA 5′ cap structure. The activity of eIF4E is regulated by two major signalling pathways: the Ras-ERK-Mnk1 pathway and the PI3K-mTOR (mammalian target of rapamycin) pathway (97) (Fig. 12). In the Ras-ERK-Mnk1 pathway, the extracellular signal-regulated kinase ERK, activated by growth factors through Ras, phosphorylates the kinase Mnk1, which, in turn, phosphorylates eIF4E. Phosphorylation of eIF4E increases its affinity for the 5′ cap structure. The activity of eIF4E is also regulated by the PI3K-mTOR pathway. The assembly of the translation initiation complex eIF4F is inhibited by the translational repressor of eIF4E-binding proteins (4E-BP1). 4E-BP1 interacts with eIF4E in its hypophosphorylated state and prevents the recognition and binding of eIF4E to the 5′ cap mRNA structure. PI3K activates mTOR, which in turn phosphorylates 4E-BP1 leading to disruption of the interaction between 4E-BP1 and eIF4E and allowing eIF4E binding to the 5′ cap structure (Fig. 12). Most recently, 1-oxo-11,12-methylen-dioxyrocaglaol (**50**) was found to strongly inhibit protein synthesis ($IC_{50}$ = 30 n*M*) in living cells, but had no inhibitory effect on protein synthesis *in vitro* in the rabbit reticulocyte cell free system (99). This finding indicates **50** does not directly inhibit the translational machinery, but rather acts through inhibition of the signaling pathway that is required for translation. Further investigation revealed **50** suppresses ERK phosphorylation and thereby inhibits ERK-Mnk1-mediated phosphorylation of eIF4E (99) (Fig. 12). Indeed, several rocaglamide derivatives, *e.g.* rocaglamide (**1**), 1-*O*-acetylrocaglamide (**4**), and 3′-hydroxyaglafoline (**19**), have been shown to inhibit ERK phosphorylation (100). Interestingly, these compounds do not inhibit ERK activity in normal lymphocytes (100). It is well known that the Ras-ERK-Mnk1 and the PI3K-mTOR pathways are frequently over-activated in many types of cancers due to gain of function mutations. Also the eIF4E, eIF4G, and eIF4A expression or activities are up-regulated in many cancers (97). Thus, targeting translational pathways is one of the mechanisms by which rocaglamide derivatives exert their antitumor functions.

**4.3.3. Apoptosis Induction—**Induction of apoptosis is now known to be also an important mechanism of rocaglamide (**1**)-mediated anticancer activity. Apoptotic cell death can be triggered through two main pathways: the extrinsic (also termed receptor-mediated) and the intrinsic (also termed mitochondrial-mediated) pathway (Fig. 13). The extrinsic apoptotic pathway is initiated by binding of ligands (*e.g.* CD95L and TRAIL) to their specific death receptors on the cell surface, which leads to the formation of the death inducing signaling complex (DISC) containing the FAS-associated death domain adaptor protein FADD and pro-caspase-8. Activation of caspase-8 at the DISC leads to activation of the effector caspase, caspase-3, which cleaves a number of target death proteins such as poly (ADP-ribose) polymerase (PARP) leading to apoptosis (101). The intrinsic pathway is initiated by various stimuli that directly or indirectly activate the mitochondrial pathway by inducing the release of cytochrome c and the formation of the apoptosome complex with Apaf-1 and pro-caspase-9. Caspase-9 is then activated at the apoptosome and, subsequently,

activates pro-caspase-3 (102). Activated caspase-8 may induce cleavage of Bid, which links the extrinsic death pathway to the intrinsic death pathway by induction of the translocation of the proapoptotic Bcl-2 family proteins Bax and/or Bak to the mitochondrial membrane. One major negative regulator of receptor-mediated apoptosis is the cellular caspase-8 (FLICE)-inhibitory protein (c-FLIP), which blocks processing and activation of caspase-8 at the DISC level (101). In the intrinsic apoptosis pathway, death and life of cells are largely controlled by pro-apoptotic, *e.g.* Bax and Bak, and anti-apoptotic proteins, *e.g.* Bcl-2, Bcl-$X_L$, XIAP, and myeloid cell leukemia-1 (Mcl-1) (102).

The first observation that rocaglamide derivatives could induce apoptotic cell death in cancer cells was reported in 2002 (24). It was shown that a fraction of the human leukemic CEM T cells die by apoptosis after treatment with didesmethyl-rocaglamide (**15**). It was also shown that didesmethyl-rocaglamide (**15**) could enhance apoptotic cell death induced by other apoptotic stimuli such as TNF-α and cisplatin (24). Thereafter, silvestrol (**35**) was also reported to have a pronounced cytotoxic rather than cytostatic effect on the human prostate carcinoma LNCaP cells (103). It was shown that treatment of LNCaP cells with silvestrol (**35**) resulted in cytochrome c release and consequently activation of caspase-9. However, no caspase-3 and caspase-7 activation were detected although the apoptotic cell death induced by silvestrol (**35**) could be inhibited by a pan-caspase inhibitor, Boc-D-Fmk (103).

Solid evidence supporting rocaglamide derivatives as being potent apoptosis inducers was provided by the study of rocaglamide (**1**) and 1-*O*-acetylrocaglamide (**4**) in leukemic cells (100). In this investigation, rocaglamide (**1**) treatment was shown to induce depolarization of the mitochondrial membrane potential and to trigger caspase-mediated apoptosis involving caspase-9, -8, -3, and -2 in different leukemic cell lines, *e.g.* the human acute T cell leukemia Jurkat, the human T cell lymphoma Hut78, the EBV-transformed human B lymphoblast SKW, and also primary tumor cells freshly isolated from patients having acute myeloid (AML), acute lymphoblastic (ALL), and chronic myeloid (CML) leukemias. Interestingly, rocaglamide (**1**) showed no or very low toxicities to normal peripheral blood T and B lymphocytes and had also very little toxicity to human bone marrow stem cells (100). Investigation of the molecular mechanisms by which rocaglamide (**1**) and 1-*O*-acetylrocaglamide (**4**) killed tumors but not normal cells revealed that these compounds preferentially induce apoptosis in malignant cells by differential modulation of the activities of ERK, p38, and JNK. It has been shown that p38 is involved in mitochondria-mediated apoptosis by promoting mitochondrial translocation of the pro-apoptotic Bcl2 family protein Bax *via* inducing Bid cleavage (104, 105). The protein kinase p38 has been also linked to activation of the mitochondrial pathway by directly phosphorylating Bax (106), Bim (107), and Bcl-2 (108) and by down-regulation of Bad phosphorylation (109). Consistent with those studies, activation of p38 and JNK by rocaglamide (**1**) and 1-*O*-acetylro-caglamide (**4**) was shown to correlate with Bid cleavage (100).

Extensive studies in the past have established that ERK is an important survival factor and, particularly, ERK has been found to be constitutively activated in the majority of cancers. Thus, targeting the ERK pathway has been considered to be one of the important strategies in anticancer therapy (110). Rocaglamide (**1**) and 1-*O*-acetylrocaglamide (**4**) were shown to induce activation of p38 and JNK accompanied by a long-term suppression of ERK activity

(100). The critical role of p38/JNK and ERK in apoptosis induction in tumor cells was further demonstrated by the rocaglamide derivative 3′-hydroxylafoline (**19**), which differs from rocaglamide (**1**) and 1-*O*-acetylrocaglamide (**4**) only in having -OH at the C-3′ position. 3′-Hydroxylafoline (**19**) had a very weak effect on the activities of p38 and ERK in tumor cells and showed only a slight apoptosis induction. In addition, malignant cells that lost their ability to respond to rocaglamide-induced activation of p38/JNK or suppression of ERK were resistant to apoptosis induction by rocaglamide (110). Furthermore, rocaglamide (**1**) and 1-*O*-acetylrocaglamide (**4**) do not affect the activities of p38, JNK, and ERK in normal lymphocytes and therefore have no or only small effects on apoptosis induction in normal lymphocytes (100).

Inhibition of protein synthesis may affect expression levels of pro- and antiapoptotic proteins, in particular, those having a short half-life. Therefore, rocaglamide-mediated translational inhibition may cause imbalances of pro- and anti-apoptosis protein levels in a tumor cell. For instance, reduced expression of the anti-apoptotic proteins Mcl-1 and survivin were observed in human breast cancer MDA-MB-231 cells after exposure to silvestrol (**35**) (94). Also, down-regulation of c-FLIP, the major inhibitor of caspase-8, was detected in tumor cells treated with rocaglamide (**1**), desmethyl-rocaglamide (**7**), 1-*O*-acetylrocaglamide (**4**), and 1-oxo-11,12-methylendioxyrocaglamide (**50**) (21, 99). Expression of the c-FLIP proteins is controlled at multiple levels. The ERK and the PI3K signaling pathways have been shown to regulate c-FLIP expression (111–113). In addition, c-FLIP protein turnover is actively regulated by ubiquitin-mediated proteasomal degradation (114). Therefore, c-FLIP proteins are short-lived proteins and are required to be constitutively synthesized in tumor cells. As described before, rocaglamide derivatives can inhibit translation (Fig. 12). Inhibition of *de novo* protein synthesis will lead to down-regulation of the expression levels of short-lived anti-apoptotic proteins such as c-FLIP. This effect is well demonstrated by a recent study showing that 1-oxo-11,12-methylendioxyrocaglamide (**50**) inhibits expression of c-FLIP at the translational level by blocking the ERK signalling pathway and thereby breaks CD95 and TRAIL resistance in human T-cell leukemia virus type-1 (HTLV-1)-associated adult T-cell leukemia/lymphoma (ATL) (99) (Fig. 13). One can predict that 1-*O*-acetylrocaglamide (**4**), desmethyl-rocaglamide (**7**), 1-*O*-formylaglafoline (**23**), silvestrol (**35**), 4′-demethoxy-3′,4′-methylenedioxy-methyl rocaglate (**48**), and 1-oxo-11,12-methylendioxyrocaglamide (**50**) may be also capable of sensitizing receptor-mediated apoptosis by down-regulation of c-FLIP expression.

CD95L and its receptor CD95 are the most intensively studied apoptotic system of the extrinsic pathway (Fig. 13). A well-known phenomenon is that a fraction of T cells die after activation by a so called activation-induced-cell-death (AICD). AICD in T cells is mediated predominantly by CD95L and CD95 (101). CD95 is abundantly expressed in many types of cells. In contrast, expression of CD95L is more restricted to certain types of cells and predominantly expressed in activated T cells. In resting T cells, CD95L is expressed at an undetectable level and its expression is rapidly up-regulated upon T cell activation. Thus, the rate of CD95-mediated apoptosis is largely determined by the levels of CD95L expression. Expression of CD95L in activated T cells is regulated by multiple inducible transcription

factors such as NF-AT, NF-κB, and AP-1 (Fos/Jun) (115). However, expression of c-FLIP in T cells is also regulated by NF-κB and NF-AT (116, 117). Therefore, T cell activation leads not only to induction of CD95L but also c-FLIP expression. Up-regulation of c-FLIP expression during T cell activation correlates with resistance to CD95/CD95L-mediated apoptosis and rescue of T cells from AICD. Rocaglamide (**1**) and desmethyl-rocaglamide (**7**) were shown to enhance CD95L-mediated AICD in malignant T cells by up-regulation of CD95L but down-regulation of c-FLIP expression (21). As mentioned in Sect. 4.2., rocaglamide (**1**) and several derivatives, such as 1-*O*-acetylrocaglamide (**4**) and 1-oxo-11,12-methylendioxyrocaglaol (**50**), can enhance T-cell-activation-induced p38 and JNK activity and thereby suppress NF-AT activity by promoting NF-AT nuclear export (25). The CD95L promoter is strongly regulated by JNK/AP-1 (115). Increase of p38/JNK activity leads to increase of AP-1 activity and consequently enhanced CD95L promoter activity (21). In contrast, c-FLIP expression in T cells is strongly regulated by NF-AT (117). Rocaglamide-mediated suppression of NF-AT resulted in down-regulation of c-FLIP expression (21) (Fig. 13). These studies suggest that rocaglamide derivatives may serve as adjuvants for death receptor-based anticancer therapies in the future.

## 5. Chemical Synthesis of Cyclopenta[*b*]benzofurans

Rocaglamide (**1**) and congeners pose an intriguing synthetic chemistry challenge: multiple functionalities, a hepta-substituted cyclopenta[*b*]benzofuran scaffold, and five contiguous, stereogenic centers. The following syntheses, presented largely in chronological order, are significant because of the daring synthetic maneuvers employed, efficiency of the transformations, and development of asymmetric processes.

### 5.1. First Approaches to the Synthesis of Rocaglamides

Before (−)-rocaglamide was synthesized, there were two significant approaches published. In 1987, *Richard J. K. Taylor* and coworkers first accessed the tricyclic rocaglate core employing the benzofuranone intermediate **126** (Fig. 14) (118, 119). The rocaglate skeleton was subsequently assembled *via* an intramolecular, 1,3-dithianyl anion-carbonyl condensation. However, in this case the 1,3-dithiane group proved difficult to remove. Later syntheses, including *Taylor*'s total synthesis, have adapted the use of key intermediate **126** as starting material.

*Taylor*'s work towards the rocaglate skeleton was then followed by *Kraus* and coworkers' synthesis of the di-*epi*-analogue of rocaglamide (Fig. 15) (120). Like *Taylor*'s approach, the investigators began their synthesis with the known intermediate **126**. The first significant step in this synthesis is a *Michael* addition of acrylonitrile (**130**) with **126**. Next, a samarium-mediated reductive cyclization was performed to afford rocaglate skeleton **132**. Later in the synthesis, a cuprate addition was conducted on unsaturated thioester **133** to provide the enol intermediate **134**, which through X-ray crystal structure analysis was shown to be the *trans*-phenyl-aryl isomer. Accordingly, the cuprate had added unexpectedly to the concave face of the bicyclic ring system. Subsequent amidation and reduction of **134** yielded rocaglamide isomer **135** that did not possess the same NMR spectra as natural rocaglamide. Although the natural product was not synthesized, *Kraus* established two key steps (*Michael*

addition of acrylonitrile and the reductive cyclization using $SmI_2$) that paved the way for future investigations in the field.

### 5.2. The First Total Synthesis of Rocaglamide

The first total synthesis of rocaglamide (**1**) was accomplished by *Barry Trost* and coworkers in 1990 (Fig. 16) (52). Asymmetric [3 + 2] cycloaddition of trimethylsi-lylmethyl precursor **136** and chiral oxazepinedione **137** afforded cyclopentene **138**, a transformation which established the absolute configuration at $C_4$. Following removal of the chiral auxiliary and ozonolysis (*not shown*), cyclopentanone **139** was next condensed with dimethylphloroglucinol **140** to furnish intermediate **141**. Regioselective transesterification of **141** with benzyl alcohol was then performed that was followed by oxidative cyclization with DDQ to furnish intermediate **142**. With the rocaglate skeleton in hand, several reactions were performed to fully functionalized intermediate **142** and also invert stereochemistry at $C_3$. The synthesis was completed in 16 steps and fully established the absolute configuration of the natural product.

### 5.3. Syntheses of Rocaglamide and Related Natural Products

Shortly after the *Trost* synthesis, in 1991 *Taylor* and coworkers reported their synthesis of racemic rocaglamide (**1**) in eight steps from the benzofuran intermediate **126** (Fig. 17) (121). The key steps utilized were (1) *Michael* addition of *trans*-cinnamaldehyde (**144**) and benzofuran **126**; and (2) intramolecular, keto-aldehyde pinacolic coupling (reductive cyclization) mediated by $SmI_2$. This step afforded high diastereoselectivity (6:1) in construction of the rocaglate scaffold. Advanced intermediate **146** was then oxidized *via Swern* oxidation and was then transformed to a dimethylamide. The synthesis was completed with a hydroxy-directed, diastereo-selective reduction of the α-hydroxy ketone **149** using $NMe_4BH(OAc)_3$ to afford (±)-rocaglamide (**1**). In 1992, *Taylor* and coworkers published another synthesis of rocaglamide involving hydrolysis of the dithiane group used in his original approach (122). These syntheses by *Taylor* are a beautiful fusion of his original approach and the *Kraus* approach to the rocaglamide skeleton and are also frequently cited and used in later syntheses of rocaglamide and related natural products.

Inspired by the approaches of *Kraus*, *Taylor*, and *Trost*, *Takumi Watanabe* and coworkers achieved the racemic synthesis of aglaiastatin, a natural product related to rocaglamide (Fig. 18) (123). As the synthesis of ABC ring system had already been developed by *Taylor*, *Watanabe* began with advanced intermediate **150** (122). Carboxylic acid **150** was subsequently coupled with 4,4-diethoxybutanamine to form amide **151**. After the secondary alcohol was selectively oxidized, anhydrous HCl was used to form an acyl iminium species, in which case excess ammonium formate in formic acid served to form the enamine leading to cyclization with an iminium ion intermediate to afford (±)-aglaiastatin (**154**) (*dr* = 2:1).

In 2001, *Dobler* and coworkers reported a total synthesis of racemic rocaglamide using the *Michael* addition performed by *Taylor*. However, instead of using $SmI_2$, *Dobler* converted aldehyde **145** to a cyanohydrin intermediate in quantitative yield (Fig. 19) (124). Acyloin (**147**) was then initiated *via* addition of LDA, followed by deprotection with $K_2CO_3$, a marked improvement from preexisting methods. Additionally, *Stiles* carboxylation

following the keto-aldehyde acyloin ring closure made the synthesis more efficient than previously reported.

### 5.4. New Approaches to Rocaglamide and Related Natural Products

The year 2004 saw a new synthetic approach to rocaglamide and related natural products employing 3-hydroxyflavones, *Porco* and coworkers found that upon photoirradiation of 3-hydroxyflavones (*e.g.* intermediate **155**), an oxidopyrylium species derived from excited-state intramolecular proton transfer (ESIPT) could be trapped with a dipolarophile (*e.g.* *trans*-methyl cinnamate **156**) (Fig. 20) (125) resulting in an overall [3 + 2] photocycloaddition to afford aglain intermediate **157**. The approach may mimic the proposed biosynthesis of the rocaglamides (*cf.* *13*–15). Forbaglin natural products (**158**) were also accessed through oxidation of the aglain intermediate, while rocaglamide and related natural products such as methyl rocaglate were obtained through an α-ketol shift, followed by an hydroxyl-directed reduction of the α-hydroxy ketone **159**. The methodology was then used to synthesize (±)-methyl rocaglate (Fig. 21) (125). Photoirradiation of 3-hydroxyflavone (**161**) and methyl cinnamate (**156**) afforded the aglain (**162**) as well as a benzo[*b*]-cyclobutapyran-8-one (**163**), which were then subjected to basic conditions to provide α-ketol rearrangement product **148**. Hydroxyl-directed reduction of α-hydroxyketone **148** yielded racemic methyl rocaglate (**18**).

To further improve their methodology, *Porco* and coworkers developed an enantioselective [3 + 2] photocycloaddition that was then used to synthesize the natural enantiomer (−)-methyl rocaglate, (−)-rocaglamide, and (−)-rocaglaol (Fig. 22) (126). Using functionalized TADDOL (127) derivatives, chiral *Brønsted* acids to enhance excited state intramolecular proton transfer, asymmetry was successfully induced with an enantiomeric excess (*ee*) of 86% using the TADDOL **164**. Recrystallization of methyl rocaglate (**18**) enhanced the *ee* to 94%, with 86% recovery. (−)-Rocaglaol (**28**) was also obtained through decarboxylation followed by diastereoselective reduction of intermediate **148**. Likewise, (−)-rocaglamide (**1**) was synthesized from **148** through a reduction/saponification/amide coupling sequence.

The work of *Thede* and *Ragot* in 2004 and 2005 focused on the synthesis of rocaglaol and analogues. While *Taylor's* approach to rocaglate natural products was quite viable, access to very electron-rich benzofuranones derived from *Hoesch* or *Friedel Crafts* reactions was limited. Using methods for unsymmetrical 3,4-diaryl-cyclopent-2-enones (128), *Thede* and *Ragot* published an imaginative approach to the molecule, which was highlighted by intramolecular epoxide ring opening (Fig. 23) (129). Although the method did not afford the natural product, it did allow for preparation of 3-*epi*-rocaglaol (**170**) and analogues through variation of aryl boronic acids on the western portion of the molecule. In 2005, *Thede* and *Ragot* developed an alternative method to synthesize rocaglaol (**28**) and alteration of the benzofuran moiety to create rocaglaol analogues (Fig. 24) (130). This was achieved through the α-arylation of ketones using *Taylor*'s method to synthesize the skeleton. The α-arylation entailed *Suzuki*-type reaction of brominated silyl enol ethers with aryl boronic acids, allowing broad variation of the benzofuran moiety.

Control of stereochemistry of the adjacent phenyl and *para*-methoxyphenyl (PMP) groups is a difficulty frequently encountered in the synthesis of rocaglates and analogues. *Philip Magnus* and coworkers synthesized (±)-1,2-anhydro methyl rocaglate stereospecifically in which the stereocontrol was generated through an *Isler-Mukaiyama* aldol reaction (conrotatory *Nazarov* reaction) (Fig. 25) (131). The synthesis commenced with coupling of 2,4,6-trimethoxyiodobenzene with 4-methoxyphenylacetylene under *Sonogashira* coupling conditions to afford intermediate **171**. Next, an oxidation was carried out with catalytic ruthenium chloride/sodium periodate to provide dione **172**, which was then treated with boron trichloride to selectively demethylate and simultaneously form a hemiketal. The hemiketal was subsequently methylated using trimethoxymethane and sulfuric acid to afford benzofuranone (**173**). Benzofuranone (**173**) was then alkylated to give substrate **174**, which was then exposed to Amberlyst 15 ion-exchange resin to afford **175**. Treatment with base and TIPSCl produced the substrate used in the conrotatory *Nazarov* cyclization. Since the reaction is stereospecific, only *cis*-aryl-phenyl diastereomer **178** was formed. Using *Wilkinson*'s catalyst, **178** was hydrosilated to give **179**, which was then desilylated and trapped with *N*-phenyltriflamide. This intermediate was then subjected to *Ortar* reaction conditions to afford a methyl ester intermediate that was further oxidized to a *tert*-butyl peroxide and subsequently reduced to yield (±)-1,2-anhydro methyl rocaglate (**180**).

In 2008, *Qin* and coworkers reported the shortest synthesis of (±)-rocaglamide and its 2,3-di-*epi*-analogue to date (Fig. 26) (132). A methoxycarbonyl group was introduced into *Michael* acceptor **181**, thus making the synthesis immensely more efficient. Samarium (II)-mediated reductive cyclization afforded keto-methyl rocaglate (**148**) which was then converted to the amide **149** and reduced with tetramethy-lammonium triacetoxyborohydride to afford the natural product **1**.

The most recent synthesis of rocaglamide was accomplished by *Alison Frontier* and coworkers (Fig. 27) (133). Benzofuran (**126**) was first alkylated with vinyl magnesium bromide and then oxidized to form aldehyde **183**. Subsequent alkylation with phenylacetylene and protection of the propargyl alcohol afforded propargyl ether **184**. Next, **184** was deprotonated with *tert*-butyllithium and the resulting allenyl anion trapped with tri-*n*-butyltin chloride to afford stannyl alkoxyallene **185**. In a key step, the allenol ether was oxidized with *meta*-chloroperbenzoic acid (*m*-CPBA) forming an epoxide intermediate **186**, which opened to form the pentadienyl cation **187** necessary for the *Nazarov* cyclization under acidic conditions. Treatment of intermediate **188** with excess DDQ led to a production of a diosphenol intermediate, which was subsequently converted to a triflate, and the latter was then carbonylated to afford intermediate **189** and further advanced to racemic rocaglamide.

### 5.5. Syntheses of Silvestrol

The enantioselective synthesis of the complex rocaglate silvestrol was reported by *Porco* and coworkers in 2007 (Fig. 28) (134). Through a convergent strategy, the rocaglate intermediate **191** and dioxanyloxy fragment **193** were connected and subsequently deprotected to form the natural product. Methoxy methyl ether protected 3-hydroxyflavone **190** was photo-excited to its oxidopyrylium tautomer and then trapped with methyl

cinnamate (**156**) mediated by TADDOL (**164**). After a ketol rearrangement/hydroxyl directed reduction sequence, the resulting cyclopenta[*b*,*c*]benzofuran intermediate was deprotected using TMSBr to remove the methoxymethyl ether (MOM), which afforded rocaglate intermediate **191** in 87% *ee* after recrystallization. Intermediate **192** was used to form an *O*-stannylene acetal, which was then combined with 2-bromo-2-methoxy acetate to afford a dioxanylone intermediate. Reduction of the dixoanylone intermediate with diisobutylaluminum hydride (DIBAL-H) afforded the dioxanyloxy fragment **193**. Using *Mitsunobu* conditions, fragments **191** and **193** were successfully coupled. Finally, hydrogenation of the coupled product gave (−)-silvestrol (**35**).

*Rizzacasa* and coworkers synthesized *epi*-silvestrol and silvestrol in a convergent fashion employing a method similar to their published pilot studies (135). Their plan was to connect the 1,4-dioxanyloxy fragment **199** with the cyclopenta-benzofuran **191** core *via Mitsunobu*-type coupling to access *epi*-silvestrol (**36**), which was subsequently converted to silvestrol (**35**) using a *Mitsunobu* reaction (Fig. 29) (136). The synthesis of the 1,4-dioxanyloxy fragment **199** commenced with glycosylation of bromide **194** using *para*-methoxybenzyl alcohol, followed by removal of the acetates *via* methanolysis. Subsequent benzylidene formation afforded acetal **195**, which was treated with $BH_3$·THF and $Cu(OTf)_2$ to selectively cleave the benzylidene and afforded the protected sugar **196**. Periodate cleavage, followed by selective reduction of the newly formed aldehydelactol, yielded the lactol as a 1:3 mixture of anomers. The resultant lactol was then selectively protected at the primary alcohol to afford TBS ether **197**, which was then methylated with high selectivity to provide axial product **198**. DDQ was then used to remove the *para*-methoxybenzyl protecting group to afford the 1,4-dioxanyloxy fragment **199**. Racemic rocaglate core **191** was synthesized using the methods developed by *Porco* and coworkers, which was then coupled with optically pure fragment **199** to afford two major axial diastereomers in equal amounts, and two equatorial diastereomers in equal amounts (2:1 ratio axial:equatorial products) in 35% overall yield. The diastereomers were then deprotected to afford (−)-*epi*-silvestrol (**36**). (−)-Silvestrol (**35**) was then achieved through a selective "double *Mitsunobu*" reaction of (−)-*epi*-silvestrol (**36**). Future studies by *Rizzacasa* and coworkers disclosed a method to resolve racemic **191** using (−)-menthol, as well as an improved *Mitsunobu* coupling of **191** and **199** using (di-2-methoxyethyl azodicarboxylate) (137).

Aside from their complexity and synthetic challenge, silvestrol and *epi*-silvestrol displayed potent anticancer activity in A549 lung cancer proliferation assays with $IC_{50}$ values of 33 n*M* and 30 n*M* (137). The synthetic analogue 4′-desmethoxy-*epi*-silvestrol was also found to be highly potent against LIM1215 colon cancer cells proliferation with an $IC_{50}$ of 10 n*M*, foreshadowing the development of cytotoxic flavagline analogues that are more potent than their parent counterparts.

### 5.6. Development of Rocaglates and Analogues as Therapeutic Agents

Recently, *Laurent De´saubry* and coworkers discovered the first synthetic rocaglamide-type compound that inhibits cell proliferation and viability at lower doses than the parent compound, rocaglaol (**28**) (Fig. 30) (138). Using *Dobler*'s procedure for the preparation of rocaglamides, the synthesis of racemic rocaglaol (**28**) and rocaglaol derivatives **202**, **203**,

and **204** were achieved. These compounds were tested on a variety of human cancer cell lines. In all cases, brominated rocaglaol **203** was the most potent, having $IC_{50}$ values lower than 1 n*M* for KB (nasopharynx), MCF7R (breast), HCT116 (colon), and HL60 (neutrophil) human cancer cell lines. No aryl substituents manifested a decrease in potency, while rocaglaol derivative **204** was highly inactive (methoxy group on the other aryl ring). Fluorescent probe **208** was synthesized from an amide coupling between fluorescent coumarin intermediate **207** and rocagloic acid intermediate **206**. The synthesis of affinity ligand **214** was initiated by amide coupling between fragments **210** and **211** to afford azide **212**, which was converted to amine **213** using $SnCl_2$ and benzene thiol. Then, **213** was conjugated to Affi-Gel 10 to afford the affinity ligand **214** used in pull down experiments that did not reveal any interaction between **214** and eukaryotic initiation factor 4A (eiF4A). Fluorescent probe **208** was shown to accumulate in the endoplasmic reticulum (ER), implying that rocaglamides bind to their target in the ER, inducing the death of cancer cells *via* activation of the AIF and caspase-12 pathways.

*Porco* and coworkers, using optimized reaction conditions and sequences, displayed the broad scope of their photocycloaddition methodology in the syntheses of rocaglate analogues (Fig. 31) (139). Using a variety of dipolarophiles, novel cycloadducts were obtained including thioester **216b**, *Weinreb* amide **216e**, and amide **216f**. The aglain intermediates were then converted to cyclopenta[*b*,*c*]-benzofurans using two methods. Cycloadducts bearing a methyl ester moiety were readily converted into rocaglate isomers, but in many cases a *Lewis* acid-catalyzed method was found to be necessary. When 25 compounds were tested for *in vitro* potency as inhibitors of eukaryotic translation, six compounds had $IC_{50}$ values lower than 10 μ*M*. Compounds **217e** and **217f** were found to be the most potent with $IC_{50}$ values of 300–400 n*M*. The positive control, silvestrol, had an $IC_{50}$ of 100 n*M* in the same assay, demonstrating excellent potency from the synthetic analogues. When tested *in vivo*, hydroxamate **217e** was the most potent, inhibiting 85% of protein synthesis over the course of an hour, similar to silvestrol.

With knowledge that bromine substituted at the C-4′ position improves cancer cell cytotoxicity, *Désaubry* and coworkers studied structure activity relationships (SAR) when C-1 and C-2 substituents are varied, and how the C-8 methoxy affected activity. The rocaglamide core was constructed through [3 + 2] photocycloaddition, followed by acyloin rearrangement (Fig. 32) (140). Compound **218** was prepared by decarboxylation and subsequent reduction. Methyl rocaglate analogues **220a-220c** were tested, and from **220a** and **220b**, amide analogues **219a** and **219b** were achieved through nucleophilic displacement using ammonia. Compounds **221a** and **221b** were prepared from **220a** and **220b** by KOH hydrolysis followed by amide coupling. Using modified 3-hydroxyflavone **205** and cinnamic amide **222**, synthetic rocaglamide **223** was efficiently prepared using a [3 + 2] photocycloaddition, ketol rearrangement, and subsequent reduction. With the C-2 analogues in hand, C-1 analogues were constructed from α-hydroxyketone **224** (Fig. 33) (140). Reduction with $Me_4NBH(OAc)_3$ afforded rocaglaol analogue **225**, which was esterified to afford analogues **226**, **227**, and **228**. When **224** was treated with sodium borohydride, *Désaubry* observed opposite selectivity from $Me_4NBH(OAc)_3$, forming *cis*-diol **229**, which was esterified to afford **230**. Oxime methyl ether **231** was reduced using

$BH_3$ to give two diasteromers **232** and **233**, which were then acylated to give corresponding esters and sulfonic esters.

An SAR investigation tested cytotoxic activity of these novel analogues against a variety of human cancer cell lines, and found that 8-demethoxy compounds **218**, **219b**, **220b**, **220c**, and **223** were less active than their 8-methoxy counterparts, suggesting a preference of a methoxy group for cytotoxicity. It was also determined that having an amide or ester substituent at C-2 was detrimental for activity against HL60R cells, suggesting a detriment to multidrug resistance as well. Although configuration of the hydroxy at C-1 was not crucial for activity, formamide analogue **237** had better activity in comparison to diastereomer **234**. Compound **237** also proved to be the best therapeutic candidate from *in vitro* studies. *In vivo* studies were then performed on mice with xenografted 3LL tumors using **237**, and reduced the growth of the tumor by 65% without any visible toxicity in the mice.

## 6. Concluding Remarks

The present review surveys and summarizes the rocaglamides (= flavaglines) and related derivatives isolated from the genus *Aglaia* (family Meliaceae). Both the unique unprecedented chemical skeleton and the interesting pharmacological properties of rocaglamides have attracted the attention of natural product chemists, cell biologists, and pharmacologists alike. The overwhelming research interests placed on the genus *Aglaia* have led to the isolation of more than 120 congeners since the first report of the prototype compound, rocaglamide (**1**), in 1982 by King *et al*. (11).

In addition to their insecticidal activity, rocaglamide derivatives revealed several other bioactivities of interest, such as anti-inflammatory, *in vitro* and *in vivo* antiproliferative, and apoptosis induction activities. While rocaglamides are unlikely to be developed into a commercial insecticide, their anti-tumor and apoptosis induction activities make them potential oncology drug candidates.

## Acknowledgments

Preparation of this chapter was supported by a grant of BMBF (to *P.P.*). A scholarship granted and financed by the Egyptian government (predoctoral fellowship for *S.S.E.*) is gratefully acknowledged.

## References

1. Newman DJ, Cragg GM, Snader KM. The Influence of Natural Products upon Drug Discovery. Nat Prod Rep. 2000; 17:215. [PubMed: 10888010]
2. Chin Y-W, Balunas MJ, Chai HB, Kinghorn AD. Drug Discovery from Natural Sources. AAPS J. 2006; 8:e239. [PubMed: 16796374]
3. Butler MS. Natural Products to Drugs: Natural Product-Derived Compounds in Clinical Trials. Nat Prod Rep. 2008; 25:475. [PubMed: 18497896]
4. Altmann K-H, Höfle G, Müller R, Mulzer J, Prantz K. The Epothilones: an Outstanding Family of Anti-Tumor Agents – From Soil to the Clinic. Prog Chem Org Nat Prod. 2009; 90:1.
5. Balunas MJ, Jones WP, Chin Y-W, Mi Q, Farnsworth NR, Soejarto DD, Cordell GA, Swanson SM, Pezzuto JM, Chai H-B, Kinghorn AD. Relationships between Inhibitory Activity against a Cancer

Cell Line Panel, Profiles of Plants Collected, and Compound Classes Isolated in an Anticancer Drug Discovery Project. Chem Biodiversity. 2006; 3:897.

6. Isman, MB.; Gunning, PJ.; Spollen, KM. Tropical Timber Species as Sources of Botanical Insecticides. In: Hedin, PA.; Hollingworth, RM.; Masler, EP.; Miyamoto, J.; Thompson, DG., editors. Phytochemicals for Pest Control, Symposium Series 658. ACS Books; Washington, DC: 1997. p. 27
7. Pannell, CM. Aglaia. In: Soepadmo, E.; Saw, LG.; Chung, RCK.; Kiew, R., editors. Tree Flora of Sabah and Sarawak. Ampang Press Sdn Bhd; Kuala Lumpur: 2007. p. 24
8. Muellner AN, Samuel R, Chase MW, Pannell CM, Greger H. *Aglaia* (Meliaceae): An Evaluation of Taxonomic Concepts Based on DNA Data and Secondary Metabolites. Am J Bot. 2005; 92:534. [PubMed: 21652432]
9. Proksch P, Edrada RA, Ebel R, Bohnenstengel FI, Nugroho BW. Chemistry and Biological Activity of Rocaglamide Derivatives and Related Compounds in *Aglaia* species (Meliaceae). Curr Org Chem. 2001; 5:923.
10. Janaki S, Vijayasekaran V, Viswanathan S, Balakrishna K. Anti-Inflammatory Activity of *Aglaia roxburghiana* var. *beddomei* Extract and Triterpenes Roxburghiadiol A and B. J Ethnopharmacol. 1999; 67:45. and references cited therein. [PubMed: 10616959]
11. King ML, Chiang C-C, Ling H-C, Fujita E, Ochiai M, McPhail AT. X-Ray Crystal Structure of Rocaglamide, a Novel Antileukemic 1*H*-Cyclopenta[*b*]benzofuran from *Aglaia elliptifolia*. J Chem Soc Chem Commun. 1982:1150.
12. Kim S, Salim AA, Swanson SM, Kinghorn AD. Potential of Cyclopenta[*b*]benzofurans from *Aglaia* Species in Cancer Chemotherapy. Anticancer Agents Med Chem. 2006; 6:319. [PubMed: 16842234]
13. Brader G, Vajrodaya S, Greger H, Bacher M, Kalchhauser H, Hofer O. Bisamides, Lignans, Triterpenes, and Insecticidal Cyclopenta[*b*]benzofurans from *Aglaia* Species. J Nat Prod. 1998; 61:1482. [PubMed: 9868148]
14. Nugroho BW, Edrada RA, Wray V, Witte L, Bringmann G, Gehling M, Proksch P. An Insecticidal Rocaglamide Derivative and Related Compounds from *Aglaia odorata* (Meliaceae). Phytochemistry. 1999; 51:367.
15. Bacher M, Hofer O, Brader G, Vajrodaya S, Greger H. Thapsakins: Possible Biogenetic Intermediates towards Insecticidal Cyclopenta[*b*]benzofurans from *Aglaia edulis*. Phytochemistry. 1999; 52:253.
16. Dreyer M, Nugroho BW, Bohnenstengel FI, Ebel R, Wray V, Witte L, Bringmann G, Mühlbacher J, Herold M, Hung PD, Kiet LC, Proksch P. New Insecticidal Rocaglamide Derivatives and Related Compounds from *Aglaia oligophylla*. J Nat Prod. 2001; 64:415. [PubMed: 11325219]
17. Schneider C, Bohnenstengel FI, Nugroho BW, Wray V, Witte L, Hung PD, Kiet LC, Proksch P. Insecticidal Rocaglamide Derivatives from *Aglaia spectabilis* (Meliaceae). Phytochemistry. 2000; 54:731. [PubMed: 11014256]
18. Greger H, Pacher T, Brem B, Bacher M, Hofer O. Insecticidal Flavaglines and Other Compounds from Fijian *Aglaia* Species. Phytochemistry. 2001; 57:57. [PubMed: 11336261]
19. Hayashi N, Lee K-H, Hall IH, McPhail AT, Huang H-C. Structure and Stereochemistry of (−)-Odorinol, an Antileukemic Diamide from *Aglaia odorata*. Phytochemistry. 1982; 21:2371.
20. Cui B, Chai H, Santisuk T, Reutrakul V, Farnsworth NR, Cordell GA, Pezzuto JM, Kinghorn AD. Novel Cytotoxic 1*H*-Cyclopenta[*b*]benzofuran Lignans from *Aglaia elliptica*. Tetrahedron. 1997; 53:17625.
21. Zhu JY, Giaisi M, Köhler R, Müller WW, Mühleisen A, Proksch P, Krammer PH, Li-Weber M. Rocaglamide Sensitizes Leukemic T Cells to Activation-Induced Cell Death by Differential Regulation of CD95L and c-FLIP Expression. Cell Death Differen. 2009; 16:1289.
22. Saifah E, Suttisri R, Shamsub S, Pengsuparp T, Lipipum V. Bisamides from *Aglaia edulis*. Phytochemistry. 1999; 52:1085. [PubMed: 10643670]
23. Engelmeier D, Hadacek F, Pacher T, Vajrodaya S, Greger H. Cyclopenta[*b*] benzofurans from *Aglaia* Species with Pronounced Antifungal Activity against Rice Blast Fungus (*Pyricularia grisea*). J Agric Food Chem. 2000; 48:1400. [PubMed: 10775404]

24. Baumann B, Bohnenstengel F, Siegmund D, Wajant H, Weber C, Herr I, Debatin K-M, Proksch P, Wirth T. Rocaglamide Derivatives are Potent Inhibitors of NF-κB Activation in T-Cells. J Biol Chem. 2002; 277:44791. [PubMed: 12237314]
25. Proksch P, Giaisi M, Treiber MK, Palfi K, Merling A, Spring H, Krammer PH, Li-Weber M. Rocaglamide Derivatives are Immunosuppressive Phytochemicals that Target NF-AT Activity in T cells. J Immunol. 2005; 174:7075. [PubMed: 15905551]
26. Greger H, Pacher T, Vajrodaya S, Bacher M, Hofer O. Infraspecific Variation of Sulfur-Containing Bisamides from *Aglaia leptantha*. J Nat Prod. 2000; 63:616. [PubMed: 10843571]
27. Wang B-G, Ebel R, Nugroho BW, Prijono D, Frank W, Steube KG, Hao X-J, Proksch P. Aglacins A–D, First Representatives of a New Class of Aryltetralin Cyclic Ether Lignans from *Aglaia cordata*. J Nat Prod. 2001; 64:1521. [PubMed: 11754603]
28. Wang B-G, Ebel R, Wang C-Y, Wray V, Proksch P. New Methoxylated Aryltetrahydronaphthalene Lignans and a Norlignan from *Aglaia cordata*. Tetrahedron Lett. 2002; 43:5783.
29. Wang B-G, Ebel R, Wang C-Y, Edrada RA, Wray V, Proksch P. Aglacins I–K, Three Highly Methoxylated Lignans from *Aglaia cordata*. J Nat Prod. 2004; 67:682. [PubMed: 15104504]
30. Saifah E, Puripattanavong J, Likhitwitayawuid K, Cordell GA, Chai H, Pezzuto JM. Bisamides from *Aglaia* Species: Structure Analysis and Potential to Reverse Drug Resistance with Cultured Cells. J Nat Prod. 1993; 56:473. [PubMed: 8496701]
31. Saifah E, Suparakchinda N. Bisamide from *Aglaia rubiginosa*. Planta Med. 1998; 64:682. [PubMed: 17253314]
32. Inada A, Shono K, Murata H, Inatomi Y, Darnaedi D, Nakanishi T. Three Putrescine Bisamides from the Leaves of *Aglaia grandis*. Phytochemistry. 2000; 53:1091. [PubMed: 10820837]
33. Seger C, Pacher T, Greger H, Saifah E, Hofer O. Aglairubine: Structure Revision of a Chemotaxonomically Interesting Bisamide in *Aglaia* (Meliaceae). Monatsh Chem. 2002; 133:97.
34. Duong TN, Edrada RA, Ebel R, Wray V, Frank W, Duong AT, Lin WH, Proksch P. Putrescine Bisamides from *Aglaia gigantea*. J Nat Prod. 2007; 70:1640. [PubMed: 17880174]
35. Greger H, Hofer M, Teichmann K, Schinnerl J, Pannell CM, Vajrodaya S, Hofer O. Amide-Esters from *Aglaia tenuicaulis* – First Representatives of a Class of Compounds Structurally Related to Bisamides and Flavaglines. Phytochemistry. 2008; 69:928. [PubMed: 18155259]
36. Puripattanavong J, Weber S, Brecht V, Frahm AW. Phytochemical Investigation of *Aglaia andramanica*. Planta Med. 2000; 66:740. [PubMed: 11199132]
37. Mohamad K, Martin M-T, Leroy E, Tempête C, Sévenet T, Awang K, Païs M. Argenteanones C–E and Argenteanols B–E, Cytotoxic Cycloartanes from *Aglaia argentea*. J Nat Prod. 1997; 60:81. [PubMed: 9051908]
38. Roux D, Martin M-T, Adeline M-T, Sevenet T, Hadi AHA, Païs. Foveolins A and B, Dammarane Triterpenes from *Aglaia foveolata*. Phytochemistry. 1998; 49:1745. [PubMed: 11711093]
39. Mohamad K, Sévenet T, Dumontet V, Païs M, Tri MV, Hadi H, Awang K, Martin M-T. Dammarane Triterpenes and Pregnane Steroids from *Aglaia lawii* and *A. tomentosa*. Phytochemistry. 1999; 51:1031.
40. Mohamad K, Martin M-T, Najdar H, Gaspard C, Sévenet T, Awang K, Hadi H, Païs M. Cytotoxic 3,4-Secoapotirucallanes from *Aglaia argentea* Bark. J Nat Prod. 1999; 62:868. [PubMed: 10395505]
41. Weber S, Puripattanavong J, Brecht V, Frahm AW. Phytochemical Investigation of *Aglaia rubiginosa*. J Nat Prod. 2000; 63:636. [PubMed: 10843575]
42. Rivero-Cruz JF, Chai H-B, Kardono LBS, Setyowati FM, Afriastini JJ, Riswan S, Farnsworth NR, Cordell GA, Pezzuto JM, Swanson SM, Kinghorn AD. Cytotoxic Constituents of the Twigs and Leaves of *Aglaia rubiginosa*. J Nat Prod. 2004; 67:343. [PubMed: 15043407]
43. Cai X-H, Luo X-D, Zhou J, Hao X-J. Dolabellane Diterpenoids from the Higher Plant *Aglaia odorata*. Helv Chim Acta. 2005; 88:2938.
44. Su B-N, Chai H, Mi Q, Riswan S, Kardono LBS, Afriastini JJ, Santarsiero BD, Mesecar AD, Farnsworth NR, Cordell GA, Swanson SM, Kinghorn AD. Activity-Guided Isolation of Cytotoxic Constituents from the Bark of *Aglaia crassinervia* Collected in Indonesia. Bioorg Med Chem. 2006; 14:960. [PubMed: 16216518]

45. Xie B-J, Yang S-P, Chen H-D, Yue J-M. Agladupols A–E, Triterpenoids from *Aglaia duperreana*. J Nat Prod. 2007; 70:1532. [PubMed: 17711345]
46. Joycharat N, Greger H, Hofer O, Saifah E. Flavaglines and Triterpenoids from the Leaves of *Aglaia forbesii*. Phytochemistry. 2008; 69:206. [PubMed: 17707871]
47. Joycharat N, Greger H, Hofer O, Saifah E. Flavaglines and Triterpenes as Chemical Markers of *Aglaia oligophylla*. Biochem Syst Ecol. 2008; 36:584.
48. Pointinger S, Promdang S, Vajrodaya S, Pannell CM, Hofer O, Mereiter K, Greger H. Silvaglins and Related 2,3-Secodammarane Derivatives – Unusual Types of Triterpenes from *Aglaia silvestris*. Phytochemistry. 2008; 69:2696. [PubMed: 18930298]
49. Seger C, Pointinger S, Greger H, Hofer O. Isoeichlerianic Acid from *Aglaia silvestris* and Revision of the Stereochemistry of Foveolin B. Tetrahedron Lett. 2008; 49:4313.
50. Hofer O, Pointinger S, Brecker L, Peter K, Greger H. Silvaglenamin – A Novel Dimeric Triterpene Alkaloid from *Aglaia silvestris*. Tetrahedron Lett. 2009; 50:467.
51. Cai X-H, Wang Y-Y, Zhao P-J, Li Y, Luo X-D. Dolabellane Diterpenoids from *Aglaia odorata*. Phytochemistry. 2010; 71:1020. [PubMed: 20338601]
52. Trost BM, Greenspan PD, Yang BV, Saulnier MG. An Unusual Oxidative Cyclization. A Synthesis and Absolute Stereochemical Assignment of (−)-Rocaglamide. J Am Chem Soc. 1990; 112:9022.
53. Ishibashi F, Satasook C, Isman MB, Towers GHN. Insecticidal 1*H*-Cyclopentate-trahydro[*b*]benzofurans from *Aglaia odorata*. Phytochemistry. 1993; 32:307.
54. Nugroho BW, Güssregen B, Wray V, Witte L, Bringmann G, Proksch P. Insecticidal Rocaglamide Derivatives from *Aglaia elliptica* and *A. harmsiana*. Phytochemistry. 1997; 45:1579.
55. Nugroho BW, Edrada RA, Güssregen B, Wray V, Witte L, Proksch P. Insecticidal Rocaglamide Derivatives from *Aglaia duperreana*. Phytochemistry. 1997; 44:1455.
56. Chaidir, Hiort J, Nugroho BW, Bohnenstengel FI, Wray V, Witte L, Hung PD, Kiet LC, Sumaryono W, Proksch P. New Insecticidal Rocaglamide Derivatives from Flowers of *Aglaia duperreana* (Meliaceae). Phytochemistry. 1999; 52:837.
57. Molleyres L-P, Rindlisbacher A, Winkler T, Kumar V. Insecticidal Natural Products: New Rocaglamide Derivatives from *Aglaia roxburghiana*. Pestic Sci. 1999; 55:494.
58. Hiort J, Chaidir, Bohnenstengel FI, Nugroho BW, Schneider C, Wray V, Witte L, Hung PD, Kiet LC, Proksch P. New Insecticidal Rocaglamide Derivatives from the Roots of *Aglaia duperreana*. J Nat Prod. 1999; 62:1632.
59. Güssregen B, Fuhr M, Nugroho BW, Wray V, Witte L, Proksch P. New Insecticidal Rocaglamide Derivatives from Flowers of *Aglaia odorata*. J Biosci (Z Naturforsch). 1997; 52c:339.
60. Dumontet V, Thoison O, Omobuwajo OR, Martin M-T, Perromat G, Chiaroni A, Riche C, Païs M, Sévenet T, Hadi AHA. New Nitrogenous and Aromatic Derivatives from *Aglaia argentea* and *A. forbesii*. Tetrahedron. 1996; 52:6931.
61. Fuzzati N, Dyatmiko W, Rahman Abdul, Achmad F, Hostettman K. Triterpenoids, Lignans and a Benzofuran Derivative from the Bark of *Aglaia elaeagnoidea*. Phytochemistry. 1996; 42:1395.
62. Ko F-N, Wu T-S, Liou M-J, Huang T-F, Teng C-M. PAF Antagonism In Vitro and In Vivo by Aglafoline from *Aglaia elliptifolia* Merr. Eur J Pharmacol. 1992; 218:129. [PubMed: 1327822]
63. Wang S-K, Cheng Y-J, Duh C-Y. Cytotoxic Constituents from Leaves of *Aglaia elliptifolia*. J Nat Prod. 2001; 64:92. [PubMed: 11170675]
64. Chaidir, Lin WH, Ebel R, Edrada RA, Wray V, Nimtz M, Sumaryono W, Proksch P. Rocaglamides, Glycosides, and Putrescine Bisamides from *Aglaia dasyclada*. J Nat Prod. 2001; 64:1216. [PubMed: 11575959]
65. Mulholland DA, Naidoo N. A Revision of the Structure of Ferrugin from *Aglaia ferruginaea*. Phytochemistry. 1998; 47:1163.
66. Dean FM, Monkhe TV, Mulholland DA, Taylor DAH. An Isoflavanoid from *Aglaia ferruginaea*, an Australian Member of the Meliaceae. Phytochemistry. 1993; 34:1537.
67. Xu Y-J, Wu X-H, Tan BKH, Lai Y-H, Vittal JJ, Imiyabir Z, Madani L, Khozirah KS, Goh SH. Flavonol–Cinnamate Cycloadducts and Diamide Derivatives from *Aglaia laxiflora*. J Nat Prod. 2000; 63:473. [PubMed: 10785416]

68. Hwang BY, Su B-N, Chai H, Mi Q, Kardono LB, Afriastini JJ, Riswan S, Santarsiero BD, Mesecar AD, Wild R, Fairchild CR, Vite GD, Rose WC, Farnsworth NR, Cordell GA, Pezzuto JM, Swanson SM, Kinghorn AD. Silvestrol and Episilvestrol, Potential Anticancer Rocaglate Derivatives from *Aglaia silvestris*. J Org Chem. 2004; 69:3350. [PubMed: 15132542]
69. Hwang BY, Su B-N, Chai H, Mi Q, Kardono LB, Afriastini JJ, Riswan S, Santarsiero BD, Mesecar AD, Wild R, Fairchild CR, Vite GD, Rose WC, Farnsworth NR, Cordell GA, Pezzuto JM, Swanson SM, Kinghorn AD. Silvestrol and Episilvestrol, Potential Anticancer Rocaglate Derivatives from *Aglaia silvestris*. J Org Chem. 2004; 69:6156.
70. Chumkaew P, Kato S, Chantrapromma K. Potent Cytotoxic Rocaglamide Derivatives from the Fruits of *Amoora cucullata*. Chem Pharm Bull. 2006; 54:1344. [PubMed: 16946551]
71. Kim S, Chin Y-W, Su B-N, Riswan S, Kardono LBS, Afriastini JJ, Chai H, Farnsworth NR, Cordell GA, Swanson SM, Kinghorn AD. Cytotoxic Flavaglines and Bisamides from *Aglaia edulis*. J Nat Prod. 2006; 69:1769. [PubMed: 17190457]
72. Kokpol U, Venaskulchai B, Simpson J, Weavers RT. Isolation and X-ray Structure Determination of a Novel Pyrimidinone from *Aglaia odorata*. J Chem Soc Chem Commun. 1994; (6):773.
73. Ohse T, Ohba S, Yamamoto T, Koyano T, Umezawa K. Cyclopentabenzofuran Lignan Protein Synthesis Inhibitors from *Aglaia odorata*. J Nat Prod. 1996; 59:650. [PubMed: 8759160]
74. Wang S-K, Duh C-Y. Cytotoxic Cyclopenta[*b*]benzofuran Derivatives from the Stem Bark of *Aglaia formosana*. Planta Med. 2001; 67:555. [PubMed: 11509980]
75. Bringmann G, Mühlbacher J, Messer K, Dreyer M, Ebel R, Nugroho BW, Wray V, Proksch P. Cyclorocaglamide, the First Bridged Cyclopentatetrahydro-benzofuran, and a Related "Open Chain" Rocaglamide Derivative from *Aglaia oligophylla*. J Nat Prod. 2003; 66:80. [PubMed: 12542350]
76. Shiengthong D, Ungphakorn A, Lewis DE, Massy-Westropp RA. New Nitrogenous Compounds – Odorine and Odorinol. Tetrahedron Lett. 1979; 24:2247.
77. Purushothaman KK, Sarada A, Connolly JD, Akinniyi JA. The Structure of Roxburghilin, a Bis-amide of 2-Aminopyrrolidine from the Leaves of *Aglaia roxburghiana* (Meliaceae). J Chem Soc Perkin Trans I. 1979:3171.
78. Saifah E, Jongbunprasert V, Kelley CJ. Piriferine, a New Pyrrolidine Alkaloid from *Aglaia pirifera* leaves. J Nat Prod. 1988; 51:80.
79. Inada A, Sorano T, Murata H, Inatomi Y, Darnaedi D, Nakanishi T. Diamide Derivatives and Cycloartanes from the Leaves of *Aglaia elliptica*. Chem Pharm Bull. 2001; 49:1226. [PubMed: 11558621]
80. Salim AA, Pawlus AD, Chai H-B, Farnsworth NR, Kinghorn AD, Carcache-Blanco EJ. Ponapensin, a Cyclopenta[*bc*]benzopyran with Potent NF-κB Inhibitory Activity from *Aglaia ponapensis*. Bioorg Med Chem Lett. 2007; 17:109. [PubMed: 17055270]
81. Salim AA, Chai H-B, Rachman I, Riswan S, Kardono LBS, Farnsworth NR, Carcache-Blanco EJ, Kinghorn AD. Constituents of the Leaves and Stem Bark of *Aglaia foveolata*. Tetrahedron. 2007; 63:7926. [PubMed: 18698338]
82. Kim S, Su B-N, Riswan S, Kardono LBS, Afriastini JJ, Gallucci JC, Chai H, Farnsworth NR, Cordell GA, Swanson SM, Kinghorn AD. Edulisones A and B, Two Epimeric Benzo-[*b*]oxepine Derivatives from the Bark of *Aglaia edulis*. Tetrahedron Lett. 2005; 46:9021.
83. Chiu SF. Recent Research Findings on Meliaceae and Other Promising Botanical Insecticides in China. J Plant Diseases and Protection. 1985; 92:310.
84. Bohnenstengel FI, Steube KG, Meyer C, Nugroho BW, Hung PD, Kiet LC, Proksch P. Structure Activity Relationships of Antiproliferative Rocaglamide Derivatives from *Aglaia* species (Meliaceae). J Biosci (Z Naturforsch). 1999; 54c:55.
85. Bohnenstengel FI, Steube KG, Meyer C, Quentmeier H, Nugroho BW, Proksch P. 1 *H*-Cyclopenta[*b*]benzofuran Lignans from *Aglaia* species Inhibit Cell Proliferation and Alter Cell Cycle Distribution in Human Monocytic Leukemia Cell Lines. J Biosci (Z Naturforsch). 1999; 54c:1075.
86. Ewete F, Nicol RW, Hengsawad V, Sukumalanand P, Satasook C, Wiriyachitra P, Isman MB, Kahn Y, Duval F, Philogène BJR, Arnason JT. Insecticidal Activity of *Aglaia odorata* Extract and

the Active Principle, Rocaglamide, to the European Corn Borer *Ostrinia nubilalis* Hübn. (Lep., Pyralidae). J Appl Ent. 1996; 120:483.

87. Koul O, Kaur H, Goomber S, Wahab S. Bioefficacy and Mode of Action of Rocaglamide from *Aglaia elaeagnoidea* (syn. *A. roxburghiana*) against Gram Pod Borer, *Helicoverpa armigera* (Hübner). J Appl Ent. 2004; 128:177.
88. O'Shea JJ, Ma A, Lipsky P. Cytokines and Autoimmunity. Nat Rev Immunol. 2002; 2:37. [PubMed: 11905836]
89. Li-Weber M, Krammer PH. Regulation of IL4 Gene Expression by T Cells and Therapeutic Perspectives. Nat Rev Immunol. 2003; 3:534. [PubMed: 12876556]
90. Yamamoto Y, Gaynor RB. Therapeutic Potential of Inhibition of the NF-kappaB Pathway in the Treatment of Inflammation and Cancer. J Clin Invest. 2001; 107:135. [PubMed: 11160126]
91. Macian F. NFAT Proteins: Key Regulators of T-Cell Development and Function. Nat Rev Immunol. 2005; 5:472. [PubMed: 15928679]
92. Li Q, Verma IM. NF-kappaB Regulation in the Immune System. Nat Rev Immunol. 2002; 2:725. [PubMed: 12360211]
93. Lee SK, Cui B, Mehta RR, Kinghorn AD, Pezzuto JM. Cytostatic Mechanism and Antitumor Potential of Novel 1*H*-Cyclopenta[*b*]benzofuran Lignans Isolated From *Aglaia elliptica*. Chem Biol Interact. 1998; 115:215. [PubMed: 9851291]
94. Cencic R, Carrier M, Galicia-Vázquez G, Bordeleau ME, Sukarieh R, Bourdeau A, Brem B, Teodoro JG, Greger H, Tremblay ML, Porco JA Jr, Pelletier J. Antitumor Activity and Mechanism of Action of the Cyclopenta[*b*]benzofuran, Silvestrol. PLoS One. 2009; 4:e5223. [PubMed: 19401772]
95. Hausott B, Greger H, Marian B. Flavaglines: a Group of Efficient Growth Inhibitors Block Cell Cycle Progression and Induce Apoptosis in Colorectal Cancer Cells. Int J Cancer. 2004; 109:933. [PubMed: 15027128]
96. Mi Q, Kim S, Hwang BY, Su BN, Chai H, Arbieva ZH, Kinghorn AD, Swanson SM. Silvestrol Regulates G2/M Checkpoint Genes Independent of p53 Activity. Anticancer Res. 2006; 26:3349. [PubMed: 17094452]
97. Silvera D, Formenti SC, Schneider RJ. Translational Control in Cancer. Nat Rev Cancer. 2010; 10:254. [PubMed: 20332778]
98. Bordeleau ME, Robert F, Gerard B, Lindqvist L, Chen SM, Wendel HG, Brem B, Greger H, Lowe SW, Porco JA Jr, Pelletier J. Therapeutic Suppression of Translation Initiation Modulates Chemosensitivity in a Mouse Lymphoma Model. J Clin Invest. 2008; 8:2651. [PubMed: 18551192]
99. Bleumink M, Köhler R, Giaisi M, Proksch P, Krammer PH, Li-Weber M. Rocaglamide Breaks TRAIL Resistance in HTLV-1-associated Adult T-cell Leukemia/Lymphoma by Translational Suppression of c-FLIP Expression. Cell Death Differ. 2011; 18:362. [PubMed: 20706274]
100. Zhu JY, Lavrik IN, Mahlknecht U, Giaisi M, Proksch P, Krammer PH, Li-Weber M. The Traditional Chinese Herbal Compound Rocaglamide Preferentially Induces Apoptosis in Leukemia Cells by Modulation of Mitogen-Activated Protein Kinase Activities. Int J Cancer. 2007; 121:1839. [PubMed: 17565740]
101. Krammer PH, Arnold R, Lavrik IN. Life and Death in Peripheral T Cells. Nat Rev Immunol. 2007; 7:532. [PubMed: 17589543]
102. Galluzzi L, Larochette N, Zamzami N, Kroemer G. Mitochondria as Therapeutic Targets for Cancer Chemotherapy. Oncogene. 2006; 25:4812. [PubMed: 16892093]
103. Kim S, Hwang BY, Su BN, Chai H, Mi Q, Kinghorn AD, Wild R, Swanson SM. Silvestrol, a Potential Anticancer Rocaglate Derivative from *Aglaia foveolata*, Induces Apoptosis in LNCaP Cells Through the Mitochondrial/Apoptosome Pathway Without Activation of Executioner Caspase-3 or −7. Anticancer Res. 2007; 27:2175. [PubMed: 17695501]
104. Zhuang S, Demirs JT, Kochevar IE. p38 Mitogen-Activated Protein Kinase Mediates bid Cleavage, Mitochondrial Dysfunction, and Caspase-3 Activation During Apoptosis Induced by Singlet Oxygen but not by Hydrogen Peroxide. J Biol Chem. 2000; 275:25939. [PubMed: 10837470]

105. Yoshino T, Kishi H, Nagata T, Tsukada K, Saito S, Muraguchi A. Differential Involvement of p38 MAP Kinase Pathway and Bax Translocation in the Mitochondria-Mediated Cell Death in TCR- and Dexamethasone-Stimulated Thymocytes. Eur J Immunol. 2001; 31:2702. [PubMed: 11536168]
106. Kim BJ, Ryu SW, Song BJ. JNK- and p38 Kinase-Mediated Phosphorylation of Bax Leads to Its Activation and Mitochondrial Translocation and to Apoptosis of Human Hepatoma HepG2 Cells. J Biol Chem. 2006; 281:21256. [PubMed: 16709574]
107. Cai B, Chang SH, Becker EB, Bonni A, Xia Z. p38 MAP Kinase Mediates Apoptosis Through Phosphorylation of BimEL at Ser-65. J Biol Chem. 2006; 281:25215. [PubMed: 16818494]
108. De Chiara G, Marcocci ME, Torcia M, Lucibello M, Rosini P, Bonini P, Higashimoto Y, Damonte G, Armirotti A, Amodei S, Palamara AT, Russo T, Garaci E, Cozzolino F. Bcl-2 Phosphorylation by p38 MAPK: Identification of Target Sites and Biologic Consequences. J Biol Chem. 2006; 281:21353. [PubMed: 16714293]
109. Grethe S, Coltella N, Di Renzo MF, Porn-Ares MI. p38 MAPK Downregulates Phosphorylation of Bad in Doxorubicin-Induced Endothelial Apoptosis. Biochem Biophys Res Commun. 2006; 347:781. [PubMed: 16843435]
110. Balmanno K, Cook SJ. Tumour Cell Survival Signalling by the ERK1/2 Pathway. Cell Death Differ. 2009; 16:368. [PubMed: 18846109]
111. Yeh JH, Hsu SC, Han SH, Lai MZ. Mitogen-Activated Protein Kinase Kinase Antagonized fas-Associated Death Domain Protein-Mediated Apoptosis by Induced FLICE-Inhibitory Protein Expression. J Exp Med. 1998; 188:1795. [PubMed: 9815257]
112. Wang W, Prince CZ, Mou Y, Pollman MJ. Notch3 Signaling in Vascular Smooth Muscle Cells Induces c-FLIP Expression via ERK/MAPK Activation. Resistance to Fas ligand-Induced Apoptosis. J Biol Chem. 2002; 277:21723. [PubMed: 11925448]
113. Panka DJ, Mano T, Suhara T, Walsh K, Mier JW. Phosphatidylinositol 3-Kinase/Akt Activity Regulates c-FLIP Expression in Tumor Cells. J Biol Chem. 2001; 276:6893. [PubMed: 11145953]
114. Poukkula M, Kaunisto A, Hietakangas V, Denessiouk K, Katajamäki T, Johnson MS, Sistonen L, Eriksson JE. Rapid Turnover of c-FLIPshort is Determined by its Unique C-Terminal Tail. J Biol Chem. 2005; 280:27345. [PubMed: 15886205]
115. Li-Weber M, Krammer PH. Function and Regulation of the CD95 (APO-1/Fas) Ligand in the Immune System. Semin Immunol. 2003; 15:145. [PubMed: 14563113]
116. Kreuz S, Siegmund D, Scheurich P, Wajant H. NF-kappaB Inducers Upregulate cFLIP, a Cycloheximide-Sensitive Inhibitor of Death Receptor Signaling. Mol Cell Biol. 2001; 21:3964. [PubMed: 11359904]
117. Ueffing N, Schuster M, Keil E, Schulze-Osthoff K, Schmitz I. Up-regulation of c-FLIP short by NFAT Contributes to Apoptosis Resistance of Short-Term Activated T Cells. Blood. 2008; 112:690. [PubMed: 18509086]
118. Katamna C. Synthesis of 2-Arylbenzofuran-3-ones. Bull Soc Chim Fr. 1970; 6:2309.
119. Davey AE, Taylor RJK. A Novel 1,3-Dithiane-based Cyclopenta-annulation Procedure: Synthesis of the Rocaglamide Skeleton. J Chem Soc, Chem Commun. 1987; 1:25.
120. Kraus GA, Sy JO. A Synthetic Approach to Rocaglamide via Reductive Cyclization of δ-Keto Nitriles. J Org Chem. 1989; 54:77.
121. Davey AE, Schaeffer MJ, Taylor RJK. Synthesis of the Novel Antileukemic Tetrahydrocyclopenta[*b*]benzofuran, Rocaglamide. J Chem Soc, Chem Commun. 1991; 16:1137.
122. Davey AE, Schaeffer MJ, Taylor RJK. Synthesis of the Novel Anti-leukemic Tetrahydrocyclopenta[*b*]benzofuran, Rocaglamide and Related Synthetic Studies. J Chem Soc, Perkin Trans 1. 1992; 20:2657.
123. Watanabe T, Takeuchi T, Kohzuma S, Umezawa K, Otsuka M. Total Synthesis of (±)-Aglaiastatin, a Novel Bioactive Alkaloid. Chem Commun. 1998; 10:1097.
124. Dobler MR, Bruce I, Cederbaum F, Cooke NG, Diorazio LJ, Hall RG, Irving E. Total Synthesis of (±)-Rocaglamide and Some Aryl Analogues. Tetrahedron Lett. 2001; 42:8281.

125. Gerard B, Jones G, Porco JA. A Biomimetic Approach to the Rocaglamides Employing Photogeneration of Oxidopyryliums Derived from 3-Hdroxyflavones. J Am Chem Soc. 2004; 126:13620. [PubMed: 15493911]
126. Gerard B, Sangji S, O'Leary DJ, Porco JA. Enantioselective Photocycloaddition Mediated by Chiral Brnsted Acids: Asymmetric Synthesis of the Rocaglamides. J Am Chem Soc. 2006; 128:7754. [PubMed: 16771486]
127. McDougal NT, Schaus SE. Asymmetric Morita-Baylis-Hillman Reactions Catalyzed by Chiral Brnsted Acids. J Am Chem Soc. 2003; 125:12094. [PubMed: 14518986]
128. Schoop A, Helmut G, Axel G. A New Analogue of Rocaglamide by an Oxidative Dihydrofuran Synthesis. Tetrahedron Lett. 2000; 41:1913.
129. Thede K, Diedrichs N, Ragot JP. Stereoselective Synthesis of (±)-Rocaglaol Analogues. Org Lett. 2004; 6:4595. [PubMed: 15548084]
130. Diedrichs N, Ragot JP, Thede K. A Highly Efficient Synthesis of Rocaglaols by a Novel α-Arylation of Ketones. Eur J Org Chem. 2005; 9:1731.
131. Magnus P, Stent MAH. Stereospecific Synthesis of (±)-1,2-Anhydro Methyl Rocaglate. Org Lett. 2005; 7:3853. [PubMed: 16119915]
132. Li H, Fu B, Wang MA, Li N, Liu WJ, Xie ZQ, Ma YQ, Qin Z. Total Synthesis and Biological Activity of (±)-Rocaglamide and its 2,3-Di-*epi* Analogue. Eur J Org Chem. 2008; 10:1753.
133. Malona JA, Cariou K, Frontier JA. Nazarov Cyclization Initiated by Peracid Oxidation: the Total Synthesis of (±)-Rocaglamide. J Am Chem Soc. 2009; 131:7560. [PubMed: 19445456]
134. Gerard B, Cencic R, Pelletier J, Porco JA. Enantioselective Synthesis of the Complex Rocaglate (−)-Silvestrol. Angew Chem Int Ed. 2007; 46:7831.
135. El Sous M, Rizzacasa MA. Biomimetic Synthesis of the Novel 1,4-Dioxanyloxy Fragment of Silvestrol and Episilvestrol. Tetrahedron Lett. 2005; 46:293.
136. El Sous M, Khoo M, Holloway G, Owen DJ, Scammells PJ, Rizzacasa MA. Total Synthesis of (−)-Episilvestrol and (−)-Silvestrol. Angew Chem Int Ed. 2007; 46:7835.
137. Adams TE, El Sous M, Hawkins BC, Hirner S, Holloway G, Khoo ML, Owen DJ, Savage GP, Scammells PJ, Rizzacasa MA. Total Synthesis of the Potent Anticancer *Aglaia* Metabolites (−)-Silvestrol and (−)-Episilvestrol and the Active Analogue (−)-4′-Desmethoxyepisilvestrol. J Am Chem Soc. 2009; 131:1607. [PubMed: 19140688]
138. Thuaud F, Bernard Y, Turkeri G, Dirr R, Aubert G, Cresteil T, Baguet A, Tomasetto C, Svitkin Y, Sonenberg N, Nebigil CG, Désaubry L. Synthetic Analogue of Rocaglaol Displays a Potent and Selective Cytotoxicity in Cancer Cells: Involvement of Apoptosis Inducing Factor and Caspase-12. J Med Chem. 2009; 52:5176. [PubMed: 19655762]
139. Roche SP, Cencic R, Pelletier J, Porco JA. Biomimetic Photocycloaddition of 3-Hydroxyflavones: Synthesis and Evaluation of Rocaglate Derivatives as Inhibitors of Eukaryotic Translation. Angew Chem Int Ed. 2010; 49:6533.
140. Thuaud F, Ribeiro N, Gaiddon C, Cresteil T, Désaubry L. Novel Flavaglines Displaying Improved Cytotoxicity. J Med Chem. 2011; 54:411. [PubMed: 21142180]

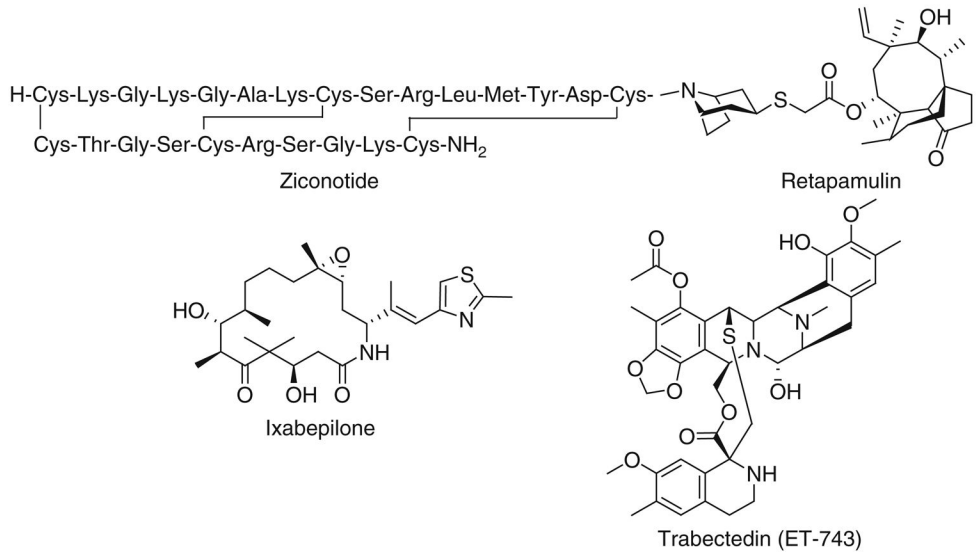


**Fig. 1.**

Chemical structures of ziconotide, ixabepilone, retapamulin, and trabectedin (ET-743)

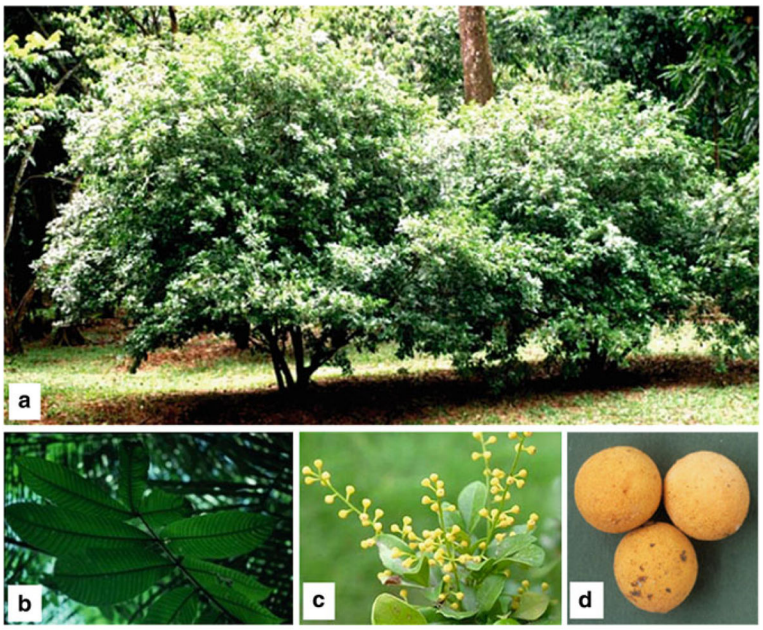


**Fig. 2.**

*Aglaia* Lour. (family Meliaceae). (a): Entire tree of *Aglaia odorata*, (b): leaves of *A. tomentosa*, (c): flowers of *A. odorata*, (d): fruits of *A. forbesi*i (photos by Dr. *B. W. Nugroho* and from http://dps.plants.ox.ac.uk/bol/aglaia and http://www.rareflora.com/aglaiaodo.html)

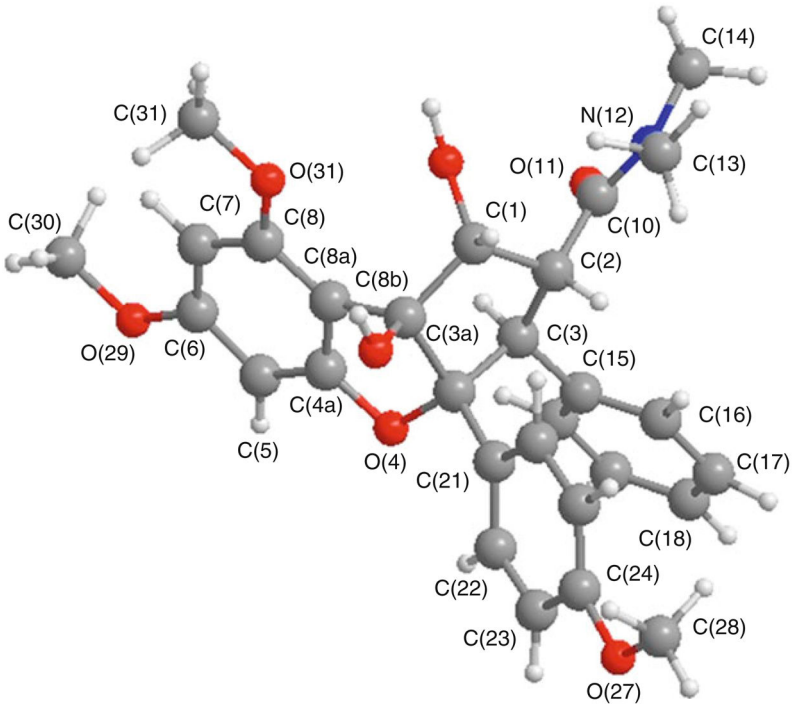


**Fig. 3.**
X-ray crystal structure of rocaglamide (**1**) (11)

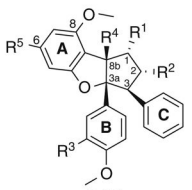

**1-38**

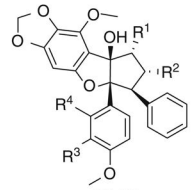

**39-47**

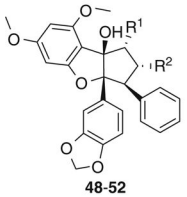

**48-52**

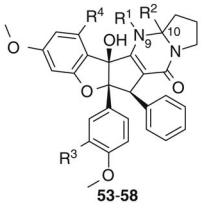

**53-58**

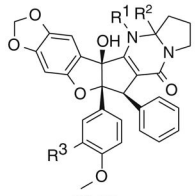

**59-62**

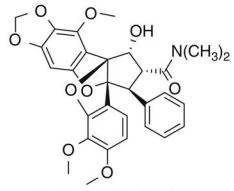

Cyclorocaglamide (**63**)

| Cpd. | Trivial Name | $R^1$ | $R^2$ | $R^3$ | $R^4$ | $R^5$ | Ref. |
|---|---|---|---|---|---|---|---|
| **1** | Rocaglamide | OH | $CON(CH_3)_2$ | H | OH | $OCH_3$ | (*11*, *60*) |
| **2** | | OH | $CON(CH_3)_2$ | OH | OH | $OCH_3$ | (*55*) |
| **3** | Aglaroxin E | OH | $CON(CH_3)_2$ | $OCH_3$ | OH | $OCH_3$ | (*55*, *57*) |
| **4** | 1-*O*-Acetylrocaglamide | $OCOCH_3$ | $CON(CH_3)_2$ | H | OH | $OCH_3$ | (*58*) |
| **5** | | $OCOCH_3$ | $CON(CH_3)_2$ | OH | OH | $OCH_3$ | (*55*) |
| **6** | | OH | $CON(CH_3)_2$ | OH | $OC_2H_5$ | $OCH_3$ | (*56*) |
| **7** | Desmethyl-rocaglamide | OH | $CONHCH_3$ | H | OH | $OCH_3$ | (*53*, *60*) |
| **8** | | OH | $CONHCH_3$ | OH | OH | $OCH_3$ | (*14*) |
| **9** | | $OCOCH_3$ | $CONHCH_3$ | H | OH | $OCH_3$ | (*58*) |
| **10** | | $OCOCH_3$ | $CONHCH_3$ | OH | OH | $OCH_3$ | (*59*) |
| **11** | | OH | $CONHCH_3$ | OH | $OC_2H_5$ | $OCH_3$ | (*56*) |
| **12** | *N*,*N*-Didesmethyl-*N*-4-hydroxybutyl-rocaglamide | OH | $CONH(CH_2)_4OH$ | H | OH | $OCH_3$ | (*54*) |
| **13** | | $OCOCH_3$ | $CONH(CH_2)_4OH$ | H | OH | $OCH_3$ | (*54*) |
| **14** | | OH | Ring[1] | H | OH | $OCH_3$ | (*54*) |
| **15** | Didesmethyl-rocaglamide | OH | $CONH_2$ | H | OH | $OCH_3$ | (*60*) |
| **16** | | OH | $CONH_2$ | OH | OH | $OCH_3$ | (*59*) |
| **17** | | $OCOCH_3$ | $CONH_2$ | H | OH | $OCH_3$ | (*56*) |
| **18** | Methyl rocaglate (Aglafoline) | OH | $COOCH_3$ | H | OH | $OCH_3$ | (*53*, *60–62*) |

| Cpd. | Trivial Name | $R^1$ | $R^2$ | $R^3$ | $R^4$ | $R^5$ | Ref. |
|---|---|---|---|---|---|---|---|
| **19** | 3'-Hydroxyaglafoline | OH | $COOCH_3$ | OH | OH | $OCH_3$ | (*14*) |
| **20** | | OH | $COOCH_3$ | $OCH_3$ | OH | $OCH_3$ | (*17*) |
| **21** | | $OCOCH_3$ | $COOCH_3$ | H | OH | $OCH_3$ | (*56*) |
| **22** | | $OCOCH_3$ | $COOCH_3$ | OH | OH | $OCH_3$ | (*59*) |
| **23** | 1-*O*-Formylaglafoline | OCHO | $COOCH_3$ | H | OH | $OCH_3$ | (*17*) |
| **24** | | OCHO | $COOCH_3$ | OH | OH | $OCH_3$ | (*17*) |
| **25** | | =NOH | $COOCH_3$ | $OCH_3$ | OH | $OCH_3$ | (*14*) |
| **26** | | OH | $COOCH_3$ | H | $OCH_3$ | $OCH_3$ | (*58*) |
| **27** | Rocagloic acid | OH | COOH | H | OH | $OCH_3$ | (*63*) |
| **28** | Rocaglaol (Aglaiastatin A) | OH | H | H | OH | $OCH_3$ | (*53*, *60*, *65*) |
| **29** | | OH | H | $OCH_3$ | OH | $OCH_3$ | (*59*) |
| **30** | | OH | H | $Sugar^2$ | OH | $OCH_3$ | (*54*) |
| **31** | | OH | H | $Sugar^3$ | OH | $OCH_3$ | (*67*) |
| **32** | | OH | H | H | $OC_2H_5$ | $OCH_3$ | (*60*) |
| **33** | | OH | H | H | $OCH_3$ | $OCH_3$ | (*58*) |
| **34** | 1-*O*-Acetylrocaglaol | $OCOCH_3$ | H | H | OH | $OCH_3$ | (*42*) |
| **35** | Silvestrol (5'''*R*) | OH | $COOCH_3$ | H | OH | $Ring^4$ | (*68*) |
| **36** | Episilvestrol (5'''*S*) | OH | $COOCH_3$ | H | OH | $Ring^4$ | (*68*) |
| **37** | 1-*O*-Formylrocagloic acid | OCHO | COOH | H | OH | $OCH_3$ | (*70*) |
| **38** | 3'-Hydroxyrocagloic acid | H | COOH | OH | OH | $OCH_3$ | (*70*) |
| **39** | Aglaroxin A | OH | $CON(CH_3)_2$ | H | H | - | (*16*, *57*) |
| **40** | Aglaroxin B | OH | $CON(CH_3)_2$ | $OCH_3$ | H | - | (*57*, *71*) |
| **41** | Aglaroxin F | OH | $CON(CH_3)_2$ | $OCH_3$ | OH | - | (*57*) |
| **42** | Aglaroxin A 1-*O*-acetate | $OCOCH_3$ | $CON(CH_3)_2$ | H | H | - | (*72*) |
| **43** | 1-*O*-Acetyl-3'-methoxyaglaroxin A | $OCOCH_3$ | $CON(CH_3)_2$ | $OCH_3$ | H | - | (*72*) |
| **44** | Pannellin | OH | $COOCH_3$ | H | H | - | (*13*, *71*) |
| **45** | 1-*O*-Acetylpannellin | $OCOCH_3$ | $COOCH_3$ | H | H | - | (*13*) |
| **46** | 3'-Methoxypannellin | OH | $COOCH_3$ | $OCH_3$ | H | - | (*13*) |
| **47** | Isothapsakon A | =O | $Chain^5$ | H | H | - | (*71*) |
| **48** | 4'-Demethoxy-3',4'-methylenedioxy-methyl rocaglate | OH | $COOCH_3$ | - | - | - | (*20*) |
| **49** | | OH | H | - | - | - | (*20*) |
| **50** | 1-Oxo-11,12-methylendioxyrocaglaol | =O | H | - | - | - | (*20*) |
| **51** | | OCHO | $COOCH_3$ | - | - | - | (*20*) |
| **52** | | $OCOCH_3$ | $COOCH_3$ | - | - | - | (*17*) |
| **53** | | $\Delta^{9,10}$ | | H | - | - | (*73*) |
| **54** | | $\Delta^{9,10}$ | | OH | - | - | (*56*) |
| **55** | Algaroxin D (Aglaiastatin) | H | H | H | - | - | (*54*, *57*, *74*) |
| **56** | Marikarin | $\Delta^{9,10}$ | | H | OH | - | (*18*) |
| **57** | 3'-Hydroxymarikarin | $\Delta^{9,10}$ | | OH | OH | - | (*18*) |
| **58** | Aglaiformosanin | $\Delta^{9,10}$ | | $OCH_3$ | $OCH_3$ | - | (*75*) |
| **59** | Algaroxin C | $\Delta^{9,10}$ | | H | - | - | (*57*) |
| **60** | Algaroxin G | $\Delta^{9,10}$ | | $OCH_3$ | - | - | (*57*) |
| **61** | Algaroxin H | H | H | $OCH_3$ | - | - | (*57*) |
| **62** | Algaroxin I | H | H | H | - | - | (*57*) |

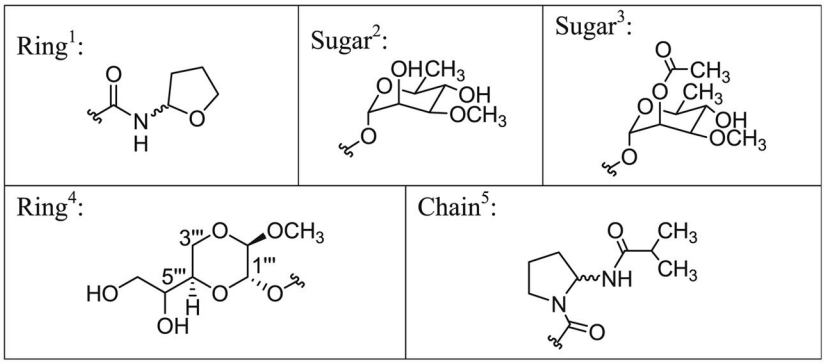

**Fig. 4.**

Rocaglamide derivatives isolated from *Aglaia* species

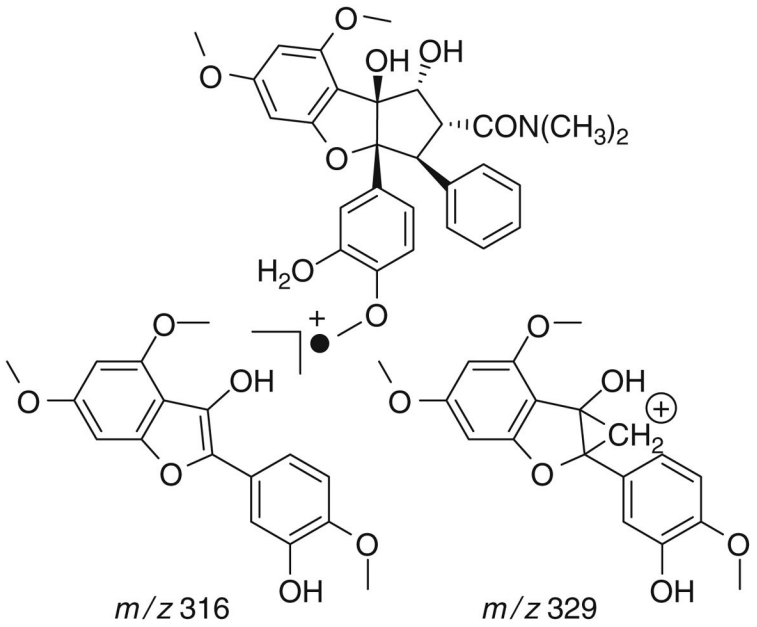


**Fig. 5.**
Plausible structures of fragment ions *m/z* 316 and 329 of compound **2** under EI–MS

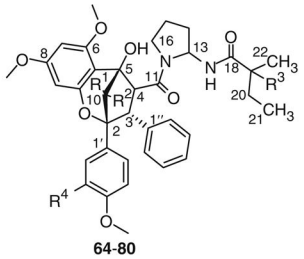

**64-80**

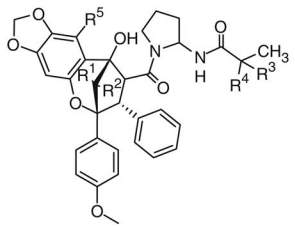

**81-89**

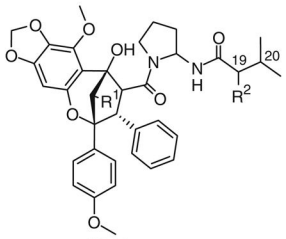

**90-92**

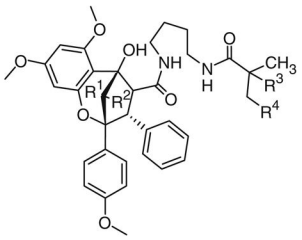

**93, 94**

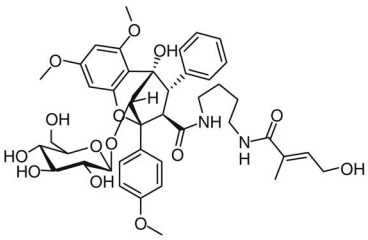

**95**

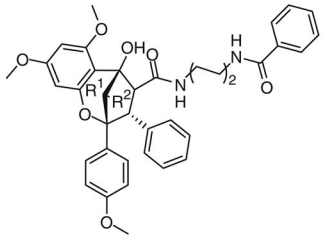

**96-100**

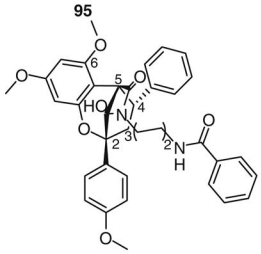

Cyclofoveoglin (**101**)

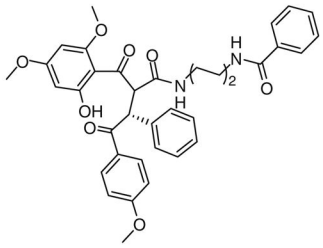

Secofoveoglin (**102**)

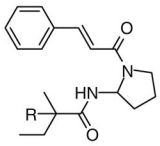

R = H: Odorine (**103**)
R = OH: Odorinol (**104**)

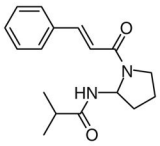

Piriferine (**105**)

| Cpd. | Trivial Name | $R^1$ | $R^2$ | $R^3$ | $R^4$ | $R^5$ | H-3, H-4 | Ref. |
|---|---|---|---|---|---|---|---|---|
| **64** | Aglain A | $OCOCH_3$ | H | H | H | - | *β,α* | (*60*) |
| **65** | 4-Epiaglain A | $OCOCH_3$ | H | H | H | - | *β,β* | (*80*) |
| **66** | Desacetylaglain A | OH | H | H | H | - | *β,α* | (*18*) |
| **67** | Aglain B | H | OH | H | H | - | *β,α* | (*60*) |
| **68** | 10-*O*-Acetylaglain B | H | $OCOCH_3$ | H | H | - | *β,α* | (*80*) |
| **69** | Aglain C | H | OH | H | H | - | *α,β* | (*60*) |
| **70** | | H | OH | H | OH | - | *α,β* | (*14*) |
| **71** | | H | OH | OH | OH | - | *α,β* | (*14*) |
| **72** | | H | OH | OH | $OCH_3$ | - | *α,β* | (*14*) |
| **73** | | H | OH | H | OH | - | *β,α* | (*14*) |
| **74** | Aglaxiflorin A | $OCOCH_3$ | H | OH | H | - | *β,α* | (*67*) |
| **75** | Aglaxiflorin B | $OCOCH_3$ | H | OH | H | - | *α,β* | (*67*) |
| **76** | Aglaxiflorin D | H | OH | OH | H | - | *α,β* | (*67*) |
| **77** | Elliptifoline | H | OH | $\Delta^{19,20}$ | H | - | *α,β* | (*63*) |
| **78** | Aglaroxin J | H | $OCOCH_3$ | H | H | - | *α,β* | (*57*) |
| **79** | Aglaroxin L | H | OH | OH | H | - | *α,β* | (*57*) |
| **80** | | H | OH | OH | H | - | *β,α* | (*57*) |
| **81** | | H | OH | OH | $C_2H_5$ | H | *β,α* | (*57*) |
| **82** | | H | $OCOCH_3$ | H | $C_2H_5$ | H | *β,α* | (*57*) |
| **83** | (13*S*)-Thapsakin B | H | OH | H | $CH_3$ | $OCH_3$ | *β,α* | (*15*) |
| **84** | (13*R*)-Thapsakin B | H | OH | H | $CH_3$ | $OCH_3$ | *β,α* | (*15*) |
| **85** | Isothapsakin B | OH | H | H | $CH_3$ | $OCH_3$ | *β,α* | (*15*) |
| **86** | Homothapsakin A | H | OH | H | $C_2H_5$ | $OCH_3$ | *α,β* | (*15*) |
| **87** | 10-*O*-Acetylthapsakin A | H | $OCOCH_3$ | H | $CH_3$ | $OCH_3$ | *α,β* | (*15*) |
| **88** | Thapsakon A | =O | | H | $CH_3$ | $OCH_3$ | *α,β* | (*15*) |
| **89** | Thapsakon B | =O | | H | $CH_3$ | $OCH_3$ | *β,α* | (*15*) |
| **90** | Edulirin A | OH | H | - | - | - | *β,α* | (*72*) |
| **91** | 10-*O*-Acetyledulirin A | $OCOCH_3$ | H | - | - | - | *β,α* | (*72*) |
| **92** | 19,20-Dehydroedulirin A | OH | $\Delta^{19,20}$ | - | - | - | *β,α* | (*72*) |
| **93** | Grandiamide A | $OCOCH_3$ | H | $\Delta^{19,20}$ | $CH_3$ | - | *α,β* | (*89*) |
| **94** | | *O*-glc | H | $\Delta^{19,20}$ | $CH_2OH$ | - | *α,β* | (*75*) |
| **96** | Pyrimidaglain A | H | $OCOCH_3$ | - | - | - | *β,α* | (*36*) |
| **97** | Pyrimidaglain B | $OCOCH_3$ | H | - | - | - | *α α* | (*36*) |
| **98** | Desacetylpyrimidaglain A | H | OH | - | - | - | *α,β* | (*46*) |
| **99** | Desacetylpyrimidaglain C | OH | H | - | - | - | *α,β* | (*46*) |
| **100** | Desacetylpyrimidaglain D | H | OH | - | - | - | *β,α* | (*46*) |

**Fig. 6.**
Aglain derivatives isolated from *Aglaia* species

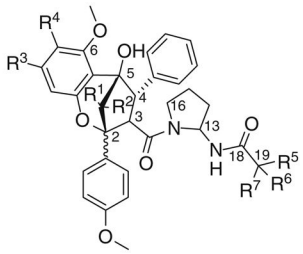

106-111

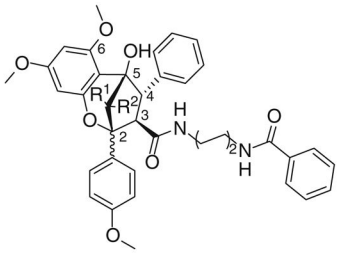

112, 113

| Cpd. | Trivial Name | $R^1$ | $R^2$ | $R^3$ | $R^4$ | $R^5$ | $R^6$ | $R^7$ | H-3, H-4 | Ref. |
|---|---|---|---|---|---|---|---|---|---|---|
| **106** | Aglaforbesin A | OH | H | $OCH_3$ | H | $C_2H_5$ | H | $CH_3$ | *α,β* | (*60*) |
| **107** | Aglaforbesin B | H | OH | $OCH_3$ | H | $C_2H_5$ | H | $CH_3$ | *α,β* | (*60*) |
| **108** | Aglaxiflorin C | H | $OCOCH_3$ | $OCH_3$ | H | $C_2H_5$ | OH | $CH_3$ | *α,β* | (*67*) |
| **109** | | H | OH | $-OCH_2O-$ | | $CH_3$ | H | $CH_3$ | *β,α* | (*71*) |
| **110** | Isoedulirin A | H | OH | $-OCH_2O-$ | | H | H | $CH(CH_3)_2$ | *α,β* | (*72*) |
| **111** | Edulirin B | H | OH | $-OCH_2O-$ | | H | H | $CH(CH_3)_2$ | *β,α* | (*72*) |
| **112** | Foveoglin A | OH | H | - | - | - | - | - | *α,β* | (*82*) |
| **113** | Foveoglin B | H | OH | - | - | - | - | - | *α,β* | (*82*) |

**Fig. 7.**

Aglaforbesin derivatives isolated from *Aglaia* species

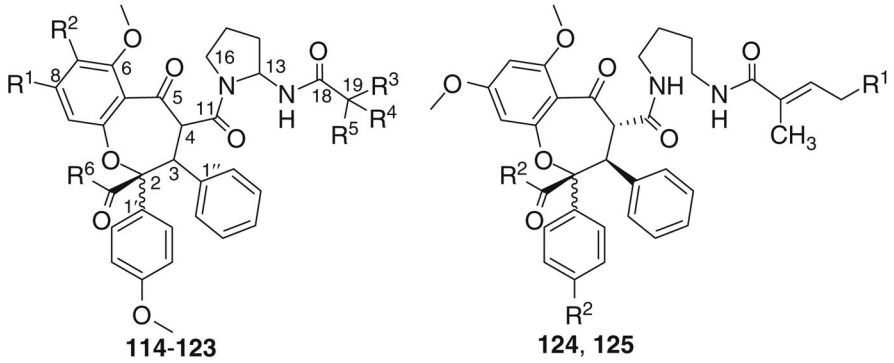


| Cpd. | Trivial Name | $R^1$ | $R^2$ | $R^3$ | $R^4$ | $R^5$ | $R^6$ | H-3, H-4 | Ref. |
|---|---|---|---|---|---|---|---|---|---|
| **114** | Forbaglin A (13*R*) | $OCH_3$ | H | $CH_3$ | H | $C_2H_5$ | $CH_3$ | *α,β* | (*60*) |
| **115** | Forbaglin B (13*S*) | $OCH_3$ | H | $CH_3$ | H | $C_2H_5$ | $CH_3$ | *α,β* | (*60*) |
| **116** | (13*S*)-Thapoxepine A | -$OCH_2O$- | | $CH_3$ | H | $CH_3$ | $CH_3$ | *α,β* | (*15*) |
| **117** | (13*R*)-Thapoxepine A | -$OCH_2O$- | | $CH_3$ | H | $CH_3$ | $CH_3$ | *α,β* | (*15*) |
| **118** | Homothapoxepine A | -$OCH_2O$- | | $CH_3$ | H | $C_2H_5$ | $CH_3$ | *α,β* | (*15*) |
| **119** | (13*S*)-Thapoxepine B | -$OCH_2O$- | | $CH_3$ | H | $CH_3$ | $CH_3$ | *β,α* | (*15*) |
| **120** | (13*R*)-Thapoxepine B | -$OCH_2O$- | | $CH_3$ | H | $CH_3$ | $CH_3$ | *β,α* | (*15*) |
| **121** | Edulisone A (13*R*) | -$OCH_2O$- | | H | H | $CH(CH_3)_2$ | $OCH_3$ | *α,β* | (*83*) |
| **122** | Edulisone B (13*S*) | -$OCH_2O$- | | H | H | $CH(CH_3)_2$ | $OCH_3$ | *α,β* | (*83*) |
| **123** | 19,20-Dehydroedulisone | -$OCH_2O$- | | $\Delta^{19,20}$ | | $C(CH_3)_2$ | $OCH_3$ | *α,β* | (*72*) |
| **124** | | *O*-glc | $OCH_3$ | - | - | - | - | *α,β* | (*64*) |
| **125** | | OH | OH | - | - | - | - | *α,β* | (*64*) |

**Fig. 8.**
Forbagline derivatives isolated from *Aglaia* species

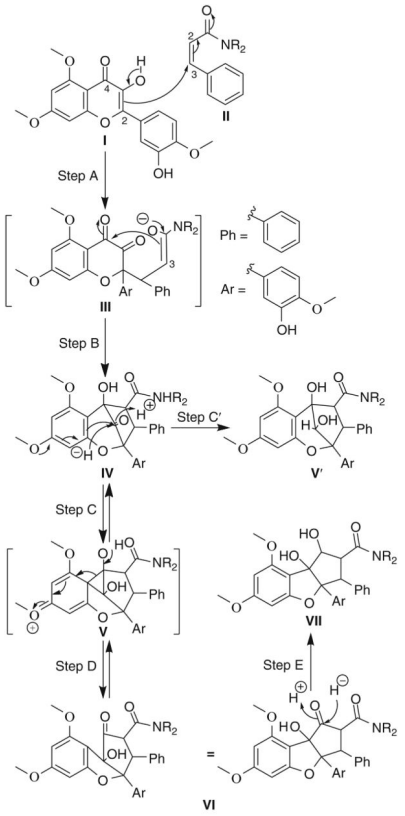


**Fig. 9.**

Postulated joint biosynthesis scheme of rocaglamide (= flavagline)-type compounds isolated from *Aglaia* species (14)

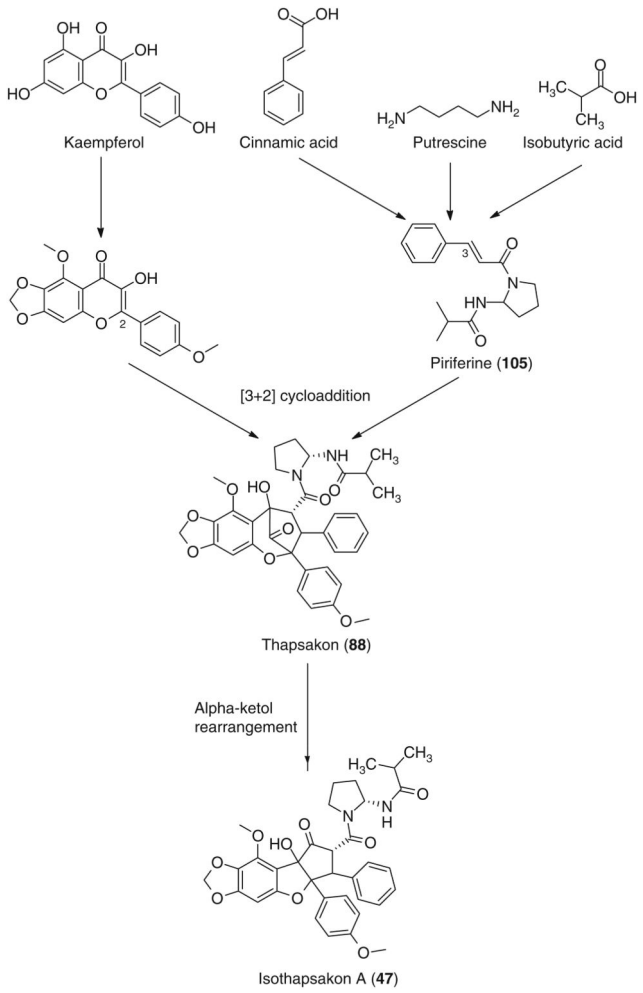


**Fig. 10.**

Proposed biosynthetic origin of isothapsakon A (**47**) and thapsakon (**88**) as bisamide-containing rocaglamide-type derivatives

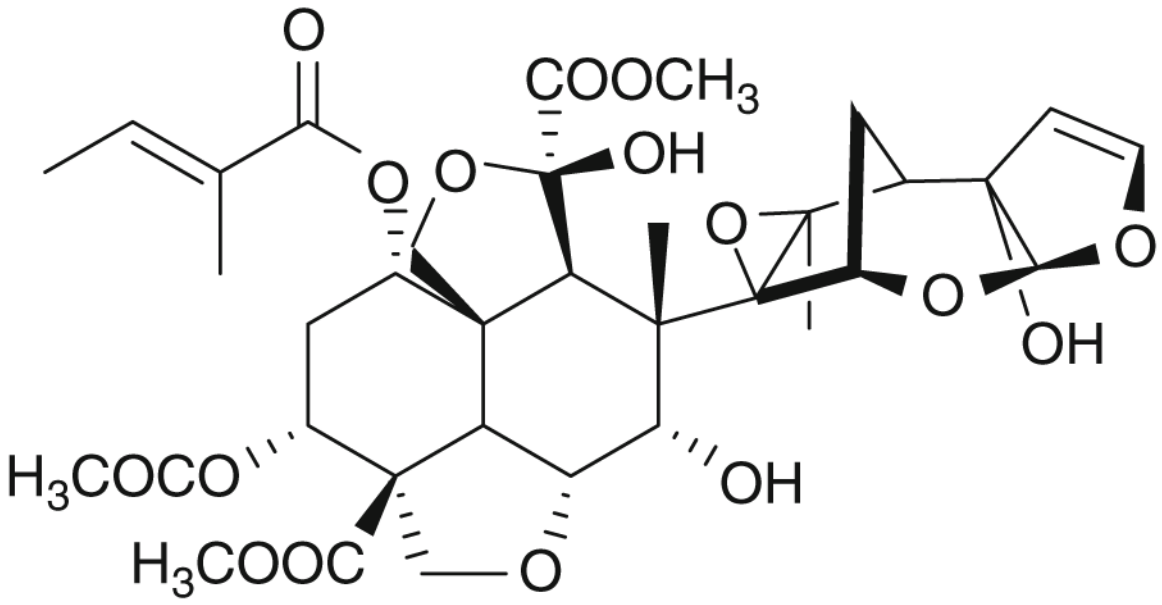


**Fig. 11.**
Chemical structure of azadirachtin from *Azadirachta indica* (family Meliaceae)

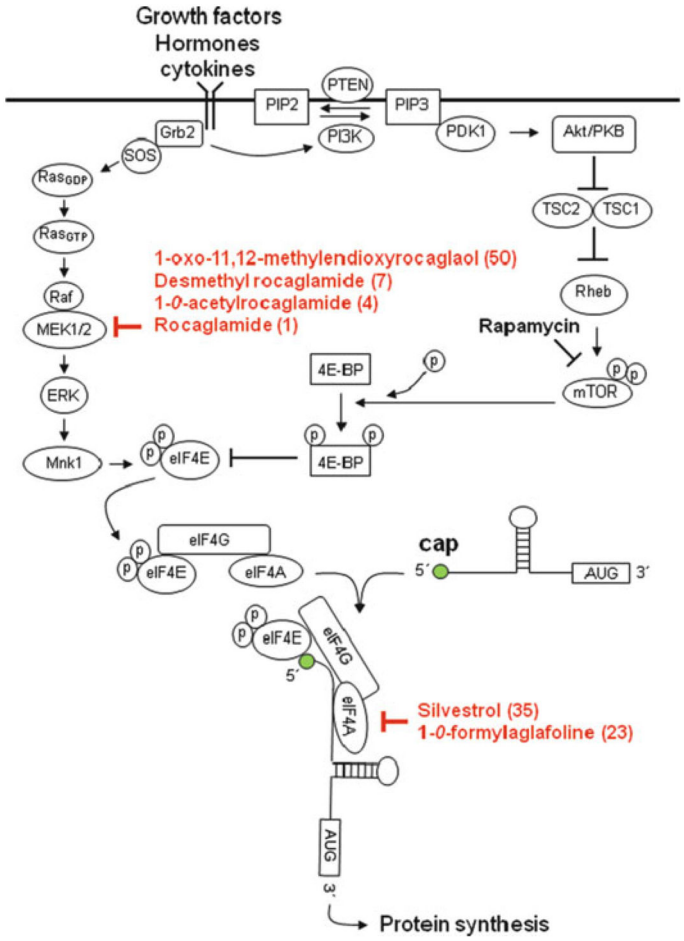


**Fig. 12.**

Inhibition of protein synthesis by rocaglamides. The Ras-Raf-MEK-ERK and the PI3K-AKT-mTOR pathways play a central role in regulation of cap-dependent translation by activation of the eukaryotic translation initiation factor 4E (eIF4E). eIF4E binds to the 5′ cap structure and assembles eIF4G and eIF4A to initiate translation. Rocaglamide congeners **23** and **35** directly bind to and inhibit eIF4A function. Rocaglamides **1**, **4**, **7** and **50** block the MEK-REK pathway and inhibit eIF4E cap binding activity

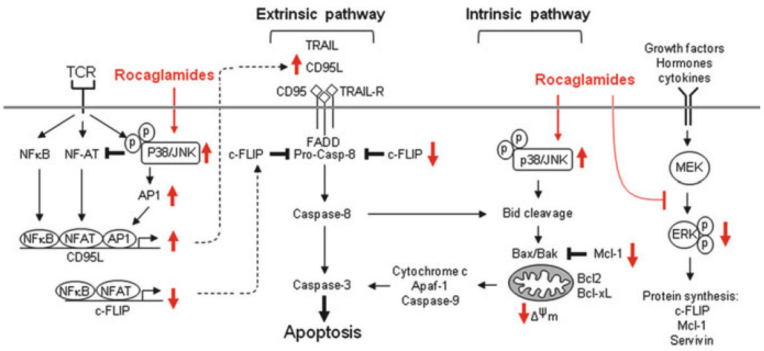


**Fig. 13.**

Apoptosis pathways affected by rocaglamides. Apoptotic cell death is regulated by two main pathways: extrinsic (receptor-mediated) and intrinsic (mitochondria-mediated) pathways. The extrinsic pathway involves ligation of death receptors (*e.g.* CD95 and TRAIL-R) with their ligands (*e.g.* CD95L and TRAIL) resulting in a sequential activation of caspase-8 and -3, which cleave target proteins leading to apoptosis. This pathway is negatively regulated by the anti-apoptotic protein c-FLIP. Intrinsic stimuli (*e.g.* anticancer drugs) directly or indirectly activate the mitochondrial pathway by inducing release of cytochrome c and activation of caspase-9. Caspase-9, in turn, activates caspase-3. This death pathway is largely controlled by the pro-apoptotic (*e.g.* Bax and Bak) and anti-apoptotic (*e.g.* Mcl-1, Bcl-2 and Bcl-xL) proteins. Activated caspase-8 may induce cleavage of Bid, which induces translocation of Bax and/or Bak to the mitochondrial membrane and amplifies the mitochondrial apoptosis pathway. Bid cleavage can be also induced by activated p38 and JNK. Several rocaglamides can activate p38 and JNK leading to Bid cleavage. Rocaglamides can also directly inhibit protein synthesis by interfering with eIF4A (see Fig. 9) or indirectly through inhibition of the MEK-ERK-eIF4E pathway. Protein synthesis inhibition will lead to down-regulation of short-lived anti-apoptotic proteins such as c-FLIP and Mcl-1. Furthermore, rocaglamides may further increase T-cell-receptor (TCR)-mediated activation of p38 and JNK leading to down-regulation of NF-AT activity and up-regulation of AP-1 activity. This event results in up-regulation of CD95L promoter activity and suppression of c-FLIP promoter activity leading to enhancing activation-induced-cell-death

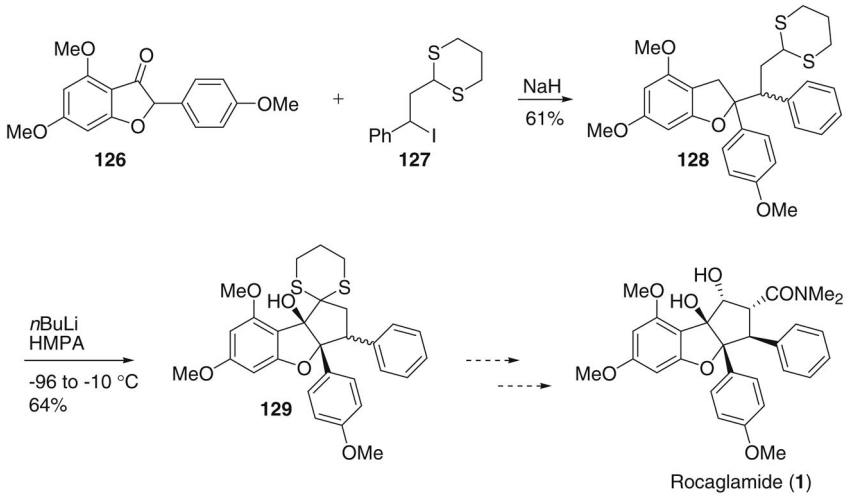


**Fig. 14.**

*Taylor*'s approach to the rocaglate skeleton (119)

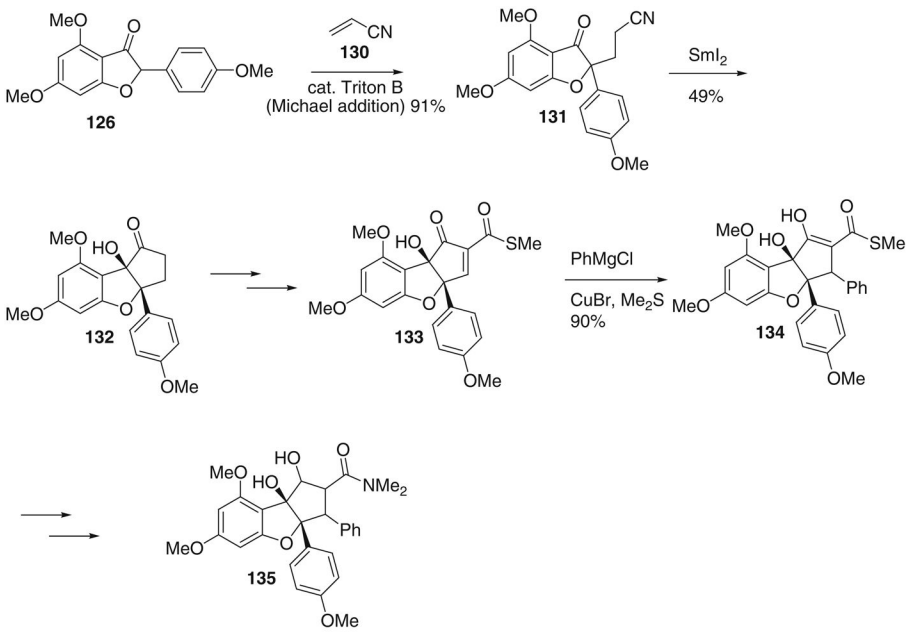


**Fig. 15.**

*Kraus*'s synthesis of a rocaglamide di-*epi*-analogue (120)

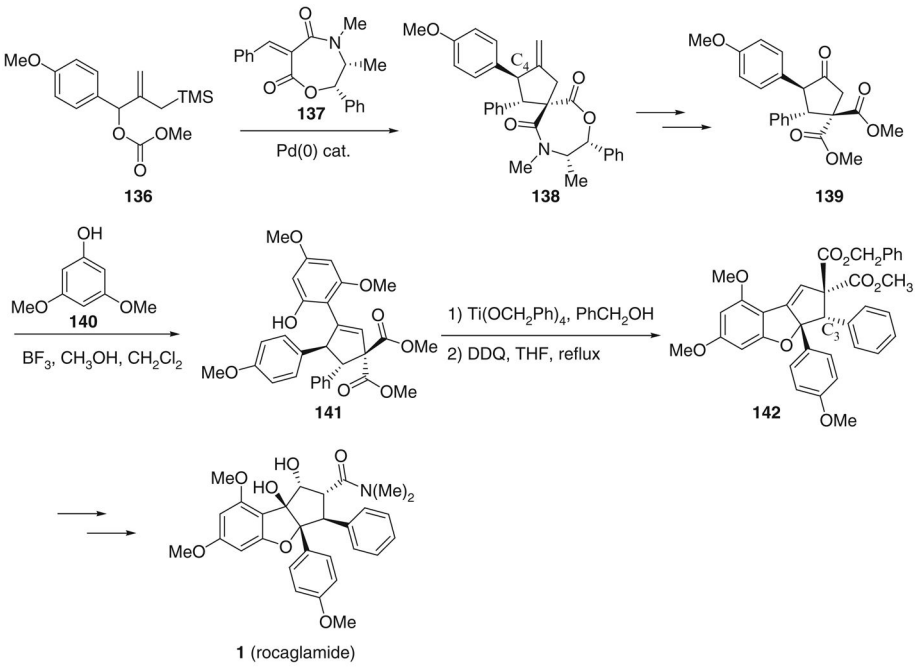


**Fig. 16.**

*Trost*'s synthesis of (−)-rocaglamide (52)

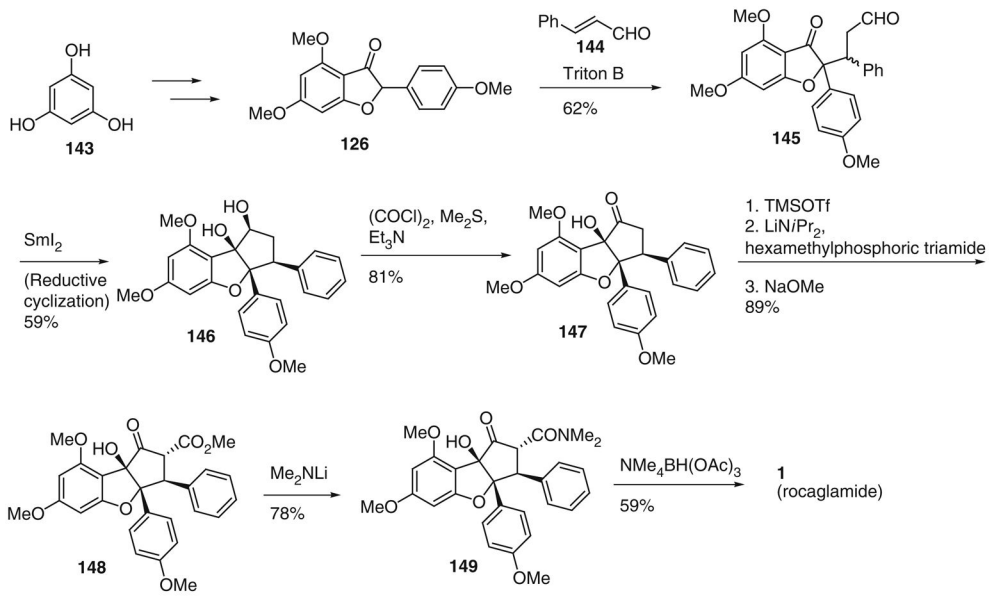


**Fig. 17.**

*Taylor*'s racemic synthesis of rocaglamide (**1**) (121)

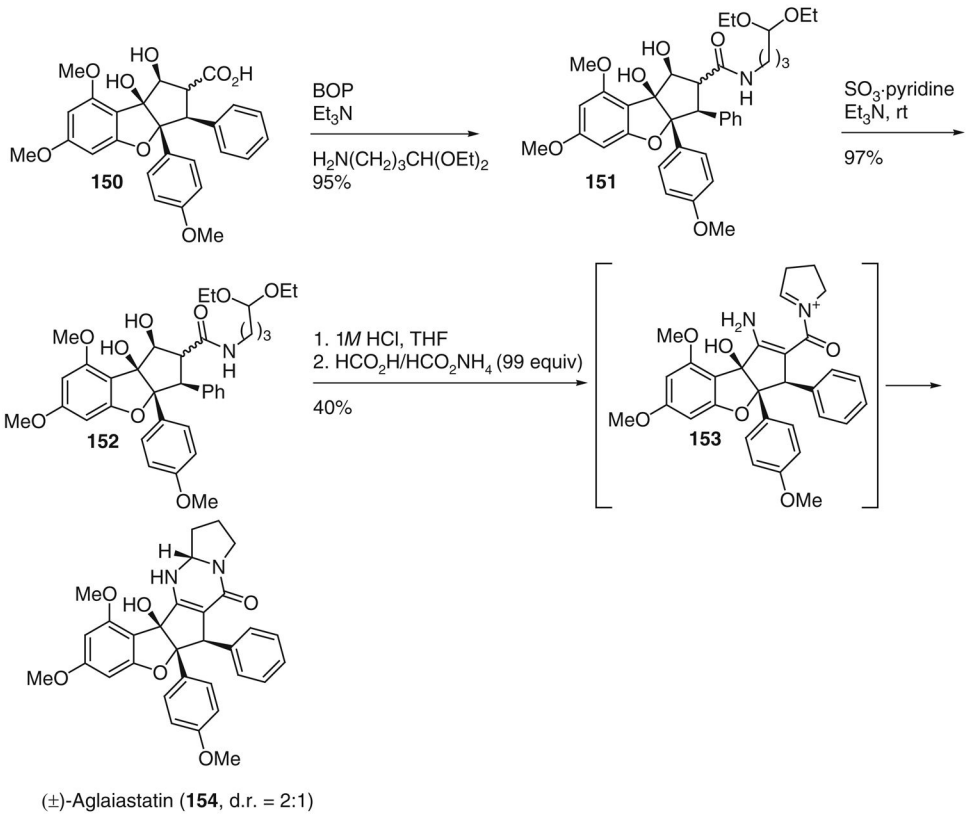


**Fig. 18.**

*Watanabe*'s synthesis of (±)-aglaiastatin (**154**) (123)

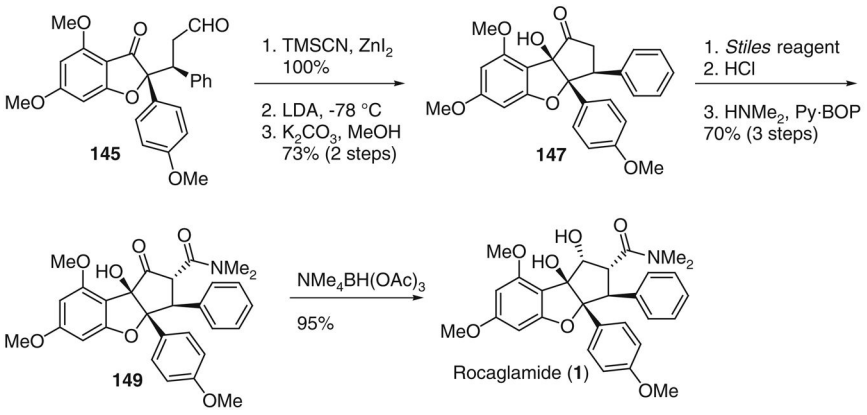


**Fig. 19.**

*Dobler*'s synthesis of racemic rocaglamide (**1**) (124)

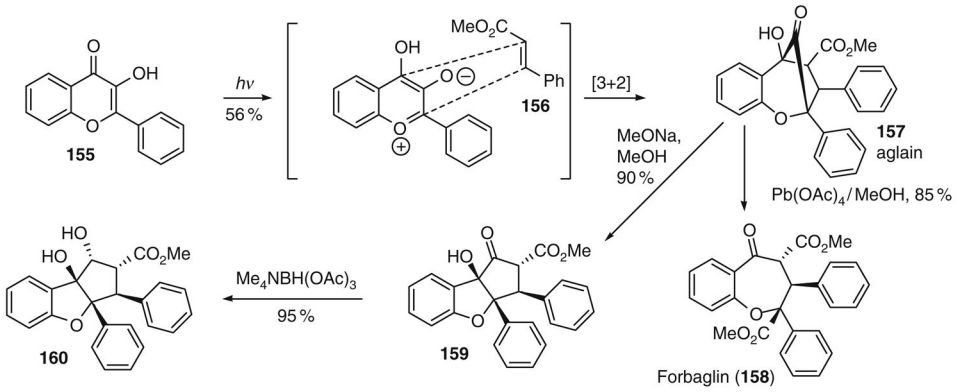


**Fig. 20.**

*Porco*'s unified approach to the aglains, forbaglins, and rocaglamides (125)

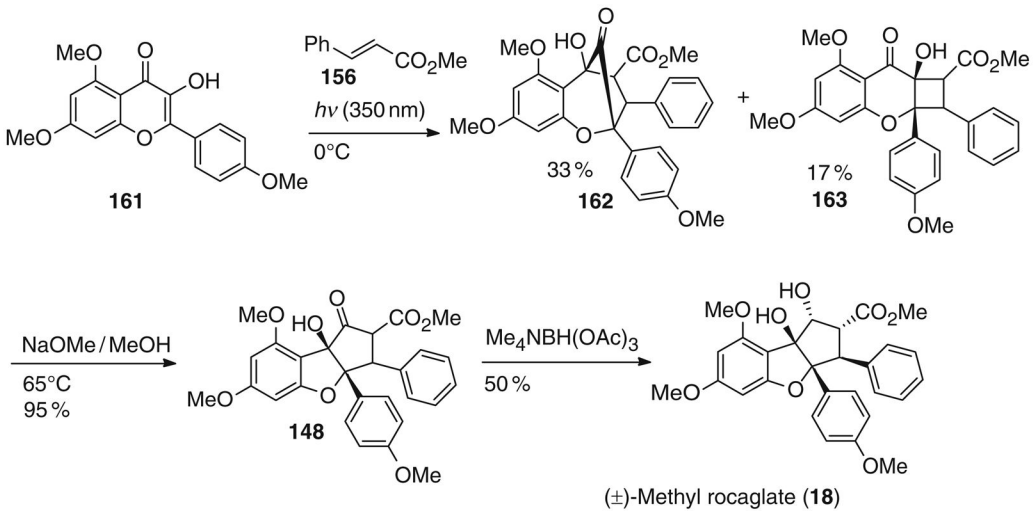


**Fig. 21.**

*Porco*'s synthesis of (±)-methyl rocaglate (**18**) (125)

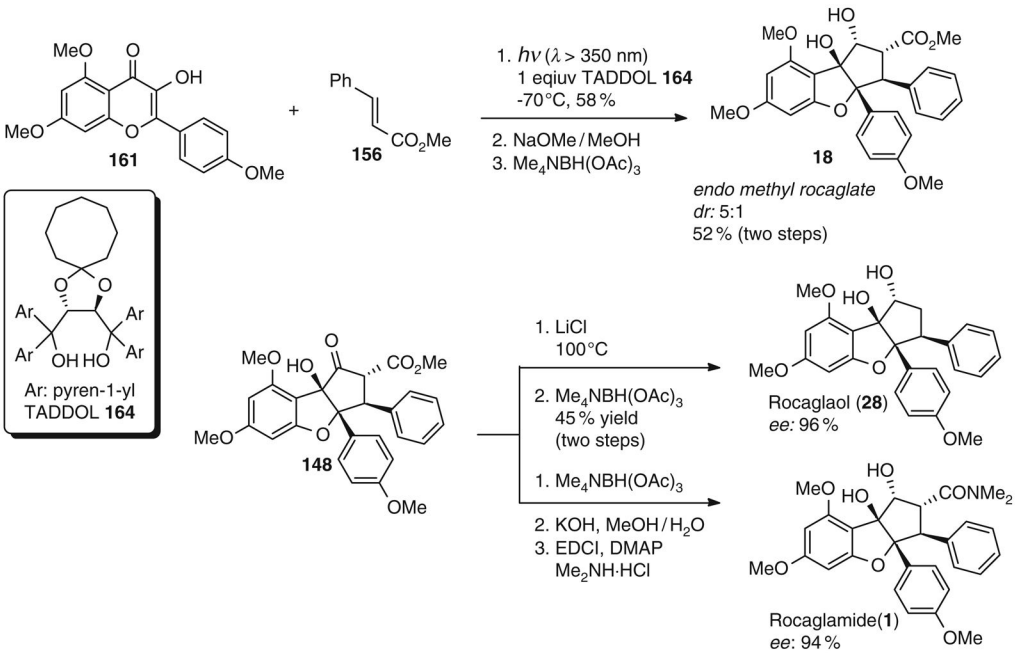


**Fig. 22.**

*Porco*'s enantioselective methodology for the synthesis of (−)-methyl rocaglate (**18**), (−)-rocaglaol (**28**), and (−)-rocaglamide (**1**) (126)

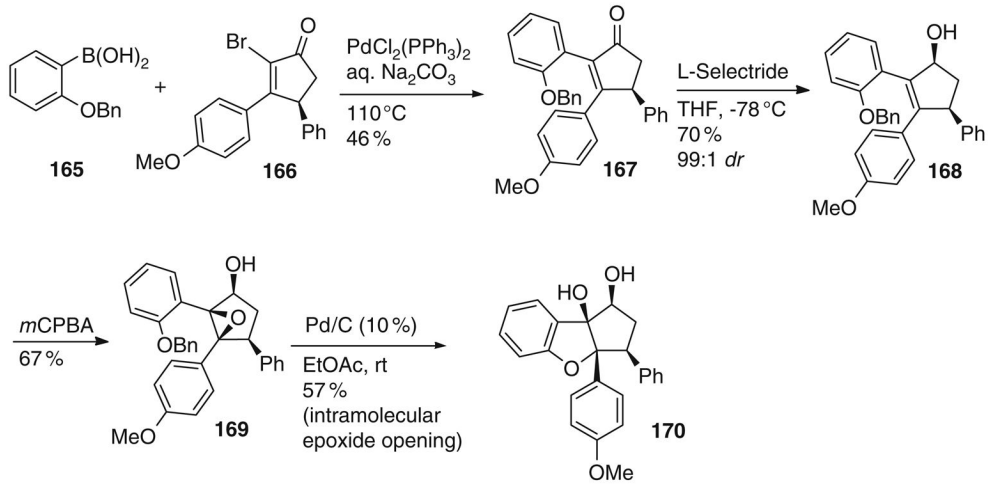


**Fig. 23.**

*Thede* and *Ragot*'s stereoselective synthesis of (±)-rocaglaol analogues (129)

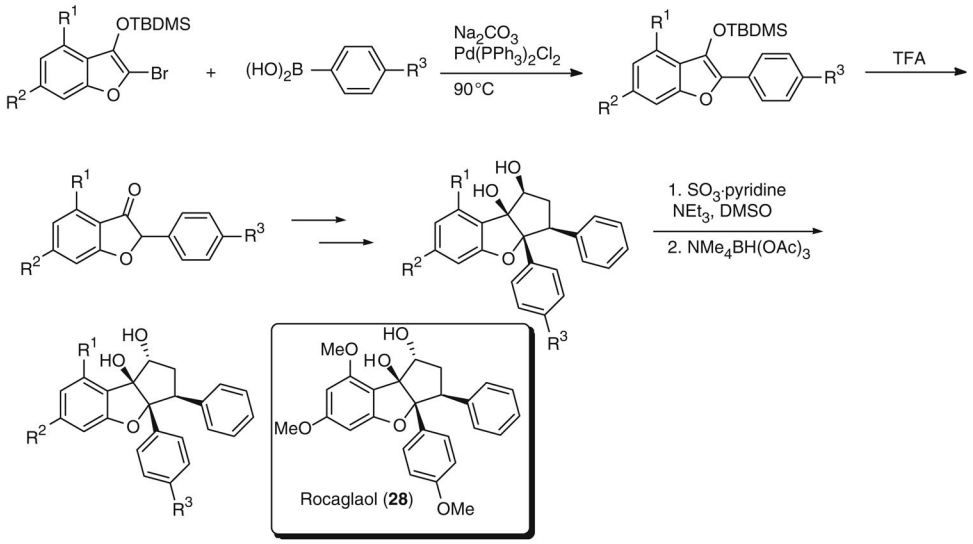


**Fig. 24.**

*Thede* and *Ragot*'s stereoselective synthesis of (±)-rocaglaol (**28**) and analogues (130)

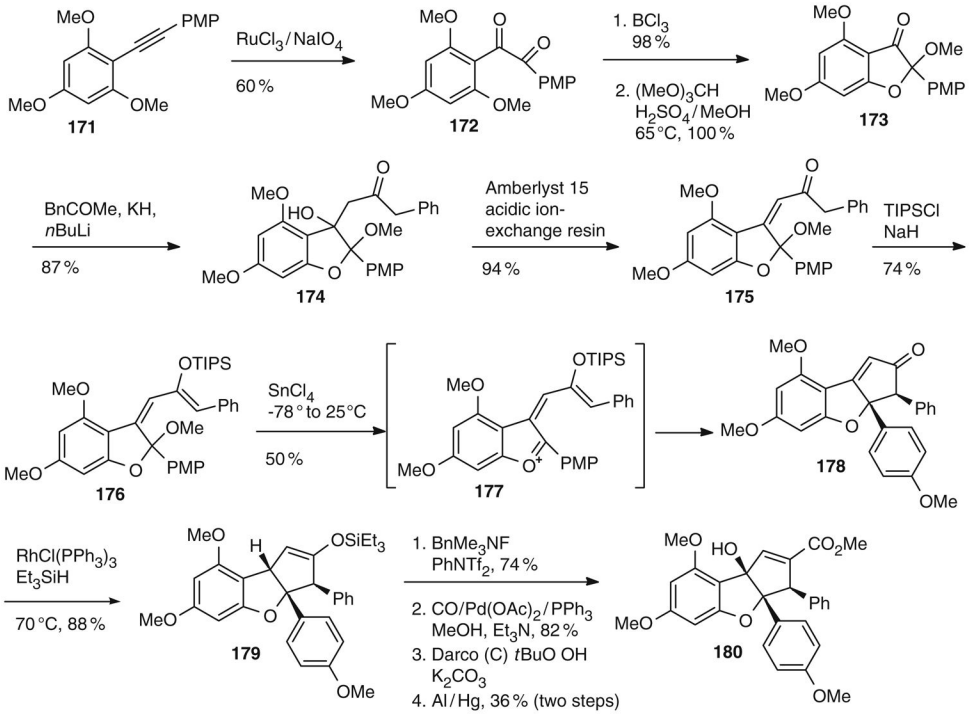


**Fig. 25.**

*Magnus*'s stereospecific synthesis of (±)-1,2-anhydro methyl rocaglate (**180**) (131)

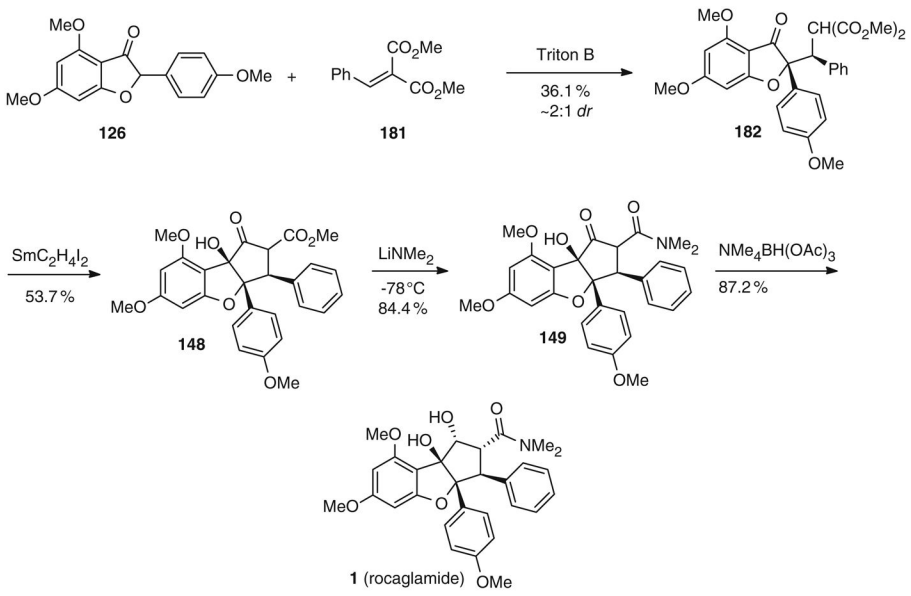


**Fig. 26.**

*Qin*'s racemic synthesis of rocaglamide (**1**) (132)

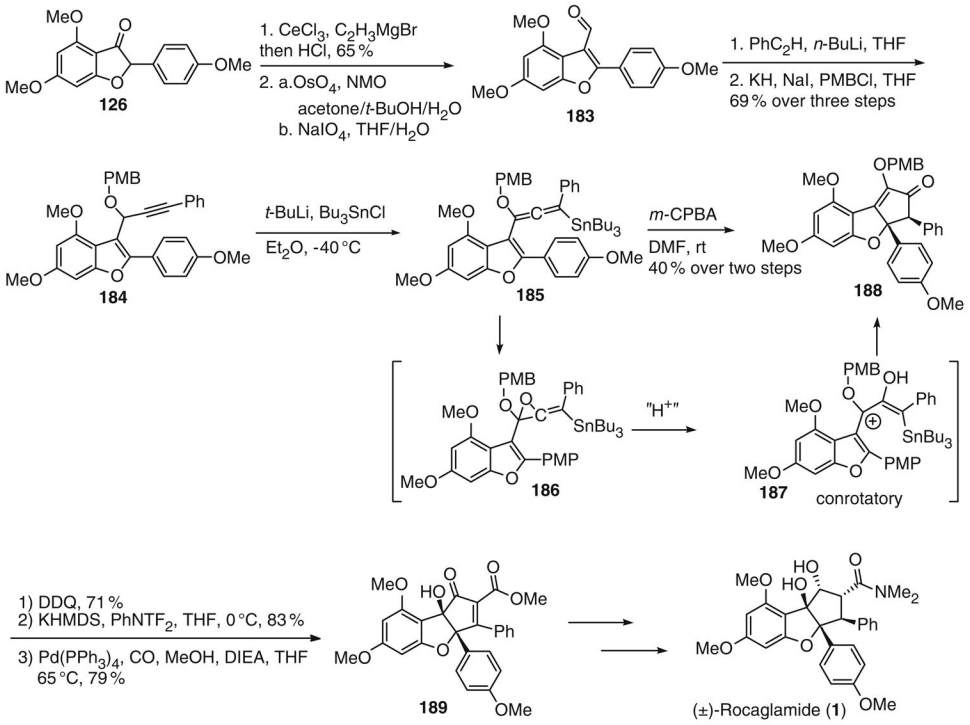


**Fig. 27.**

*Frontier*'s synthesis of (±)-rocaglamide (**1**) *via Nazarov* cyclization (133)

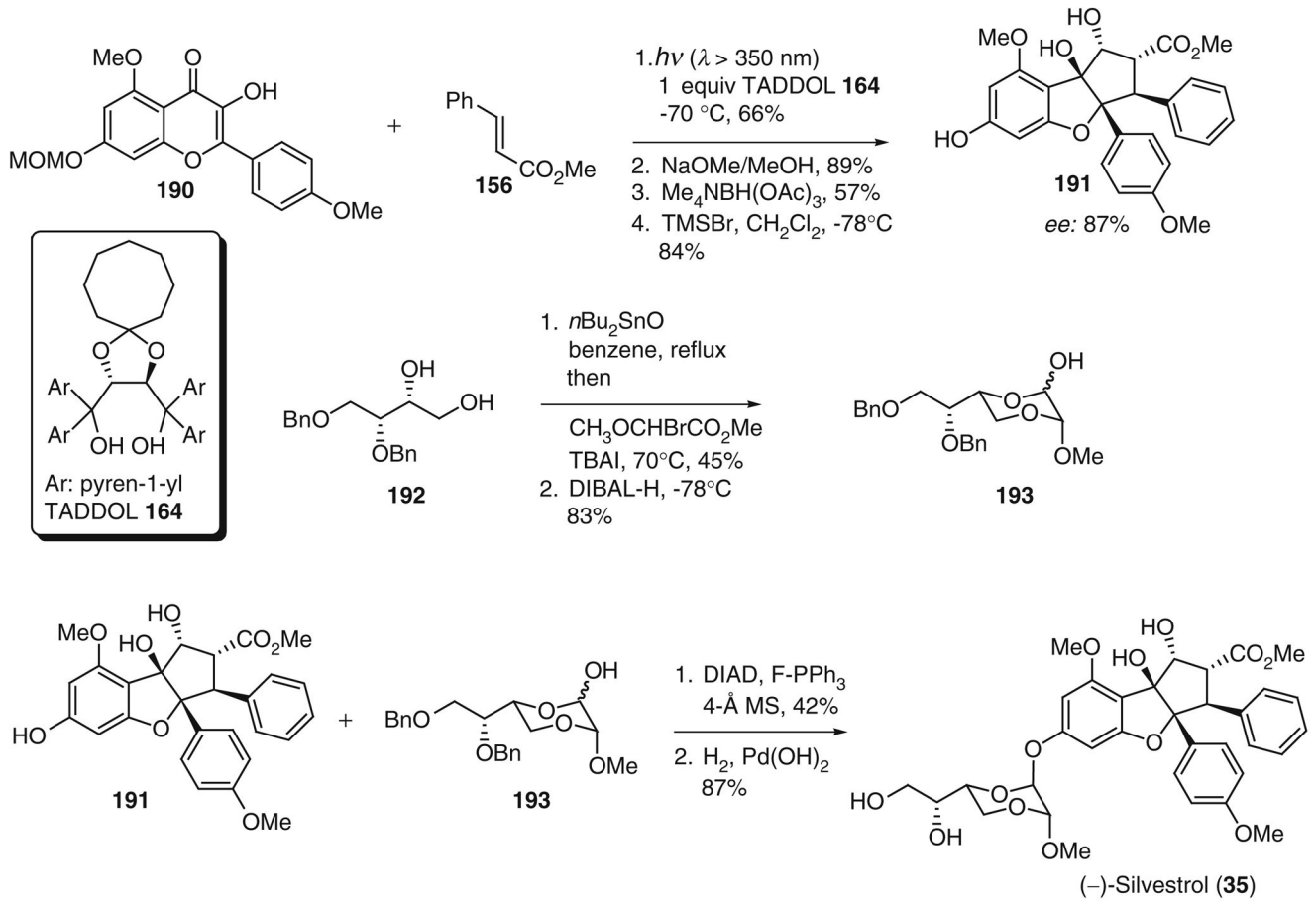


**Fig. 28.**

*Porco*'s enantioselective synthesis of (−)-silvestrol (**35**) (134)

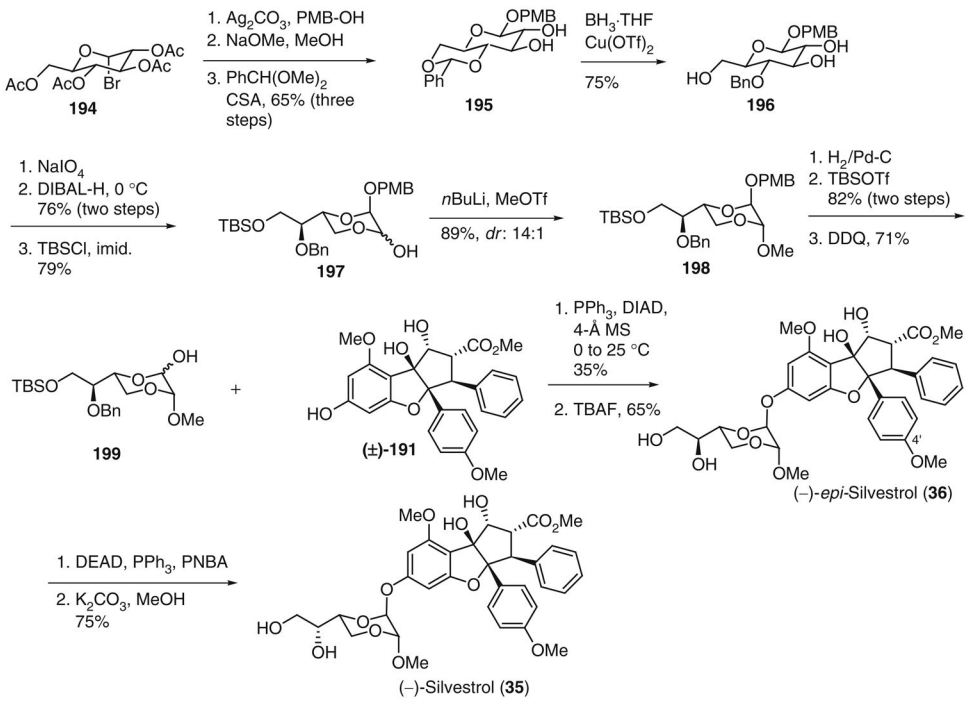


**Fig. 29.**

*Rizzacasa*'s syntheses of (−)-silvestrol (**35**) and (−)-*epi*-silvestrol (**36**) (136)

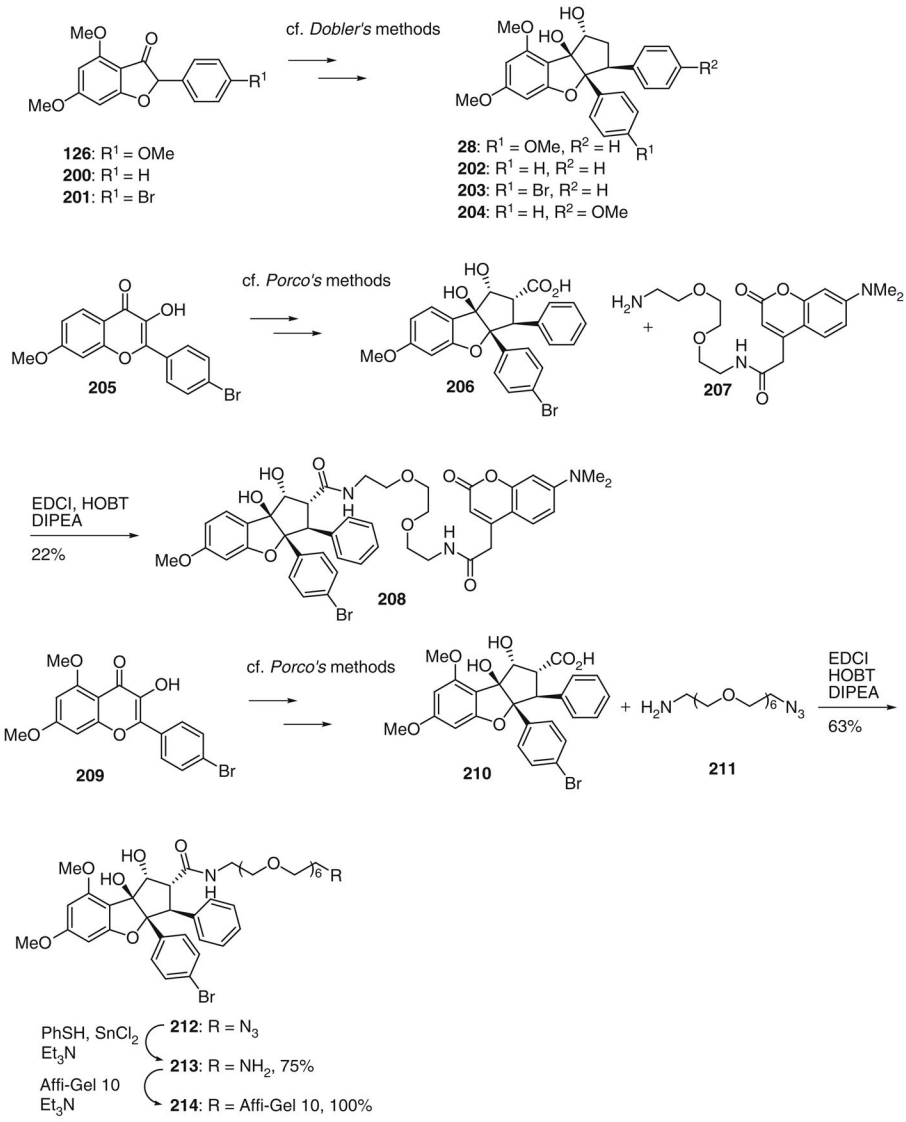


**Fig. 30.**

*Désaubry*'s synthetic rocaglaol derivatives **28** and **202**–**204**, fluorescent probe **208**, and affinity ligand **214** (138)

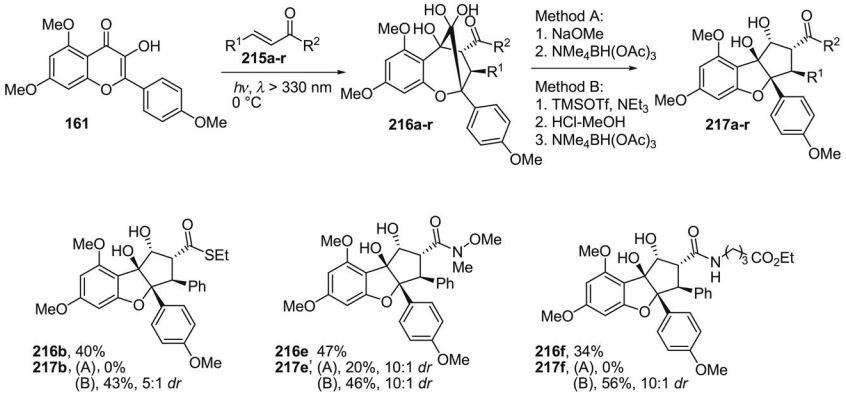


**Fig. 31.**

Scope of [3 + 2] photocycloaddition to produce analogues of rocaglamide (139)

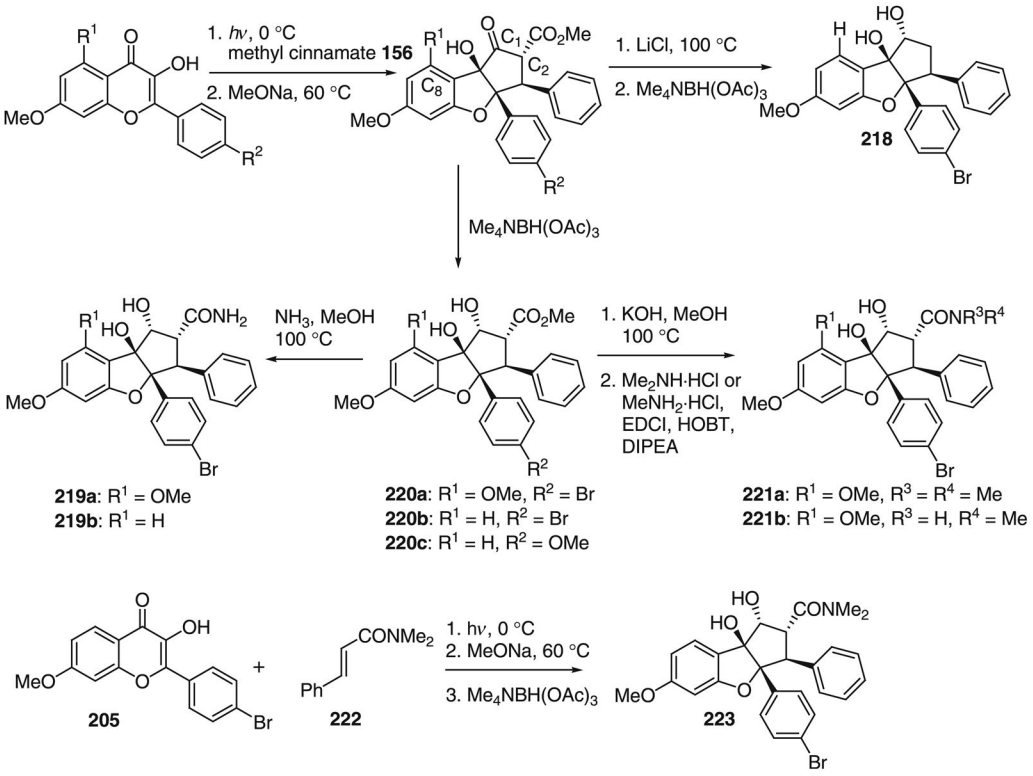


**Fig. 32.**

*Désaubry*'s rocaglamide and rocaglaol analogues (140)

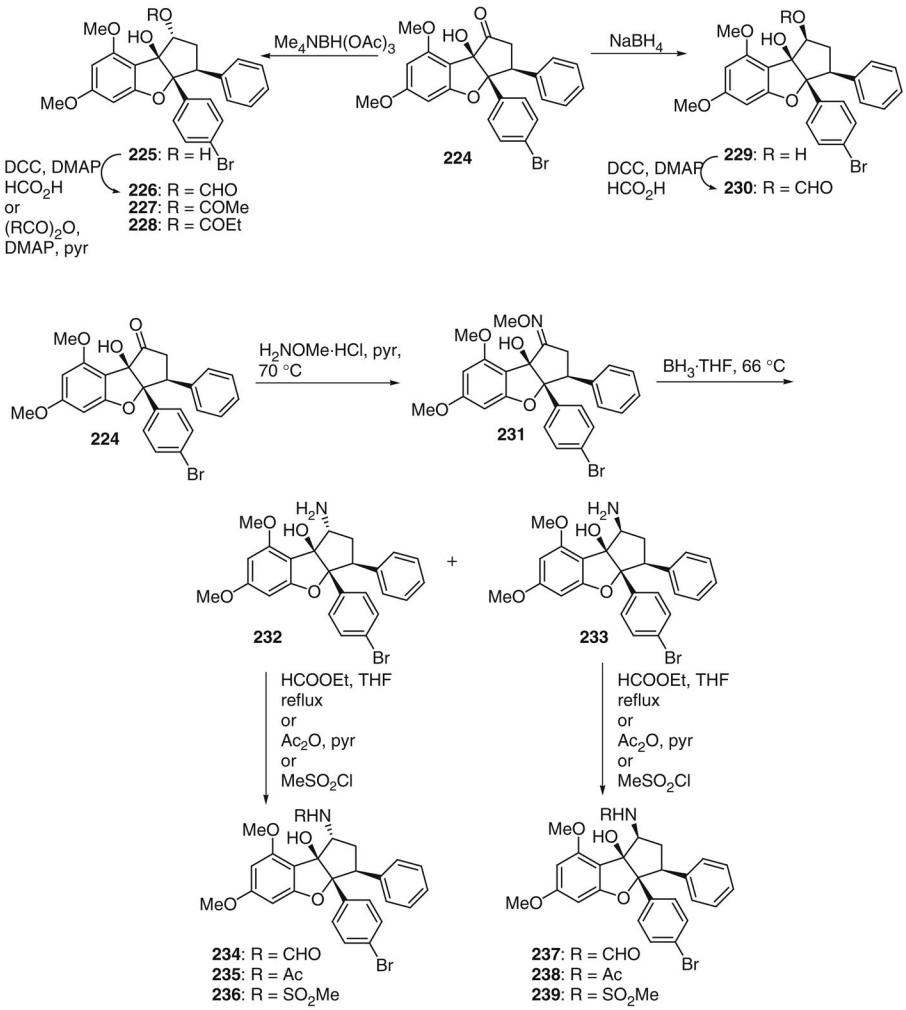


**Fig. 33.**

*Désaubry*'s rocaglamide and rocaglaol analogues varied at C-1 (140)